

Proteomics-based Identification and Characterization of Components  
in the avrRpm1-RPM1 “Gene-for-Gene” Defense Response

D i s s e r t a t i o n

zur Erlangung des akademischen Grades

doctor rerum naturalium (Dr. rer. nat)

vorgelegt der

Naturwissenschaftlichen Fakultät I  
Biowissenschaften

der Martin-Luther-Universität Halle-Wittenberg

von

Ivy Widjaja

geb. am: 2 November 1974 in: Surabaya, Indonesia

Gutachter /in

1. Prof. Dr. Dierk Scheel
2. Prof. Dr. Ralf Bernd Klösgen
3. Prof. Dr. Ralf Oelmüller

Halle (Saale), 28.05.2009

Herewith, I declare that this thesis and its content was made solely based on my work as a PhD student of Martin-Luther-Universität Halle Wittenberg. This work was done independently without any help from others. Other resources and supports than that are stated in this thesis were not used. All citations are cited literally and the sources are acknowledged accordingly in this thesis as references.

I certify that this thesis has never been submitted to other faculties or universities for examination.

Halle,

Ivy Widjaja

Parts of this thesis have been published in the following paper and posters

Journal paper:

Widjaja I, Naumann K, Roth U, Wolf N, Mackey D, Dangl JL, Scheel D, Lee J (2008) Combining sub-proteome enrichment and Rubisco depletion enables identification of low abundance proteins differentially regulated during plant defense. *Proteomics* (in press)

Posters:

Widjaja I, Lee J, Belkhadir Y, Dangl JL, and Scheel D. Proteomic Study of Plant Defense Mechanism Using a “Gene-for-Gene” Model in Arabidopsis. *Molecular Interactions*, 18-20<sup>th</sup> July 2005, Berlin

Widjaja I, Dangl JL, Scheel D and Lee J. Post Translational Modification of the Lipid Raft Protein, Remorin during Gene-for-Gene Interaction; A Proteomics Approach. *International Meeting “Communication in Plants and their Response to the Environment”*, 10-12<sup>th</sup> May 2007, Halle/Saale

Widjaja I, Dangl JL, Scheel D and Lee J. Post Translational Modification of the Lipid Raft Protein, Remorin during Gene-for-Gene Interaction; A Proteomics Approach. *3<sup>rd</sup> Plant Science Student Conference 2007*, 6-8<sup>th</sup> June 2007, Halle/Saale

Widjaja I, Dangl JL, Scheel D and Lee J. Post Translational Modification of the Lipid Raft Protein, Remorin during Gene-for-Gene Interaction; A Proteomics Approach. *14<sup>th</sup> International Workshop on Plant Membrane Biology*, 26-30<sup>th</sup> June 2007, Valencia

## Contents

I. Introduction.....	1
1. Pathogen Associated Molecular Pattern-Triggered Immunity (PTI).....	2
2. Effector-Triggered Immunity (ETI).....	3
2.1. Effector proteins.....	4
2.1.1. Type Three Secretion System.....	5
2.1.2. Strategies used by bacterial pathogens to suppress plant defense..	6
2.1.3. Enzyme activities of effectors to promote bacterial virulence.....	10
2.2. Resistance proteins.....	11
2.2.1. Different classes of resistance proteins.....	11
2.2.2. Functional domain of resistance protein.....	12
2.3. “Gene-for-Gene” interaction.....	14
2.3.1. Direct “Gene-for-Gene” interaction.....	14
2.3.2. Indirect “Gene-for-Gene” interaction.....	14
2.3.3. Components of R gene signal transduction.....	15
3. The “avrRpm1-Rpm1” model system.....	16
4. Proteomics for plant defense study.....	18
5. Aim of this work.....	20
II. Material and methods.....	21
1. Protein biochemical techniques.....	21
1.1. Total protein extraction.....	21
1.2. Microsomal fraction extraction.....	21
1.3. Rubisco depletion from total protein.....	21
1.4. Rubisco depletion from microsomal protein.....	22
1.5. Rubisco depletion using Seppro IgY Rubisco (Genway) spin column.....	22
1.6. 2-DE.....	22
1.7. Image analysis using Proteomweaver.....	23
1.8. Protein identification using PMF MALDI-TOF/MS.....	23
1.9. Western blot.....	24
1.10. Immunoprecipitation.....	24
1.11. Dephosphorylation assay (Phosphatase treatment).....	24
1.12. Generation and purification of anti-Remorin (AtREM1.2).....	25
1.13. Lipid rafts/Detergent Resistant Membranes (DRM) isolation.....	25
1.14. Co-immunoprecipitation using anti-RIN4 and anti-Remorin.....	26
2. Molecular biological and cloning procedures.....	26
2.1. DNA extraction and Southern blot.....	26
2.2. RNA extraction and Northern blot.....	27
2.3. Radioactive DNA labelling and hybridization.....	27
2.4. Reverse-Transcription-PCR (RT-PCR).....	28
2.5. Selection of T-DNA insertional (SALK) lines.....	28
2.6. Cloning of the AtREM1.2-CFP/YFP/Strep/RNAi constructs.....	28
2.7. Cloning of the pER8-AtREM1.2 and pER10-AtREM1.2 constructs.....	29
2.8. Cloning of AtREM1.2-RNAi into pCB302.....	29
2.9. Cloning At2g20630 and At1g11650 into pENTR-TOPO vector.....	29
2.10. Agrobacterium transformation.....	29
3. Plant growth, treatment and transformation.....	30
3.1. Plant growth and treatment.....	30
3.2. Arabidopsis transformation using floral dip protocols.....	30
3.3. Trypan Blue staining.....	31

3.4.	DAB staining.....	31
3.5.	Bacterial growth curve assay.....	31
3.6.	Ion leakage assay.....	32
3.7.	Agrobacterium transient expression in <i>Nicotiana benthamiana</i> .....	32
4.	Hormone analysis.....	32
4.1.	JA and OPDA measurement.....	32
4.2.	SA measurement.....	33
4.3.	ET measurement.....	34
III.	Results.....	35
1.	Proteomics analysis of differentially regulated protein during avrRpm1-Rpm1 interaction.....	35
1.1.	Differential regulation of proteins in total protein extract.....	36
1.2.	Differential regulation of proteins in microsomal protein extract.....	37
1.3.	Rubisco depletion from total protein and microsomal fractions.....	39
1.4.	Comparison between Rubisco depletion using PEG fractionation and commercial Rubisco-removal spin column.....	40
1.5.	Differential regulation of proteins of different biological functions.....	42
1.6.	Candidates signaling proteins are post-transcriptionally of post-translationally regulated.....	43
2.	Functional analysis of the putative Protein Phosphatase 2C (At2g20630).....	45
2.1.	PP2C up-regulation is specific for avrRpm1.....	46
2.2.	At2g20630 T-DNA insertion mutants do not express PIA1.....	47
2.3.	The <i>pial</i> mutants showed enhanced resistance to <i>Pto</i> DC3000( <i>avrRpm1</i> ), but not to <i>Pto</i> DC3000.....	48
2.4.	Expression of the RPM1-responsive gene, <i>MMP2</i> , is enhanced in the <i>pial</i> mutants.....	50
2.5.	PIA1 regulates the induction of pathogenesis- and stress-related genes.....	51
2.6.	Differential regulation of pathogenesis- and stress-related genes in the <i>pial</i> mutants corresponds to changes in plant hormones involved in defense.....	52
2.7.	PIA1 does not regulate phosphorylation of RIN4 and AtREM1.2.....	54
2.8.	Screening for putative PIA1 targets by Proteomics analysis of the <i>pial</i> mutants.....	55
3.	Functional analysis of AtREM1.2 (At3g61260).....	57
3.1.	$\alpha$ -Remorin recognized protein spots identified as AtREM1.2.....	57
3.2.	Up-regulation of AtREM1.2 observed on the silver-stained 2D gels was confirmed by 2D-Western using $\alpha$ -Remorin.....	59
3.3.	AtREM1.2 is up-regulated by avrRpm1 and avrB, but not by avrRpt2.....	60
3.4.	Up-regulation of AtREM1.2 was continued until 6 hpi when HR occurred, and the expression went back to basal levels at 10 hpi.....	61
3.5.	AtREM1.2 is present in the detergent resistant membrane (lipid raft membrane) fraction.....	62
3.6.	Dephosphorylation assay confirms AtREM1.2 phosphorylation during RPM1-mediated resistance.....	62
3.7.	Interaction between AtREM1.2 and RIN4 was not detected.....	63
3.8.	Over expression of <i>AtREM1.2</i> did not cause necrosis, but silencing of <i>AtREM1.2</i> produced subtle necrosis during the Agrobacterium-mediated transient expression.....	64
3.9.	Inducible expression and silencing of <i>AtREM1.2</i> did not cause any change in HR formation.....	65

3.10.	Inducible expression and silencing of <i>AtREM1.2</i> did not change the susceptibility against virulent strain <i>Pto</i> DC3000.....	67
3.11.	Silencing of <i>AtREM1.2</i> increased resistance against <i>Pto</i> DC3000 ( <i>avrRpm1</i> ), but induced expression of <i>AtREM1.2</i> did not influence the resistance against the avirulent strain.....	68
3.12.	Silencing of <i>AtREM1.2</i> did not change the RIN4 phosphorylation.....	69
3.13.	Silencing of <i>AtREM1.2</i> did not change the expression of selected RPM1-marker genes.....	70
3.14.	<i>AtREM1.2</i> transgene could not be induced in the <i>rpm1-3</i> line.....	71
IV.	Discussion.....	73
1.	Proteomics analysis of differentially regulated proteins during <i>avrRpm1-Rpm1</i> interaction.....	73
1.1.	Combination of microsomal enrichment and fractionation-based Rubisco depletion reveals novel candidates with potential signaling roles in RPM1-mediated resistance.....	73
1.2.	Potential functions/roles of the candidates.....	75
2.	Functional analysis of PIA1 for RPM1-mediated defense response.....	77
2.1.	PIA1 does not regulate cell death formation and ROS production, but negatively regulates disease resistance mediated by RPM1.....	78
2.2.	PIA1 regulates pathogenesis- and stress-related gene expression.....	81
2.3.	Searching for PIA1 target proteins.....	83
2.4.	PIA1 regulates an <i>avrB</i> -independent pathway in RPM1-mediated defense response.....	84
3.	Functional analysis of <i>AtREM1.2</i> (At3g61260) for defense response mediated by <i>avrRpm1-RPM1</i> interaction.....	85
3.1.	<i>AtREM1.2</i> regulation during the RPM1-mediated defense response might occur <i>via</i> phosphorylation and distribution to lipid rafts, but not by interaction with RIN4.....	87
3.2.	<i>AtREM1.2</i> may play a role in maintaining cell integrity.....	90
3.3.	Silencing <i>AtREM1.2</i> increases resistance specifically to <i>Pto</i> DC3000 ( <i>avrRpm1</i> ).....	91
3.4.	<i>AtREM1.2</i> does not regulate RIN4 phosphorylation and the expression of RPM1 marker genes <i>MMP2</i> , <i>RIPK</i> and <i>TonB</i> .....	92
4.	Summary.....	93
V.	References.....	95

## Appendix

## List of Abbreviations

ACS6	1-aminocyclopropane-1-carboxylic acid (ACC) synthase-6
<i>Apaf-1</i>	<i>Apoptotic protease activating factor-1</i>
Bax	Bcl-2-associated X protein
<i>Bcl-2</i>	B-cell lymphoma 2
BiP	Luminal binding protein
CC	Coiled-coil motif
<i>CED4</i>	<i>Caenorhabditis elegans apoptotic adaptor 4</i>
CEL	Conserved effector locus
CHORD	Cysteine and histidine-rich domain
<i>coi1</i>	<i>coronatine insensitive 1</i>
Co-IP	Co-immunoprecipitation
Col-0	<i>Arabidopsis</i> accession Columbia
COR	Coronatine
<i>cpr</i>	<i>constitutive expressor of PR genes</i>
CTR1	Constitutive triple response 1
DRM	Detergent-resistant membrane
DSM	Detergent-soluble membrane
<i>EDS1</i>	<i>Enhanced disease susceptibility 1</i>
<i>EF1<math>\alpha</math></i>	Elongation factor-1 $\alpha$
<i>ein2</i>	<i>ethylene insensitive 2</i>
ET	Ethylene
ETI	Effector-triggered immunity
ETS	Effector-triggered susceptibility
flg22	22 amino acid domain in bacterial flagellin
FLS2	Flagellin insensitive 2
GPI	Glycophosphatidylinositol
<i>grp7</i>	<i>glycine-rich RNA-binding protein 7</i>
GST	Glutathione S-transferase
HR	Hypersensitive response
<i>hrc</i>	<i>HR and conserved</i>
<i>hrp</i>	<i>HR and pathogenicity</i>
HSP	Heat shock protein
IPG	Immobilized pH gradient
JA	Jasmonic acid
LC-MS/MS	Liquid chromatography Tandem Mass Spectrometry
MALDI-TOF/MS	Matrix-assisted laser desorption ionization-time of flight/mass spectrometry
MAPK	Mitogen-activated protein kinase
MEK	Mitogen-activated protein kinase kinase (also known as MKK)
<i>Mla</i>	<i>Mildew-resistance locus A</i>
<i>MLO</i>	<i>Mildew-resistance locus O</i>
<i>MMP2</i>	Matrix metalloprotease involved in cytoskeletal re-organisation
MP2C	Alfalfa PP2C regulating MAPK signaling
NADPH	Nicotinamide adenine dinucleotide phosphatase hydrogen
<i>nahG</i>	<i>salicylate hydroxylase</i>
NB-LRR	Nucleotide binding leucine-rich repeat
<i>NDR1</i>	<i>Non-race-specific disease resistance 1</i>
NLS	Nuclear localization signal
<i>NPRI</i>	<i>Nonexpressor of PR-1</i>

<i>OPDA</i>	<i>Oxo-phytodienoic acid</i>
ORF	Open reading frame
<i>PAD4</i>	<i>Phytoalexin-deficient 4</i>
PAL	Phenylalanine ammonia lyase
PAMP	Pathogen-associated molecular patterns
PCD	Programmed cell death
<i>PDF1.2</i>	<i>Plant defensin 1.2</i>
<i>PEN1</i>	<i>PENETRATION MUTANT 1</i>
PIA1	PP2C induced by avrRpm1
PMF	Peptide mass fingerprinting
PP2C	Protein phosphatase-2C
PR	Pathogenesis-related
<i>Prf</i>	<i>Pseudomonas resistance and fenthion sensitivity</i>
ProMoST	Protein Modification Screening Tool
PRR	Pattern recognition receptor
PrxIII	Peroxiredoxin III
PSII-P	Photosystem II
PTI	PAMP-triggered immunity
RAP2.6	Related to AP2 - 6
RAR1	Required for Mla12 resistance
Rcr3	Required for <i>Cladosporium fulvum</i> resistance 3
RIN4	RPM1-interacting protein 4
<i>RIPK</i>	<i>RPM1</i> -induced protein kinase
RLK	Receptor like kinase
RLP	Receptor like protein
RNA BP	RNA binding protein
ROR2	Required for <i>mlo</i> -specific resistance 2
ROS	Reactive oxygen species
<i>rpm1</i>	An allele of <i>RPM1</i> with a stop codon at amino acid 87
R.T.	Room temperature
RT-PCR	Reverse transcriptase polymerase chain reaction
Rubisco	Ribulose-1,5-biphosphate carboxylase/oxygenase
SA	Salicylic acid
SAG	Salicylic acid glycoside
SAR	Systemic acquired resistance
SDS-PAGE	Sodium dodecyl sulfate polyacrylamide gel electrophoresis
<i>SGT1</i>	Suppressor of G-two allele of <i>skp1</i>
SH2	Src homology 2 domain
Src	Proto-oncogenic tyrosine kinase
SUMO	Small ubiquitin-related modifier
TAIR	The arabidopsis information resource
TAO1	Target of avrB operation 1
T-DNA	Transferred DNA of the tumor-inducing (Ti) plasmid
TIR	Toll-interleukin-1 receptor motif
<i>TonB</i>	A gene encoding product of unknown function predicted to localize to the chloroplast
TM	Transmembrane
TMV	Tobacco Mosaic Virus
TTSS	Type Three Secretion System
Upa20	Upregulated by AvrBs3-20
<i>VSP2</i>	<i>Vegetable storage protein 2</i>

## I. Introduction

Plants, unlike animals, lack mobile cells and adaptive immune system. They rely on the innate immune system that provides immediate defenses against infection by other organisms (Ausubel, 2005; Nürnberger et al., 2004; Sanabria et al., 2008). The innate immune system is thought to constitute an evolutionary older defense strategy and is a dominant immune system in plants, fungi, insects and primitive multi-cellular organisms (Charles et al., 2001). In contrast to the more evolved adaptive immune system, innate immunity does not provide a long-lasting protective immunity against subsequent attack by a specific pathogen (Bruce et al., 2002; Nürnberger et al., 2004). The innate immune system is composed of cells and mechanisms that defend the host in a non-specific manner, which means that it recognizes and responds to all pathogens in a generic way (Bruce et al., 2002). The adaptive immune system composed of B and T cells, is able to recognize and remember specific pathogen. In animals, specialized cell types like macrophages, neutrophils, and dendritic cells are the main components of immune systems, while in plants each single cell is autonomously capable of sensing and mounting defense against pathogens (Bruce et al., 2002; Nürnberger et al., 2004).

Plant innate immunity consists of two different immune systems, the pathogen-associated molecular pattern (PAMP)-triggered immunity (PTI) that uses pattern recognition receptors (PRRs) and the effector-triggered immunity (ETI) that relies on so-called NB-LRR proteins with nucleotide-binding and leucine-rich repeat domains (Chisholm et al., 2006; Jones and Dangl, 2006). These two types of plant immunity represent evolution of the plant immune system in order to defend themselves against the evolving pathogens. Co-evolution of plant-pathogen is best described by the four phased “zigzag model” from Jones and Dangl (2006) (Fig. 1). In this model, phase 1 is represented by PTI, where PRRs recognize the PAMPs and mount defense mechanisms to halt further colonization by pathogen. In phase 2, pathogens deploy effector(s) to disturb PTI and render plants susceptible; this results in the effector-triggered susceptibility (ETS). In phase 3, the susceptible plants evolve NB-LRR proteins to recognize a specific effector and trigger the ETI. In phase 4, pathogens escape the ETI by diversifying the recognized effectors or acquiring additional effectors that suppress the existing ETI, resulting again in ETS. Subsequently, plants evolve new NB-LRR proteins to recognize the new effectors and thereby again achieve ETI (Jones and Dangl, 2006). Presumably, such alternating phases of ETS and ETI can repeat itself during the “arms-race” co-evolution of plants and pathogens.

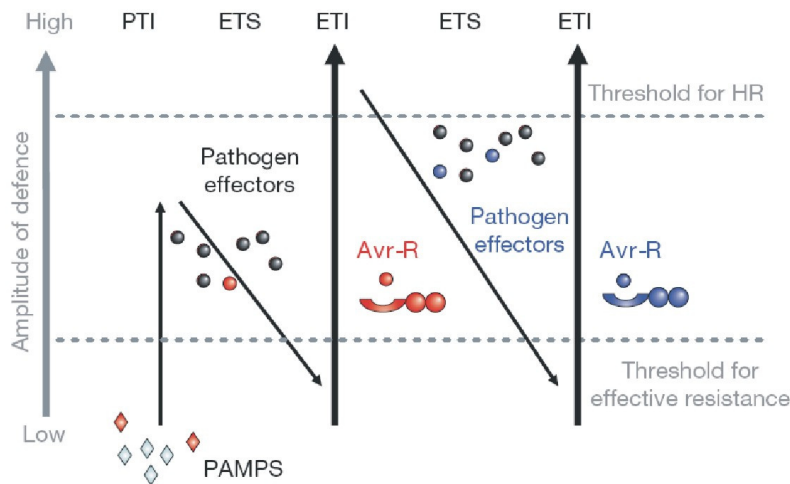


**Fig. 1** Zigzag model from Jones and Dangl (2006)

### 1. Pathogen Associated Molecular Pattern-Triggered Immunity (PTI)

PAMP is the term initially used in the animal immune system to refer to the pathogen-derived molecules, which bind to the PRR and trigger the expression of immune response genes and the production of antimicrobial compounds (Ausubel, 2005; Nürnberger et al., 2004). PAMPs are essential for the pathogen lifestyle, structurally conserved in the microbe and are normally not present in the host (Nürnberger et al., 2004). Many PAMPs in the animal system can also act as general elicitors for defense responses in plants; this finding provides the evidence that plants and animals share similarities in the activation of their innate immune systems. PAMPs that are known to induce defense responses in plants are multiple cell-surface components of gram-negative bacteria including lipopolysaccharide, a major constituent of the outer membrane; and flagellin, the protein subunit from the flagellum. Major constituents of the cell wall of higher fungi, like chitin and ergosterol, can also act as PAMPs (Nürnberger et al., 2004). PAMP recognition is often mediated through receptors with an extracellular LRR domain. In plants, these receptors are exclusively localized in the plasma membrane, while in animal system they may also be localized intracellularly (Nürnberger et al., 2004).

A well-studied model system for PTI is the activation of defense responses by flagellin, a protein subunit of bacterial flagella. Flg22, a 22 amino acid domain that is conserved at the N-terminal fragment of flagellin, can induce defense responses in many plants, including *Arabidopsis* and tomato (Felix et al., 1999). In *Arabidopsis*, flg22 is recognized by FLS2, a receptor like kinase (RLK) consisting of an extracellular LRR and an intracellular serine/threonine kinase domain (Asai et al., 2002; Gomez-Gomez and Boller, 2000). Flg22 induces the production of reactive oxygen species (ROS), activation of mitogen-

activated protein (MAP) kinases and induction of defense-genes (Asai et al., 2002; Felix et al., 1999). Zipfel et al. (2004) showed the role of flagellin perception for disease resistance in *Arabidopsis*. Pretreatment of wild type *Arabidopsis* with flg22 one day before challenge with pathogenic *Pseudomonas syringae* pv. *tomato* DC3000 (*Pto* DC3000) reduced bacterial growth compared to the *fls2* mutant that received the same pretreatment, indicating that induced disease resistance required FLS2 perception of flg22 (Zipfel et al., 2004). Subsequently, the authors found that the *fls2* mutant showed faster and more severe disease symptoms compared to wild type *Arabidopsis* only after spray inoculation with *Pto* DC3000 suggesting that flg22 perception probably restricts early steps of bacterial invasion (Zipfel et al., 2004).

PTI serves as a basal and broader defense against an entire group of microorganisms, which remains operative in susceptible and resistant plants (Jones and Dangl, 2006). It does not prohibit pathogen colonization but limits the extent of its spread (Nürnberger et al., 2004). This basal or general defense is also important for the activation of non-host resistance, a term used when all members of a plant species exhibit resistance to all members of a given pathogen species (Thordal-Christensen, 2003). Non-host resistance is an evolutionary ancient, multilayered resistance mechanism consisting of constitutive and inducible components (Thordal-Christensen, 2003). Constitutive or preformed barriers present on the plant surface consist of wax layers, rigid cell wall, antimicrobial enzymes or secondary metabolites; all of them prevent the ingress of pathogens (Nürnberger et al., 2004). When pathogens are able to defeat the preformed barrier, they still have to encounter the extracellular PRR, which upon recognition of PAMPs will trigger PTI (Nürnberger et al., 2004).

## **2. Effector-Triggered Immunity (ETI)**

Individual phytopathogenic races or strains of a given pathogen species can overcome PTI by acquisition of virulence factors (effectors), thus making plants susceptible to pathogen colonization. Co-evolution of individual cultivars of the otherwise susceptible plant species results in the evolution of resistance proteins that specifically recognize the pathogen race-specific factors and allow the plant to resist this particular pathogen strain/race by activation of ETI (Jones and Dangl, 2006; Nürnberger et al., 2004). This type of resistance is known as host resistance (cultivar specific resistance), and it conforms to Flor's "Gene-for-Gene" hypothesis (see Section 2.3), which is genetically determined by complementary pairs of pathogen-encoded avirulence (*Avr*) genes and plant resistance (*R*) genes. When either of the

two components is absent, infection can occur (Nürnberg et al., 2004; Van der Biezen and Jones, 1998).

The defense responses initiated in PTI and ETI are surprisingly similar. Like PTI, ETI is often associated with rapid calcium and ion fluxes, an extracellular oxidative burst, induction of defense-genes, callose apposition for cell wall reinforcement and, additionally, localized programmed cell death (PCD) that presumably halts growth of biotrophs – referred to as hypersensitive response (HR) (Belkadir et al., 2004). The HR is, however, not always present in ETI. The *Arabidopsis dnd* (*defense no death*) mutant still mounts effective disease resistance against *P. syringae* pv. *glycinea* without producing HR (Clough et al., 2000). On the other hand, there are cases of HR-like cell death triggered by PAMPs, such as the *Phytophthora*-derived oligopeptide elicitor, pep13, in potato (Halim et al., 2004). Even though PTI overlaps significantly with ETI, it is temporally slower and of lower amplitude. Thus, ETI apparently accelerates and amplifies PTI that constitutes the basal defense response (Belkadir et al., 2004). Navarro et al. (2004) found that approximately 45% of the flagellin-activated genes were also induced three hours post inoculation in the ETI. This suggests that effector proteins might trigger a common gene subset very early after race-specific recognition and therefore enhance the PAMP-mediated defense response.

## 2.1. Effector proteins

Most pathogenic microbes are able to produce effectors to promote pathogenicity by suppressing plant defense responses. Gram negative bacteria gain entry into intercellular space (apoplast) of plants *via* wounds or stomata, and subsequently deliver their effectors into the plant cytoplasm using Type Three Secretion System (TTSS) (Grant et al., 2006). Compared to those from fungi, oomycetes and viruses, bacterial effectors are better characterized and are more extensively described in section 2.1.1 - 2.1.3 below.

Haustoria, specialized infection structures, are used by fungi and oomycetes to deliver effectors into the apoplast of plants (Chisholm et al., 2006; Schulze-Lefert and Panstruga, 2003). Little is known about the intracellular delivery mechanisms of fungal/oomycete pathogens. Recent studies reveal a highly conserved amino acid motif RXLR-EER in different oomycetes effectors. The RXLR motif is similar to a host targeting signal required for translocation of malarial proteins into host cells in *Plasmodium* species, suggesting that it is required for translocating secreted oomycete proteins from the apoplast into plant cells (Rehmany et al., 2005). The *Phytophthora infestans* RXLR-EER-containing protein Avr3a is able to trigger hypersensitive cell death after recognition within plant cells that contain the

corresponding R3a resistance protein. However, replacement of the RXLR-EER motif in Avr3a results in failure to induce HR, demonstrating that this motif is required for translocation (Whisson et al., 2007).

Most effectors promote their pathogenicity by suppressing components of PTI, ETI and non-host resistance in plants (Nomura et al., 2005). The *Cladosporium fulvum* Avr2 effector is a cysteine-rich protein that binds and inhibits the secreted tomato cysteine protease Rcr3, which possibly has antimicrobial activity. In resistant plants, this inhibition induces a conformational change in Rcr3 that triggers the Cf-2 protein to activate HR (Rooney et al., 2005). Another effector from *C. fulvum*, Avr4, contains a chitin-binding domain that binds chitin from fungal cell walls; thus preventing its degradation by plant chitinases to release PAMPs for triggering defense responses (van den Burg et al., 2003). Viral effectors that suppress plant defense mechanisms are poorly described but since one main anti-viral mechanism is RNA silencing, many viral effectors will likely suppress the host RNA silencing response (Chisholm et al., 2006).

### **2.1.1. Type Three Secretion System**

Gram negative bacteria deliver effectors into the host cells *via* TTSSs. The TTSS components are encoded by *hrp* (HR and pathogenicity) and *hrc* (HR and conserved) genes (Alfano and Collmer, 2004). Together with harpins, helper proteins and specific transcriptional regulatory proteins, they are encoded in *hrp* gene clusters; these are often flanked by mobile transposon elements and this has been suggested to facilitate transfer of virulence to pathogen strains through exchange of these so-called pathogenicity islands (Grant et al., 2006).

To transport bacterial effector proteins, the TTSS has assembled extracellular needle/pilus-like appendages, called the Hrp pilus. The Hrp pilus acts as a tunnel that links the type III “secretion” embedded in the bacterial cell wall and the type III “translocon” in the host plasma membrane. The secretion allows the exit of effector proteins across the bacterial cell wall, while the translocon allows the translocation of effectors into the host cell (Büttner and Bonas, 2003; Lee et al., 2005). Specialized chaperone proteins often guide incompletely folded type III effector proteins to the cytoplasmic face of the apparatus for ATP-dependent unfolding and entry into the TTSS (Grant et al., 2006).

### 2.1.2. Strategies used by bacterial pathogens to suppress plant defense

Plant pathogens such as *Pto* DC3000 can secrete approximately 30 effector proteins into the host cells (Chang et al., 2005). Collectively, these effectors manipulate the host cells to promote their growth and dissemination. Each effector has its specific function and acts on specific target(s) in the host cells. In the following sections, some of the known effector functions in suppression of plant defense responses are described.

#### a. Suppressors of cell wall-based defense

Plants can mount active cell wall-based defense that limit the ability of bacterial and fungal pathogens to establish infectious growth. This cell wall-based defense is manifested as papillae formation at the penetration site, which consists of callose, cross-linked phenolics and hydroxyproline-rich glycoprotein deposits. Papillae are thought to form a strong reinforcement of the cell wall to limit pathogen infection (Abramovitch and Martin, 2004). The suppression of cell wall-based defense by effectors was discovered from the observation that papillae were formed during infection with TTSS mutants, but not with wild-type phytopathogenic bacteria, suggesting that certain effectors secreted by the TTSS actively suppress papillae formation (Mudgett, 2005).

Hauck et al. (2003) found out that extensins, hydroxyproline-rich proteins and germin-like protein, which are known as components of papillae, were repressed by the TTSS in SA-independent manner. In further studies, the authors showed that a *hrcC* mutant can induce a large number of highly localized callose deposits in leaves of wild-type *Arabidopsis*. This observation was severely compromised when AvrPto-expressing *Arabidopsis* were treated with the *hrcC* mutant. Moreover, the expression of AvrPto was sufficient to allow substantial multiplication of the *hrcC* mutant in the transgenic plants. Taken together, these results suggest that AvrPto is suppressor of cell wall-based defense. Since the *hrcC* mutant grew at the same level in *nahG* plants, which are defective in SA-mediated pathways, compared to wild type, the AvrPto suppression is considered to be SA-independent (Hauck et al., 2003).

Two other effectors from *Pto* DC3000 also suppress callose deposition. AvrE and HopPtoM are effectors encoded by the conserved effector locus (CEL), a gene cluster that is widely conserved among diverse *P. syringae* pathovars. The  $\Delta$ CEL mutant was able to activate callose deposition in wild-type *Arabidopsis*, but failed to elicit high levels of callose-associated defense in *nahG* plants. The  $\Delta$ CEL mutant also multiplied more aggressively in SA-deficient plants than in wild-type plants. Complementation of AvrE and HopPtoM could restore the ability of  $\Delta$ CEL mutant to cause disease, leading to conclusion that AvrE and HopPtoM are suppressors of SA-dependent cell wall-based defense (DebRoy et al., 2004).

AvrRpt2 from *Pto* strain 1065 and AvrRpm1 from *P. syringae* pv. *maculicola* strain M2 (*Pma* M2) are two effectors that inhibit defense responses induced by flg22, including callose deposition. Besides suppression on callose deposition, AvrRpt2 also inhibited activation of *GST6* transcription and blocked accumulation of *PR-1*, both components of PAMP-induced resistance. The ability to inhibit components of PAMP-induced basal defense is, however, not a general characteristic for all effectors, since AvrRpm1 only inhibited *GST6* transcription, but not accumulation of *PR-1*; and AvrPphE did not inhibit callose deposition (Kim et al., 2005).

b. Suppressors of programmed cell death (PCD).

A programmed cell death localized to infection sites (HR) is an important mechanism of plant defense to halt pathogen growth and is therefore a target of some effectors. AvrPtoB is an effector from *Pto* DC3000, which is also widely conserved among diverse genera of plant pathogens, including *Xanthomonas* spp., *Erwinia* spp. and many strains of *P. syringae*. Both AvrPtoB and AvrPto interact with the tomato Pto serine/threonine kinase, and subsequently activate a Prf-dependent disease resistance. Co-expression of AvrPto and Pto in *Nicotiana benthamiana* allows the activation of HR, indicating that the Pto-mediated defense pathway is present in *N. benthamiana*. Nevertheless, HR activation was not observed when AvrPtoB and Pto were co-expressed in *N. benthamiana*. In fact, the AvrPto/Pto dependent cell death was suppressed when AvrPtoB was also co-expressed in *N. benthamiana*, thus suggesting that AvrPtoB might act as suppressor of the Pto defense pathway in *N. benthamiana*, but not in tomato. The expression of AvrPtoB in *N. benthamiana* is sufficient to block the HR triggered by a constitutively activated mutant Pto kinase; and also inhibits HR triggered by interaction between tomato Cf-9 resistance protein and *C. fulvum* Avr-9 peptide elicitor in *N. benthamiana*. These results support the idea that AvrPtoB functions downstream of disease resistance proteins to suppress the HR. AvrPtoB also protects plants from HR-like PCD induced by Bax, a proapoptotic protein in the *Bcl-2* family that initiates PCD in animal cells. In yeast, AvrPtoB protects the cell from stress-induced PCD mediated by hydrogen peroxide, menadione and heat shock. This broad activity of AvrPtoB in inhibiting cell death suggests that AvrPtoB acts as a general cell death inhibitor (Abramovitch et al., 2003).

Cell death suppression has also been demonstrated for several other effectors. AvrPphC blocks the HR triggered by AvrPphF in the Canadian Wonder bean cultivar, while AvrPphF blocks the HR caused by unknown *Pph* effector in Tendergreen bean cultivar. AvrPtoB, AvrPphE<sub>Pto</sub>, AvrPpiB1<sub>Pto</sub>, HopPtoE or HopPtoF suppress HopPsyA-dependent HR in tobacco (Abramovitch and Martin, 2004; Mudgett, 2005).

Some effector proteins do not directly suppress the HR, rather they interfere with recognition events, which is important to trigger the HR. This is exemplified by AvrRpt2 interference with the HR triggered by AvrRpm1. Interaction between AvrRpm1 and its cognate resistance protein, RPM1, results in a visible HR at five hours post inoculation. In contrast, interaction between AvrRpt2 and RPS2 results in weaker HR at ~20 hours post inoculation. When both of the *avr* genes were expressed together, the HR triggered on either accession was indicative only of the slower AvrRpt2-RPS2 interaction, suggesting that expression of *AvrRpt2* interferes with the AvrRpm1-RPM1 interaction (Ritter and Dangl, 1996). Recent studies have elucidated the mechanism of AvrRpt2 interference with AvrRpm1-mediated HR. AvrRpt2 is a cysteine protease that cleaves RIN4, a protein required by AvrRpm1 to activate the RPM1-dependent HR. Elimination of RIN4 by AvrRpt2 prevents AvrRpm1 from activating RPM1-mediated HR (Axtell and Staskawicz, 2003; Mackey et al., 2002).

c. Activators of plant transcription

Members of the AvrBs3 effectors family from *Xanthomonas* spp. like AvrBs3, PthA, AvrXa7, Avrb6 and AvrXa10 are assumed to function in the plant nucleus to alter transcription during infection as a mean to down-regulate host defense. Effectors from the AvrBs3 family possess a distinct phenotype: a C-terminal nuclear localization signal (NLS), an acidic transcriptional activation domain (AAD) and a central repeat region, all of which are essential for the effector activity (Chisholm et al., 2006; Mudgett, 2005). Removal of the C-terminal 38 codons containing the putative AAD, but retaining the NLS sequence, from AvrXa10 of *X. oryzae* pv. *oryzae*, was concomitant with the loss of avirulence activity. Likewise, mutations in NLS sequences of AvrXa10 caused a loss in avirulence activity. The ability to modulate plant transcription by AvrBs3 effectors was proven by activation of transcription in yeast and *Arabidopsis* when AvrXa10 was fused to the coding sequence of the Gal4 DNA binding domain (Zhu et al., 1998).

AvrBs3 from *X. campestris* pv. *vesicatoria* (*Xcv*) elicits hypertrophy of mesophyll cells in susceptible host, but upon recognition of the pepper *Bs3* *R* gene induces disease resistance. Recent studies by Römer et al. (2007) demonstrated that the recognition specificity resides in the promoter of *Bs3*. When the *Bs3* promoter was fused to the *Bs3-E* (*Bs3* functional allele with distinct recognition specificities from the tomato cultivar Early California Wonder) coding sequence, it mediated exclusively *AvrBs3* recognition. Whereas *Bs3-E* promoter fused to the *Bs3* coding sequence mediate exclusively recognition of *avrBs3Δrep16* (*AvrBs3* mutant lacking repeat units 11 to 14). Thus the promoter and not the

coding sequence determine recognition specificity of the *Bs3* alleles (Römer et al., 2007). Subsequent analysis of host genes that are up-regulated by AvrBs3 in a compatible *Xcv*-pepper interaction identified *Upa20* as a regulator of cell enlargement that stimulates cell growth. *Upa20* encodes a transcription factor and it was shown that AvrBs3 binds to the *Upa20* promoter. AvrBs3 derivatives consisting of only the repeat region bound to *Upa20* promoter less efficiently than the wild-type protein; in contrast, AvrBs3 lacking the repeat region did not bind to *Upa20* promoter. These results show that AvrBs3 binds to a conserved element in the *Upa20* promoter *via* its central repeat region and induces gene expression through its activation domain, suggesting that AvrBs3 induces reprogramming of host cell by mimicking a transcription factor (Kay et al., 2007).

d. Activators of the JA pathway

Three signaling molecules are known to regulate plant defense responses. SA-dependent signaling is critical in establishing local and systemic resistance, primarily against biotrophic pathogens. JA-dependent signaling is induced in response to mechanical wounding, herbivore predation and attack by necrotrophic pathogens. ET-dependent signaling is important for the plant's response to necrotrophic pathogens, mechanical wounding and wounding induced by herbivores. These pathways do not function exclusively, but influence one another, for example the SA- and JA-dependent signalings are mutually antagonistic in some species. This fact has been exploited by bacterial pathogens to overcome SA-dependent signaling defense responses (Kunkel and Brooks, 2002). Some of the *P. syringae* strains produce the phytotoxin coronatine (COR), which was shown to contribute to virulence in *Pto* DC3000 by promoting bacterial growth and chlorosis in plants. Coronatine shares structural similarity with JA and methyl-JA (MeJA). A JA-insensitive mutant (*jai1*) of tomato was shown to be unresponsive to COR and highly resistant to *Pto* DC3000; and treatment of wild-type plants with exogenous MeJA complemented the virulence defect of a bacterial mutant deficient in COR production. All the evidences lead to the conclusion that COR promotes bacterial virulence by activating the host's JA signaling pathway (Zhao et al., 2003).

Coronatine also suppresses plants innate immunity by inhibiting stomatal closure. When *Arabidopsis* leaves were treated with *Pto* DC3000, within the first two hours there was a reduction in the number of open stomata, but the stomata were re-opened after three hours incubation. This stomatal closure was shown to be induced by PAMPs, such as flagellin and lipopolysaccharide. The ability of re-opening stomatal closure was severely compromised in the COR-deficient *Pto* DC3000 mutant. This implies that coronatine suppresses the PAMP-

triggered stomatal defense that is important to prevent bacterial entry into the plant (Melotto et al., 2006).

Suppression of plant defense by activating the JA-dependent pathway is not only achieved by production of coronatine. He et al (2004) screened bacterial effectors that are able to induce the JA-dependent signaling pathway. *RAP2.6* is an *Arabidopsis* ethylene response factor (*ERF*) family transcription factor that is strongly induced by virulent *P. syringae* strains. Both of TTSS and COR are required for *RAP2.6* induction, suggesting that *RAP2.6* induction depends on JA signaling. A highly sensitive *RAP2.6* promoter-firefly luciferase (*RAP2.6-LUC*) reporter line was developed to monitor activities of various bacterial virulence genes in *RAP2.6* induction. The authors identified five effectors that contribute to *RAP2.6* induction: AvrB, AvrRpt2, AvrPphB, HopPtoK, and AvrPphE<sub>Pto</sub> (He et al., 2004).

### 2.1.3. Enzyme activities of effectors to promote bacterial virulence

Bacterial and fungal effectors have been shown to possess enzyme activities for modifying host protein for pathogen benefits. Some of those are detailed below.

#### a. Ubiquitin ligase activity

An acidic C-terminal domain of AvrPtoB shows remarkable homology to the RING-finger and U-box families of proteins involved in ubiquitin ligase complexes in eukaryotes. AvrPtoB was later demonstrated to possess ubiquitin ligase activity *in vitro*. Mutation of key residues eliminated the ubiquitin ligase activity of AvrPtoB *in vitro* and abrogated AvrPtoB anti-PCD and virulence activities in tomato. These results suggest that AvrPtoB functions as an E3 ligase in infected cells and transfers ubiquitin or ubiquitin like molecules to cellular proteins involved in the regulation of PCD (Janjusevic et al., 2006).

#### b. Cysteine protease activity

Cysteine protease activity has been shown for several effector proteins. XopD, AvrXv4 and AvrBsT from *Xanthomonas campestris* are cysteine proteases that disrupt protein sumoylation *in planta*. Numerous SUMO-protein conjugates in host plants are presumably targeted by pathogens to disrupt many cellular events, since SUMO controls many diverse cellular processes including nuclear transport, enzyme activities, transcription and the cell cycle (Chisholm et al., 2006; Mudgett, 2005). Shao and colleague (2003) showed that AvrPphB from *P. syringae* cleaves PBS1, a protein kinase, which is required for the AvrPphB/RPS5-mediated resistance, and this protease activity is necessary for the induction of HR (Shao et al., 2003). The *P. syringae* effector AvrRpt2 is also a cysteine protease, of

which its activity is required for the elimination of RIN4, a protein with role(s) as a basal defense regulator (Axtell et al., 2003).

c. Phosphatase activity

The C-terminus of HopPtoD2 from *Pto* exhibits a predicted protein fold conserved in many protein tyrosine phosphatases (PTP). Biochemical analysis confirms that the PTP domain encodes a tyrosine phosphatase and is able to hydrolyze a PTP substrate. HopPtoD2 phosphatase activity is required for optimal pathogen growth in a susceptible host; it also suppresses the HR induced in *N. benthamiana* by ectopic expression of *NtMEK2<sup>DD</sup>*, a constitutively active MAPK kinase involved in plant defense signaling. In summary, HopPtoD2 prevents plant from mounting a defense response and probably dephosphorylates a substrate downstream of *NtMEK2* in the MAPK pathway (Mudgett, 2005).

## 2.2. Resistance Proteins

### 2.2.1. Different classes of resistance proteins

Resistance proteins, as the name suggests, are required for conferring resistance to specific pathogen strains and can be grouped in different classes (Fig. 2). The largest class is a protein family containing a nucleotide binding (NB) site and leucine-rich repeat (LRR) domains, shortened as NB-LRR proteins. The NB-LRR class can be further divided into two classes based on the N-terminal domains - either an N-terminal coiled-coil (CC) sequence or a Toll-interleukin-1 receptor (TIR) sequence. R proteins belonging to the CC NB-LRR class are RPM1, RPS2 and RPS5 that confer resistance to the bacterial effectors AvrRpm1/AvrB, AvrRpt2 and AvrPphB from *P.syringae*, respectively. TIR NB-LRR class is represented by RPW8 that confers resistance to *Erisyphé chichoracearum*, RPP2/4/5/10/14 that confer resistance to *Hyaloperonospora parasitica* and RPS4 that confer resistance to AvrRps4 from *Pto* (Chisholm et al., 2006; Glazebrook, 2001; Martin et al., 2003).

A second major class of R proteins contains an extracellular LRR protein (eLRR). Based on their domain structure, this class can be divided into three subclasses: RLP, RLK and PGIP. The RLP class (receptor-like protein) comprises R proteins that contain eLRR and transmembrane (TM) domain. The best characterized RLPs are the Cf proteins from tomato that interact with Avr proteins from *C. fulvum*. RLKs (receptor-like kinase) contain eLRR, TM domain and cytoplasmic kinase. While RLKs are typically described as receptors of PAMPS (eg. FLS2 for flg22, (Gomez-Gomez and Boller, 2000)), certain R proteins also have such protein structure. For instance, the rice Xa21 RLK that confers resistance to *X. oryzae* pv. *oryzae* (Shen and Ronald, 2002). The PGIP (polygalacturonase-inhibiting protein) class

has homology to the amino terminus of PGIPs, which are ubiquitous plant cell wall proteins that are directed against fungal polygalacturonase (Chisholm et al., 2006; Fritz-Laylin et al., 2005).

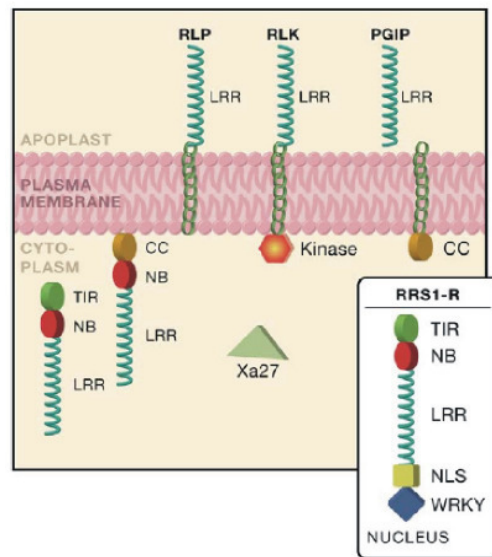


**Fig. 2** Different classes of resistance proteins (Chisholm et al., 2006).

The majority of characterized R proteins can be grouped to the above classes, but there are also examples of R proteins with novel structural motifs distinct from already mentioned structures. The tomato Pto that induces resistance against AvrPto from *Pto* does not contain any LRR or transmembrane spanning domain, but has a serine/threonine kinase catalytic region and a myristoylation motif at its N terminus (Loh et al., 1998; Martin et al., 1993). RRS1-R that confers resistance against *Ralstonia solanaceum* is a TIR-NB-LRR protein that also contains a carboxy-terminal nuclear localization signal and WRKY transcriptional activation domain (Deslandes et al., 2003). The most recent addition to this list includes the *Bs3* gene, which encodes a flavin monooxygenase (Römer et al., 2007), where resistance specificity resides in the promoter of the gene rather than the encoded protein.

### 2.2.2. Functional domains of resistance protein

#### a. LRR domain

The repetitive segment within the LRR motif is typically 20 – 30 amino acids long and contains a conserved consensus sequence LxxLxxLxLxxNxLt/sgxIpxxLG (Jones and Jones, 1997). LRR domains are present in many proteins of diverse function, ranging from viruses to eukaryotes, and appear to be involved in protein-protein interaction. Most variation between resistance genes and their closely related homologies occurs within the LRR, suggesting the role of LRR as a determinant of recognition specificity (Dodds et al., 2001; Martin et al.,

2003). The evidence that LRRs determine recognition specificity comes from the study of flax resistance proteins. The *L* locus in flax contains a single gene of the TIR-NB-LRR class and 11 alleles with different specificities of resistance to rust fungus isolates. The L6 and L11 proteins recognize distinct avirulence products from the fungus, yet they differ only in the LRR domain. When chimeric genes encoding the L2 LRR domain were fused to the L6 or L10 TIR-NB domain, the L2 specificity was expressed. Similarly, the flax P and P2 proteins differ in only ten amino acids but show different resistance specificities. By introducing six amino acid differences in the xxLxLxx motif of the P protein into the P2 protein, resistance specificity identical to P protein was observed (Dodds et al., 2001; Ellis et al., 1999).

b. NB domain

The NB domain has been found in several protein families, including ATPases and G proteins, thus the NB domain may affect R protein function through nucleotide binding or hydrolysis (Chisholm et al., 2006; Martin et al., 2003). NB domains share sequence similarities with the NB domains of apoptosis regulators such as *CED4* from *Caenorhabditis elegans* and *Apaf-1* from human, suggesting that R proteins may control plant cell death via the NB domain (Chisholm et al., 2006; Martin et al., 2003).

c. CC motif

The CC motif is present in many proteins involved in diverse biological processes. Like LRR, it has been implicated in protein-protein interaction, including oligomerization. There is no clear answer regarding the function of CC motifs in R proteins, but the distinct requirements on downstream signaling components between CC-NB-LRR proteins and TIR-NB-LRR proteins suggest that this domain may be involved in signaling rather than recognition (Martin et al., 2003).

d. TIR motif

TIR domains are implicated in several functions. They may function in signaling by the requirement on distinct downstream signaling components, like the CC motif (Martin et al., 2003). They also contribute to the proper function of R proteins as has been shown by Dinesh-Kumar et al. (2000). The *N*-gene from tobacco confers resistance against Tobacco Mosaic Virus (TMV). Deletion analysis in the TIR domain of *N* produces loss-of-function *N* alleles, while amino acid substitutions in this domain lead to a partial loss-of-function phenotype (Dinesh-Kumar et al., 2000). The L6 and L7 proteins from flax differ only in the TIR domain; and when this region was exchanged between the two proteins, the pathogen specificities were also altered. This leads to the assumption that TIR domains also play a role in pathogen recognition (Ellis et al., 1999).

### 2.3. “Gene-for-Gene” interaction

The “Gene-for-Gene” hypothesis was introduced by Flor (1971) to describe a specific interaction between pathogen *Avr* (avirulence) gene and the corresponding plant disease resistance (*R*) gene. When the corresponding *R* and *Avr* genes are present in both host and pathogen, it results in disease resistance. In the absence of one of the components, disease results (Flor, 1971). This is, in essence, the ETI described above. So far, there are two models for *Avr* and *R* protein recognition, one involves a direct interaction between them, and the other involves *R*-protein complexes where *Avr* and *R* proteins indirectly interact.

#### 2.3.1. Direct “Gene-for-gene” interaction

The interaction between the flax *L* locus and the corresponding *AvrL* genes provides evidence for a direct *Avr-R* gene interaction. Using a yeast two-hybrid assay, Dodds et al. (2006) demonstrated a physical interaction between specific variants of *AvrL* proteins with their cognate *L* proteins (Dodds et al., 2006). Direct interaction was also shown by *Pi-ta* from rice and *Avr-Pita* from *Magnaporthe grisea*. *Avr-Pita* binds specifically to the LRR domain of the *Pi-ta* protein, both in the yeast two-hybrid system and in an *in vitro* binding assay. Single amino acid substitution in the *Pi-ta* LRR domain or in the *Avr-Pita* 176 sequences that results in loss of resistance in the plant also disrupt the physical interaction, both in yeast and *in vitro* (Jia et al., 2000). *Pop2* from *Ralstonia solanacearum* binds directly to the *RRS1-R* protein from *Arabidopsis thaliana* in the yeast two hybrid systems. In contrast to the *Pi-ta* protein, the interaction requires the full length *R* protein (Deslandes et al., 2003).

It is suggested that the direct interaction leads to a relatively rapid evolution of new virulence phenotype. Pathogen effectors that are recognized through direct interaction may overcome resistance through sequence diversification, and *R* proteins also undergo similar diversification to overcome successful pathogens. This can be observed by genetic diversity in *avrL* and *L* locus, which is consistent with a co-evolutionary arms race between these corresponding *Avr* and *R* genes (Dodds et al., 2006).

#### 2.3.2. Indirect “Gene-for-Gene” interaction/Guard hypothesis

Besides the direct *Avr-R* recognition cited above, there are not much data supporting a direct interaction for others *Avr-R* proteins. One of the possible explanations is that instead of interacting directly, *R* proteins recognize the avirulence proteins through their action on the host target. This assumption is based on the observation that many avirulence proteins are actually required for pathogen virulence in susceptible hosts lacking the cognate *R* gene.

Hence, R proteins appear not to evolve to recognize Avr proteins directly, but rather to recognize the action of virulence factor as they modify host targets. This is referred to as “Guard Hypothesis”, which postulates that R proteins guard the host target (“guardee”) of avirulence protein and upon detection of “guardee” modification, defense is activated (Belkhadir et al., 2004).

The guard hypothesis entails some consequences. R proteins are likely to be part of a multiprotein complex, in which they constitutively bind to the host target, and then dissociate after modification of the complex by type III effectors, or form a new interaction with a cellular target that leads to activation. In this way R proteins are subjected to negative regulation/stabilization and only are activated upon effectors’ action (Belkhadir et al., 2004). A well-studied model supporting the Guard hypothesis is RIN4, a protein of unknown function, which is required for RPM1- and RPS2-mediated disease resistance (Mackey et al., 2003; Mackey et al., 2002). RIN4 interacts physically with either RPM1 or RPS2 *in vivo* (Mackey et al., 2003; Mackey et al., 2002). It is phosphorylated upon infection with *P. syringae* expressing the type III effectors *AvrB* or *AvrRpm1* and activate RPM1-mediated resistance (Mackey et al., 2002). *AvrRpt2*, a sequence-unrelated type III effector, causes the posttranscriptional disappearance of RIN4 and activates RPS2-mediated resistance (Mackey et al., 2003). *rin4* null mutants are lethal in an *RPM1 RPS2* background; and this lethal phenotype is fully eliminated only in the *rin4/rps2/rpm1* triple mutant (Belkhadir et al., 2004; Mackey et al., 2003). Thus, RIN4 is the host target of *AvrB*, *AvrRpm1* and *AvrRpt2*, which binds to RPM1 and RPS2 and negatively regulates the inappropriate activation of these R proteins.

### 2.3.3. Components of R gene signal transduction

The search for downstream signaling components of R gene-mediated resistance was mainly done by screening for mutants that are compromised in the disease resistance. Mutations in *EDS1* (*enhanced disease susceptibility 1*) and *PAD4* (*phytoalexin-deficient 4*) for example, block resistance mediated by TIR-NB-LRR resistance genes (Aarts et al., 1998; Glazebrook et al., 1997), while mutations in *NDR1* (*non-race-specific disease resistance 1*) and *PBS2* (*AvrPphB susceptible 2*) block resistance mediated by CC-NB-LRR resistance genes (Aarts et al., 1998; Warren et al., 1999). This suggests that there are at least two downstream signaling pathways activated by R gene and activation of each pathway depends on the R protein structure (Glazebrook, 2001). *EDS1* encodes a protein that has similarity in its amino-terminal portion to the catalytic site of eukaryotic lipases. It functions upstream of

SA-dependent *PR1* accumulation and is not required for JA-dependent *PDF1.2* expression (Falk et al., 1999). The predicted protein sequence from *PAD4* displays similarity to triacyl glycerol lipases. *pad4* has a defect in accumulation of SA upon pathogen infection, suggesting that *PAD4* participates in a positive regulatory loop that increases SA levels and activates SA-dependent defense responses (Jirage et al., 1999).

*NDR1* encodes a protein with unknown function, which is plasma membrane-localized, and predicted to be GPI-anchored (Coppinger et al., 2004). Day et al (2006) demonstrated that NDR1 interacted with RIN4 on the cytoplasmic N-terminal portion of NDR1 and that this interaction is required for the activation of RPS2-mediated resistance (Day et al., 2006). *pbs2* was discovered from screening for loss of RPS5-mediated resistance upon recognition to *P. syringae* expressing *avrPphB*. Later it was found that the mutation in *PBS2* is *AtRAR1*, the *Arabidopsis* ortholog of barley *RAR1*, which is required for full HR and complete resistance mediated by many highly related *Mla R* alleles. RAR1 itself is a protein that consists of the zinc-coordinating CHORD I and CHORD II domains and the central CCCH domain (Tornero et al., 2002). The dependency on downstream signaling described above is not a general rule for all *R*-genes. For instance, *RPP7* and *RPP8* do not require either *EDS1* or *NDR1*, while *RPP13* does not require *EDS1*, *PAD4*, *PBS2* or *NDR1*.

Other signaling components beside the above-mentioned genes affect hormone signaling. Some of them act in the SA-dependent signaling pathway, such as *NPR1/NIM1* (*non expressor of PR genes 1* or *non-inducible immunity 1*), *SAI1* (*salicylic acid insensitive 1*), *EDS4*, *EDS5/SID1* (*salicylic acid induction deficient 1*), and *EDR1* (*enhanced disease resistance 1*). Others that act in the JA/ET-dependent signaling pathway comprised of *OPR3* (*12-oxophytodienoic acid reductase 3*) and *COI1* (*coronatine insensitive 1*) (Glazebrook, 2001)

### 3. The “*avrRpm1-Rpm1*” model system

One of the best studied resistance mechanisms is the *Arabidopsis* “*avrRpm1-RPM1*” model system. The resistance gene *RPM1* confers resistance to pathogen with the avirulence gene *AvrRpm1*, which was isolated from *P. syringae* pv. *maculicola* strain M2 (*Pma* M2) (Ritter and Dangl, 1995). *AvrB*, another effector from *P. syringae* with no sequence similarity to *AvrRpm1*, also interacts with *RPM1* and triggers resistance (Mackey et al., 2002) (Fig 3a). *RPM1* has been shown to be a peripheral membrane protein that likely resides on the cytoplasmic face of the plasma membrane (Boyes et al., 1998). *AvrRpm1* and *AvrB* are similarly localized when expressed in the plant (Nimchuk et al., 2000), but the physical

interaction between AvrRpm1 or AvrB and RPM1 has never been observed. The *Arabidopsis* RIN4 protein was discovered in a yeast two-hybrid screen for plant proteins that interact with AvrB and subsequently shown to co-immunoprecipitate with AvrB, AvrRpm1 and RPM1. Reduction of RIN4 protein levels inhibits both the hypersensitive response and the restriction of pathogen growth controlled by RPM1. AvrB and AvrRpm1 cause hyperphosphorylation of RIN4 independent of RPM1 during infection, which was suggested to reflect the virulence activity of these effector molecules. Additionally, “knock-down” plants with reduced levels of RIN4 protein demonstrate a constitutive activation of defense responses in the absence of pathogens, implying that the normal function of RIN4 is to negatively regulate defense responses. These data fit the guard hypothesis in which AvrB and AvrRpm1 modify RIN4 to interfere with its regulation of defense responses, but the RIN4 modifications are perceived by RPM1, which subsequently triggers disease resistance (Mackey et al., 2002).

Interestingly, another unrelated type III effector from *P. syringae*, AvrRpt2, also targets RIN4 and induces its post transcriptional disappearance (Fig. 3b). This effect is independent of RPS2, the *Arabidopsis* R protein that recognize AvrRpt2. Over expression of RIN4 inhibits the RPS2-dependent HR and partially suppresses the ability of RPS2 to inhibit growth of *Pto* DC3000(*avrRpt2*). Conversely, disruption of *RIN4* results in lethality due to the constitutive activation of RPS2. RPS2 and RIN4 physically associate in the plant. This implies that RIN4 is the target of the AvrRpt2 virulence function, and that perturbation of RIN4 activates RPS2. Thus, RIN4 is a point of convergence for the activity of at least three unrelated *P. syringae* type III effectors (Axtell and Staskawicz, 2003; Mackey et al., 2003). It is hypothesized that AvrB and AvrRpm1 evolved to suppress PAMP-triggered defense responses mediated by RIN4. Subsequently, the plant developed RPM1 to detect these perturbations. The AvrRpt2 effector may have later evolved as a mechanism to interfere with the RPM1 disease-resistance pathway and restore pathogen virulence. Finally, RPS2 evolved to recognize the protease activity of AvrRpt2, which in turn restored resistance in the host plant (Chisholm et al., 2006). This hypothesis fits the phases of ETI and ETS described in the “zig-zag” model (Jones and Dangl, 2006) for co-evolution between pathogen and host plants.

Downstream signaling of AvrRpm1-RPM1 disease resistance requires the presence of several genes, among them are *RAR1* and *NDR1*. The HR induction mediated by RPM1 is severely attenuated, but not eliminated in *rar1*. Resistance to *Pto* DC3000(*avrRpm1*) is also inhibited in *rar1*. *ndr1* retains the ability to induce an RPM1-dependent HR, but the resistance to *Pto* DC3000(*avrRpm1*) is only partially diminished. The *rar1/ndr1* double mutant, which expresses the *rar1* phenotype for severe attenuation of RPM1-dependent HR, also resembles

the fully susceptible *rar1* in bacterial growth assay. Thus, *RAR1* appears to act in the same pathway as *NDR1* during RPM1-dependent responses (Tornero et al., 2002).

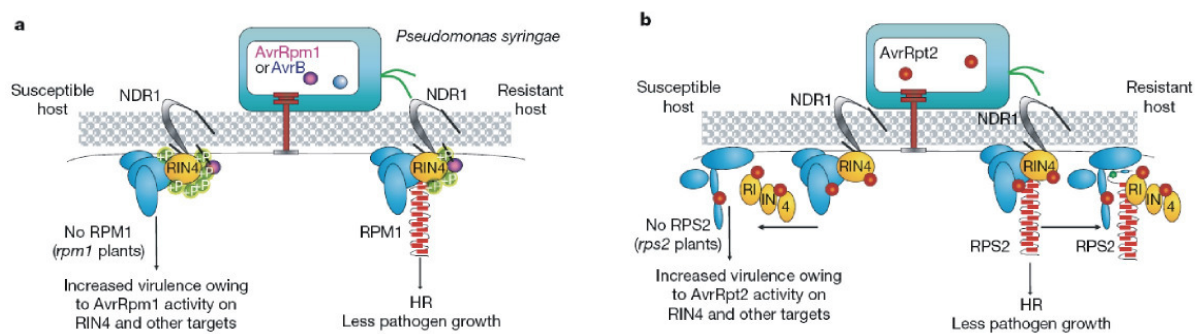


**Fig. 3** RPM1 (a) and RPS2 (b) protein complex, consisting of avr protein, R protein, host target and signaling components (Jones and Dangl, 2006).

Besides downstream signaling molecules, R proteins also require protein partners that link them to other components essential for the R protein function (Belkhadir et al., 2004). Cytosolic HSP90s are required for some NB-LRR functions and interact *in vivo* with RPM1 (Hubert et al., 2003). Three point mutations in the *Arabidopsis HSP90-2* gene can specifically impair RPM1 signaling. This results in increased growth of *Pto* DC3000(*avrRpm1*) and alters, but does not completely abolish, RPM1-mediated HR. Furthermore, RAR1 and SGT1, which are required for the function of many R proteins, also associate independently with HSP90 (Hubert et al., 2003). These data suggest that RAR1, SGT1 and HSP90 may work simultaneously to regulate downstream signaling events (Hubert et al., 2003).

#### 4. Proteomics for plant defense study

Proteomics has become an essential tool to complement transcriptomics studies with the aim to identify new targets not covered by mRNA analysis. In contrast to the relative ease of mRNA extraction and experimental manipulation for transcriptomics analysis, proteins present numerous challenges: their physicochemical and structural complexities complicate their extraction, solubilization, handling, separation and identification; and so far there is no technology equivalent to PCR, which is available to amplify low abundance proteins. Despite all these difficulties, proteomics is still a promising approach due to various limitations in transcriptomics analysis. One of the most important limitation is that mRNA levels often have a poor correlation with the levels of corresponding protein (Anderson and Anderson, 1998; Gygi et al., 1999; Ideker et al., 2001). Moreover, regulation of cellular events can occur at the protein level with no apparent changes in mRNA abundance. Post-translational modification of proteins can result in a dramatic increase in protein complexity without a concomitant

increase in gene expression. Therefore, proteome reflects the expression of the molecules that more directly influence cellular biochemistry, compared to mRNA which represents information intermediates. The ability to isolate sub-cellular protein fractions can also give an insight into sub-cellular localization and even function; or to isolate multi-subunit protein complexes whose constituents can not be predicted from DNA sequences or mRNA abundance (Rose et al., 2004).

In a classical proteomics approach, two-dimensional gel electrophoresis (2-DE) is used for protein separation and quantification, followed by identification of the target candidates by mass spectrometry (MS) (Görg et al., 2004; Schratzenholz, 2004). In a more recent approach, liquid chromatography (LC), isotopic labeling and tandem MS are combined as an alternative towards gel-free proteomics. This approach offers highly automated protein separation and identification, allowing high throughput analysis of complex protein samples (Hunt et al., 1986; Patterson and Aebersold, 2003; Washburn et al., 2001). Despite recent advances in LC-based approaches, 2-DE is still a promising strategy in proteomics. A complementary analysis of the *Mycobacterium tuberculosis* proteome using both gel-based and gel-free approaches has revealed that both approaches do not provide identical results. Each technique showed biases for and against specific classes of proteins. The 2-DE approach provides more coverage of low molecular weight proteins, while the LC-MS/MS approach recovers high molecular weight proteins better than 2-DE. Despite the argument that 2-DE is not suitable for analyzing membrane proteins, it is reported to cover hydrophobic proteins slightly better than the LC-based method (Schmidt et al., 2004). Moreover, the 2-DE-based approach has an advantage to quantify the abundance of protein down to the level of protein isoforms, which is still difficult with LC-MS/MS based approaches. This is particularly vital for the detection of differential post-translational modification which is, in most cases, important for regulating biological function (Schmidt et al., 2006; Schmidt et al., 2004). Therefore, both techniques should be used complementarily.

So far, the approach to study *R* gene-mediated resistance is mainly based on transcriptomics studies and screening for mutants with altered resistance leading to the discovery of genes required for resistance (de Torres et al., 2003; Tao et al., 2003; Tornero et al., 2002; Truman et al., 2006). Using 2-DE, Jones et al. (2004) analyzed protein changes characteristic of the establishment of basal resistance and *R* gene-mediated resistance by comparing responses to *Pto* DC3000, a *hrp* mutant and *Pto* DC3000 expressing *AvrRpm1*, respectively. Their data suggest that bacterial challenge generally induces the accumulation of antioxidant glutathione S-transferase and peroxiredoxins. However, individual members of

these protein families may be specifically modified, which is dependent on the virulence factors of the DC3000 strain (Jones et al., 2004). Subsequently, the same authors investigated the characteristic protein changes of basal defense and *R* gene-mediated resistance by applying different fractionation strategies. Proteins found to show significant changes after bacterial challenge are representative of two main functional groups: defense-related antioxidants and metabolic enzymes. Significant changes to photosystem II and two components of the mitochondrial permeability transition were also identified (Jones et al., 2006)

## 5. Aim of this work

Despite the recent studies on *R* gene-mediated resistance, which reveal many “*Avr-R*” gene partners, very little is known about the signaling events required to activate *R* protein-mediated resistance. The aim of this study is to identify protein(s), which may play a role in early signaling of *RPM1*-mediated resistance by a proteomics approach. A transgenic *Arabidopsis* line with the bacterial *AvrRpm1* avirulence gene under the control of a dexamethasone-responsive promoter was used to profile proteins specifically involved in the *avrRpm1*-*RPM1* interaction without interference from additional bacterial components. 2-DE combined with different prefractionation strategies was used to enrich potential signaling proteins that are presumably of low abundance. To elucidate the role of the proteins identified from 2-DE analysis, functional analysis using mutant/transgenic plants modulated in the expression of selected candidates was performed. This study aims to identify novel candidate signaling proteins to improve the understanding of the *RPM1*-mediated resistance mechanism.

## II. Materials and methods

### 1. Protein biochemical techniques

#### 1.1. Total protein extraction

Ground leaves (500 mg) were extracted with 1.5 mL of extraction buffer (5% glycerol, 5 mM EDTA, 0.1%  $\beta$ -Mercaptoethanol, 100 mM HEPES-KOH pH 7.5, 1% proteinase inhibitor cocktails) and centrifuged for 10 min at 18,000 x *g* at 4°C. The supernatant was mixed with an equal volume of phenol and centrifuged for 10 min at 7,850 x *g* at 4°C. The lower phase was re-extracted twice with an equal volume of re-extraction buffer (20 mM KCl, 10 mM EDTA, 0.4%  $\beta$ -Mercaptoethanol, 100 mM Tris-HCl pH 8.4) then centrifuged for 10 min at 7,850 x *g* at 4°C. The final lower phase was precipitated by adding 5 volumes of precipitation solution (100 mM CH<sub>3</sub>COONH<sub>4</sub> in methanol) for at least 2 h at -20°C. After centrifugation for 10 min at 7,850 x *g* at 4°C, the protein pellet was consecutively rinsed with precipitation solution and washing solution (80% ethanol in 50 mM Tris-HCl pH 7.5). and solubilized in 150  $\mu$ L of solubilisation buffer (7 M urea, 2 M thiourea, 50 mM DTT, 2% IPG buffer, 4% CHAPS, 0.4% SDS, 5 mM K<sub>2</sub>CO<sub>3</sub>).

#### 1.2. Microsomal fraction extraction

Ground leaves (2.5 g) were homogenized by 2 rounds of 30 s in a Polytron (Kinematica) in 20 mL of extraction buffer I (100 mM NaCl, 20 mM DTT, 0.33 M sucrose, 0.1% protease inhibitor cocktails, 1 mM PMSF, 50 mM Tris pH 8.0). The extract was cleared by filtration through Nylon Net Filters (Millipore) and centrifugation for 20 min at 3,000 x *g* at 4°C. The microsomal pellet was obtained by centrifugation for 2 h at 138,000 x *g* at 4°C and then extracted in 700  $\mu$ L of extraction buffer II (100 mM NaCl, 20 mM DTT, 1% protease inhibitor cocktails, 0.1% Triton X-100 and 0.1% NP-40, 50 mM Tris pH 9.6) by vortexing for 30 min (R.T.). The remaining insoluble debris was removed by centrifugation for 10 min at 20,000 x *g* at 4°C. The supernatant was mixed with equal volume of Phenol and processed as described for total protein extraction.

#### 1.3. Rubisco depletion from total protein

Ground leaves (2 g) were extracted in 12 mL of extraction buffer (20 mM MgCl<sub>2</sub>, 2%  $\beta$ -Mercaptoethanol, 0.1% protease inhibitor cocktails, 1 mM PMSF, 1% PVPP, 2% NP-40, 500 mM Tris-HCl pH 8.3). The extract was cleared by filtration through Nylon Net Filters (Millipore) and centrifugation for 15 min at 12,000 x *g* at 4°C. The supernatant was mixed with 50% PEG solution to make a final concentration of 10% PEG. After incubation for 30

min, the mixture was centrifuged for 10 min at 1,500 x *g* at 4°C to obtain 10% PEG pellet. The remaining supernatant was adjusted to a final concentration of 20% PEG with 50% PEG solution. The mixture was incubated for another 30 min and centrifuged for 15 min at 12,000 x *g* at 4°C to obtain 20% PEG pellet. The remaining supernatant was precipitated with acetone. The 10% PEG pellet, 20% PEG pellet and supernatant precipitate were washed with ice-cold acetone containing 0.07% β-Mercaptoethanol and solubilized in 250 μL of solubilisation buffer.

#### 1.4. Rubisco depletion from microsomal protein

Ground leaves (8 g) were subjected to microsomal fraction extraction. The microsomal pellet was extracted in 4 mL of buffer II containing Mg/NP40 (100 mM NaCl, 20 mM DTT, 20 mM MgCl<sub>2</sub>, 0.1% protease inhibitor cocktails, 1 mM PMSF, 2% NP-40, 0.1% Triton X-100, 50 mM Tris pH 9.6) and incubated for 30 min with shaking (R.T.). The remaining insoluble debris were removed by centrifugation for 15 min at 12,000 x *g* at 4°C and subjected to PEG precipitation as described above.

#### 1.5. Rubisco depletion using Seppro IgY Rubisco (Genway) spin column

Total protein extract was obtained from 500 mg of leaves and the protein concentration determined by 2D Quant Kit (GE Healthcare). Two hundreds microgram of protein were diluted with TBS buffer (150 mM NaCl, 10 mM Tris-HCl pH 7.4) to a final volume of 500 μL. The diluted sample was subjected to immunocapture of Rubisco according to the manufacturer's instruction. The bound protein and flow through were collected and the protein was precipitated by TCA/Acetone precipitation. The pellet was washed thrice with ice-cold acetone containing 0.07% β-Mercaptoethanol and solubilized in 30 μL of solubilisation buffer.

#### 1.6. 2-DE

Protein concentration was determined using 2D Quant Kit (GE Healthcare) according to the manufacturer's instruction. One hundred and fifty microgram of total protein was re-suspended in 450 μL of rehydration buffer (8 M urea, 2% CHAPS, 2.8% DTT, 0.5% IPG buffer, 0.002% BPB) and the mixture was centrifuged for 5 min at 13,000 x *g* to remove non-soluble material. The samples were loaded onto 24 cm 4 ~ 7 IPG strip (GE Healthcare) and actively rehydrated using an IPGphor (GE Healthcare) for 12 h at 50 V. Isoelectric focusing was performed using the following program: 200 V for 1 h, 500 V for 1 h, 1000 V for 1 h,

gradient to 8000 V for 1.5 h, and constant 8000 V for 72 kVhr. After focusing, the IPG strip was equilibrated for 15 min (R.T.) in equilibration buffer (6 M urea, 30% glycerol, 2% SDS, 50 mM Tris-HCl pH 8.8) containing 1% DTT, followed by equilibration buffer containing 2.5% iodoacetamide. The second dimension separation on 12% polyacrylamide gel was performed using Ettan DaltII system (GE Healthcare). The gels were stained with Silver Stain according to Blum (Blum et al., 1987).

### 1.7. Image analysis using Proteomweaver

The silver stained gels were scanned using ImageScanner (GE Healthcare) and analyzed using Proteomweaver (BioRad). After spot detection, gels were fully matched and normalized by determining normalization factor for all pairs of gels using a precision normalization algorithm. These were then used to calculate intensity factor for each gel, which brought the normalization factors as close to one as possible. To find up-regulated or down-regulated proteins, a filter was implemented to search for spots with regulation factor of  $\geq 1.5$  or  $\leq 0.75$  compared to the control. The resulting spots were subsequently analyzed statistically to fulfill significance of  $P < 0.05$  (Student's t-test). Only data reproducibly obtained in 3 independent biological replicates are considered.

### 1.8. Protein identification using PMF MALDI-TOF/MS

Protein spots were excised from 2D gels using a scalpel. The gel plugs were destained with an equal mixture of 30 mM  $K_3[Fe(CN)_6]$  and 100 mM  $Na_2S_2O_3$  and dried in a SpeedVac for 30 min. The dried gel plugs were swollen with 5 ng/ $\mu$ L trypsin solution in digestion buffer containing 10 mM  $NH_4HCO_3$  and 5% ACN for 30 min on ice and digested at 37°C for 4 - 5 h. The peptide fragments were extracted using extraction buffer containing 50% ACN and 0.1% TFA. The extract was spotted onto pre-structured MALDI sample support (AnchorChip 384/600; Bruker) and mixed with 2,5-DHB as MALDI matrix. After crystallization the samples were analyzed on Bruker's RELFEX III using Reflecton mode. The MALDI-TOF spectrum was analyzed by FlexAnalysis 2.0 (Bruker) and internally calibrated using trypsin autolysis peaks. Protein identification by PMF was performed using Mascot software, allowing 1 missed tryptic cleavage and partial oxidation of methionine as well as modification of cysteines to complete alkylation. The search was against database from TAIR and proteins obtained MOWSE scores over 57 ( $P < 0.05$ ) were considered identified.

### 1.9. Western Blot

Protein was separated on 12% SDS-PAGE gel and transferred to nitrocellulose membrane (Hybond-ECL; Amersham Biosciences). The blot was incubated in TBST (140 mM NaCl, 0.1% Tween-20, 20 mM Tris HCl pH 7.6) containing 5% skimmed milk at 4°C overnight. The blots were consecutively incubated for 1 h (R.T.) with primary antibody and secondary antibody with washing in TBST. Anti-HA mouse was used at dilution of 1:1000 (Eurogentec); anti-HA rat of 1:1000 (Roche), anti-mouse HRP of 1:8000 (Eurogentec); anti-rat AP of 1:2000 (Boehringer Mannheim GmbH); anti-Remorin of 1:500 (generated in this work); anti-rabbit HRP of 1:5000 (Pierce Biotechnology); Anti-RIN4 of 1:5000 (Mackey et al., 2002); anti-rabbit True Blot of 1:1000 (eBioscience); anti-BiP of 1:700 (Stressgen); anti-AHA2 of 1:1000 (Palmgren and Christensen, 1994); anti-streptactin AP of 1:4000 (IBA GmbH).

### 1.10. Immunoprecipitation

The anti-HA was bound to protein A sepharose (GE Healthcare) with ratio of 1 µg antibody to 2.5 µL protein A sepharose and incubated at 4°C overnight on an orbital shaker. To remove the unbound antibody, the beads were washed with PBS. Cross linking was done by incubation with 25 mM DMP (Pierce Biotechnology) in cross linking buffer (0.2 M Triethanolamine pH 8.2) for 1 h (R.T.). To quench the remaining cross linking solution, an excess of 40 mM Tris HCl pH 8.0 was added and incubated for 1 h (R.T.). The beads were washed with PBS prior to addition of protein extract. An aliquot of protein extract containing 1 mg of total protein was mixed with 100 µL of anti-HA bound protein A sepharose and incubated at 4°C overnight on an orbital shaker. The remaining supernatant was removed and the beads were washed with PBS. To elute the bound protein the beads were resuspended in SDS sample buffer and heated at 95°C for 5 min.

### 1.11. Dephosphorylation assay (Phosphatase treatment)

Ground leaves (8 g) were subjected to microsomal fraction extraction and the microsomal pellet was dissolved in 4 mL of buffer (100 mM NaCl, 20 mM DTT, 1% protease inhibitor cocktails, 0.1% Triton X-100 and 0.1% NP-40, 50 mM Tris pH 9.6) containing 2 mM MnCl<sub>2</sub>. The extract was cleared by centrifugation at 12,000 x g for 15 min at 4°C. The supernatant was divided into two aliquots. One aliquot was added with 400 U of λ Phosphatase (Upstate cell signaling solutions) and the other aliquot is without addition of λ Phosphatase. Both aliquots were incubated at 30°C for 20 min. After incubation the reactions

were subjected to PEG fractionation to obtain a 10% PEG pellet. The pellet was dissolved in solubilization buffer and resolved on 2D gel.

#### 1.12. Generation and purification of Anti-Remorin (AtREM1.2)

A peptide sequence, with potential antigenic properties, specific for the Remorin AtREM1.2 (At3g61260) was chosen. This specific peptide sequence (DVAEEKIQNPPPEQI; with an additional N-terminal cysteine for coupling purpose) was used to produce antisera against AtREM1.2 (by the antibody production facilities of Sigma Genosys). Purification of anti-remorin was done by peptide affinity purification. The free sulfhydryl at terminal cysteine of the peptide was immobilized to iodoacetyl groups on the SulfoLink Coupling Gel (Pierce Biotechnology) by incubation for 15 min with mixing and 30 min without mixing (R.T.) in the coupling buffer (50 mM Tris HCl pH 8.5, 5 mM EDTA). The non-immobilized peptide was removed and the slurry was washed with 3 volumes of coupling buffer. The non-specific binding sites of the SulfoLink coupling gel were blocked with 50 mM L-Cysteine HCl in coupling buffer by incubation (R.T.) for 15 min with mixing and 30 min without mixing. The remaining blocking solution was cleared, and the slurry was washed with 6 volumes of 1 M NaCl and equilibrated with PBS buffer. The crude antisera were centrifuged to remove debris, diluted with PBS buffer and mixed with the peptide-coupled SulfoLink gel slurry. The mixture was incubated for 1 h (R.T.) and washed extensively with PBS buffer. The bound antibody was eluted by applying 100 mM Glycine pH 2.5 - 3.0. One milliliter fractions were collected into tubes with 100  $\mu$ l of 1 M Tris pH 7.5 for immediate neutralization and monitored by absorbance at 280 nm. The fractions of interest were pooled and exchanged to PBS buffer using PD10 column (GE Healthcare).

#### 1.13. Lipid rafts/Detergent-Resistant Membranes (DRM) isolation

Microsomal pellet was obtained from 30 g of leaves according to the protocols for microsomal fraction extraction. The pellet was extracted in 1 mL of pre-cooled TNE buffer (25 mM Tris HCl pH 7.5, 150 mM NaCl, 5 mM EDTA) containing 2% Triton X-100 at 4°C for 30 min. The insoluble material was removed by centrifugation at 12,000  $\times$  g for 15 min at 4°C. The supernatant was adjusted to 1.8 M sucrose/TNE by addition of three volumes of pre-cooled 2.4 M sucrose/TNE. This mixture was then overlaid with sucrose step gradients 1.6 - 1.4 - 0.15 M and centrifuged at 285,000  $\times$  g in a Beckman SW41Ti for 18 h at 4°C. The DRM were collected in the region of 1.4 - 1.6 M interfaces. The DRM was diluted with 5 volumes of TNE buffer and centrifuged at 89,000  $\times$  g in a Beckman TLA100.3 for 2 h at 4°C. The

pellet was dissolved in SDS sample buffer (100 mM Tris HCl pH 6.8, 20% glycerol, 4% SDS).

#### 1.14. Co-immunoprecipitation using anti-RIN4 and anti-Remorin

Microsomal pellet was obtained from 10 g of leaves following the protocols for microsomal fraction extraction. The pellet was dissolved in 2 mL of buffer (50 mM HEPES pH 7.4, 50 mM NaCl, 10 mM EDTA, protease inhibitors, 0.1% Triton X-100, 0.1% NP-40). Insoluble material was pelleted by centrifugation at 20,000 x g for 20 min at 4°C. The supernatant was pre-cleared by adding 25 µL of anti-rabbit IgG magnetic beads (New England Biolabs) and incubated for 1 h at 4°C on an orbital shaker. The cleared supernatant was collected; 500 µL aliquot was taken and combined with either of the following antibodies: 3 µL of anti-RIN4 or 3 µL of pre-immune of anti-Remorin or 3 µL of anti-Remorin. These mixtures were incubated for 2 h on ice. A 25 µL aliquot of anti-rabbit IgG magnetic beads was added to each mixture and all the mixtures were rolled at 4°C overnight. The beads were washed 2 times with buffer containing 50 mM HEPES pH 7.4, 50 mM NaCl, 10 mM EDTA, 0.1% Triton X-100, 0.1% NP-40. Bound protein was eluted with 30 µL of SDS sample buffer containing 1% DTT, boiled at 95°C for 5 min and loaded onto SDS PAGE gel. The sample was probed with anti-RIN4 and anti-Remorin.

## 2. Molecular biological and cloning procedures

### 2.1. DNA extraction and Southern Blot

Ground leaves (100 mg) were extracted in EB buffer containing 100 mM Tris HCl pH 8.0, 50 mM EDTA, 500 mM NaCl, 1.5% SDS and 10 mM β-Mercaptoethanol. After incubation for 10 min at 65°C, 300 µL of 5 M KOAc pH 4.8 was added. The mixture was incubated for 1 h at 4°C and then centrifuged at 18,900 x g for 10 min at 4°C. The supernatant was collected and mixed with 800 µL of phenol/chloroform/isoamylalcohol (25:24:1), and then centrifuged at maximum speed for 5 min. The upper aqueous phase was collected and mixed with 500 µL of isopropanol. The mixture was centrifuged at maximum speed for 10 min to pellet the DNA. The pellet was washed with 70% ethanol and dissolved in 50 µL of 10 mM Tris HCl pH 8.0 with addition of RNaseA (ca. 100 µg/mL). The DNA was digested with the indicated restriction enzymes prior to electrophoresis. After the digestion the DNA was mixed with DNA sample marker and separated on a 1% agarose gel with 20 - 50 V for 4 - 8 h. The gel image with a ruler alongside the gel was taken under the UV light. After denaturation and neutralization, the gel was transferred onto nylon membrane with 20X SSC solution

overnight according to standard procedures (Sambrook et al., 1989) and then cross linked under UV exposure.

## 2.2. RNA extraction and Northern Blot

Frozen ground leaves (100 mg) were thawed by addition of 1 mL of Trizol solution and mixed vigorously. After incubation for 5 min (R.T.), the sample was mixed vigorously with 0.2 mL of  $\text{CHCl}_3$ , incubated for 5 min (R.T.) and centrifuged at 12,000 x g for 15 min at 4°C. The top aqueous phase was collected and mixed with 0.5 mL of isopropanol, incubated for 15 min (R.T.) and centrifuged at 12,000 x g for 15 min at 4°C. The pellet was washed with 70% ethanol, air-dried and resuspended in RNase free water. Five microgram of RNA in 3.3  $\mu\text{L}$  of water was mixed with 1.5  $\mu\text{L}$  of 10X GB buffer (200 mM MOPS, 50 mM NaAc, 10 mM EDTA pH 7.0 containing ethidium bromide), 2.7  $\mu\text{L}$  of formaldehyde and 7.5  $\mu\text{L}$  of formamide. The mixture was heated at 60°C for 15 min and cooled on ice. Loading dye was added to the mixture and separation was performed on a 1% formaldehyde-containing gel (Sambrook et al., 1989) with 100 V for 1 - 2 h in 1X GB buffer. The gel image with a ruler was taken under UV light. The gel was blotted onto a nylon membrane with 20X SSC solution.

## 2.3. Radioactive DNA labeling and hybridization

The membrane was first pre-hybridized in hybridization buffer containing 0.1% PVP, 0.1% Ficoll, 0.1% BSA in 0.9 M NaCl, 50 mM  $\text{NaH}_2\text{PO}_4$ , 5 mM EDTA, 0.1% SDS pH 7.0, freshly heat-denatured herring sperm DNA (50  $\mu\text{g}/\text{mL}$ ) and 50% formamide at 42°C for 4 h in the orbital shaker. DNA encompassing the ORFs of the genes of interest were amplified by PCR. Using this template, random primers and klenow enzyme from Amersham megaprime DNA Labelling Kit (GE Healthcare), probes containing radioactively labeled  $\alpha$ - $^{32}\text{P}$ -dATP were synthesized at 37°C for 10 min. The excessive amount of radioactive dATP was removed using Probe Quant G-50 micro columns (GE Healthcare). The labeled fragments was denatured at 95°C for 5 min and cooled on ice before mixing with hybridization buffer. Hybridization was done overnight at 42°C. After the hybridization, the membrane was washed with 2X SSC containing 1% SDS for 25 min (R.T.) and with pre-heated 0.2X SSC containing 0.2% SDS at 65°C for 20 min. Finally the membrane was dried, covered in plastic foil, exposed to a phosphor screen overnight, and scanned at 200 micron pixel size resolution using a Typhoon Scanner 9410 series (GE Healthcare).

#### 2.4. Reverse-Transcription-PCR (RT-PCR)

RNA was treated with Deoxyribonuclease I (Fermentas) prior to reverse transcription (RT) to remove contaminating genomic DNA. The first strand cDNA synthesis was prepared by incubating the DNase-treated RNA with oligo d(T) primer at 70°C for 5 min and the reaction was added with ribonuclease inhibitor and 10 mM dNTP mix in the RT appropriate buffer. The reaction was incubated at 37°C for 5 min. M-MuLV reverse transcriptase (Fermentas) was added and RT was performed at 37°C for 1 h. The reaction was stop by heating at 70°C for 10 min and the resulting cDNA product used for PCR. Primers combination used in PCR are listed in the table A1 in the appendix.

#### 2.5. Selection of T-DNA insertional (SALK) lines

T-DNA insertional mutants of the genes of interest (At3g61260, AtREM1.2; At2g20630, PP2C and At1g11650, RNA BP) were obtained from the SALK Institute collection. To obtain homozygous line, the insertion lines were screened by PCR using specific T-DNA primers combination consisted of LP (left genomic primer), RP (right genomic primer) and LBa1 (left border primer of T-DNA insertion). To determine the exact location of the T-DNA insertion, the PCR products of the flanking genomic sequences (using LBa1 and RP primers) were sequenced.

#### 2.6. Cloning of the AtREM1.2-CFP/YFP/Strep/RNAi constructs

To prepare attB-flanked PCR products, template-specific primers for AtREM1.2 with 12 bases of *attB1* and *attB2* at their 5'-ends were designed (5'-AAAAGCAGGCTCCATGGCGGAGGAACAGAAGATAGC-3' and 5'-AGAAAGCTGGGTTGAAACATCCACAAGTTGC-3'). These primers were used in a 2-step PCR reaction to generate, from wild type *Arabidopsis* DNA, a genomic DNA fragment of AtREM1.2 flanked by attB sites. The PCR product was purified using PEG precipitation. Briefly, an aliquot of PCR product was mixed with TE buffer (10 mM Tris HCl pH 8.0, 1 mM EDTA) (1:10). Solution containing 30% PEG8000 in 30 mM MgCl<sub>2</sub> was added to the mixture (1:2) and centrifuged at 10,000 x g for 15 min (R.T.). The DNA pellet was washed with 70% ethanol and dissolved in EB buffer (10 mM Tris HCl pH 8.5). Using BP recombination reaction the fragment was cloned into pDONR 201 (Invitrogen). The product of BP reaction was transferred to *Escherichia coli* DH5 $\alpha$  by incubation on ice for 30 min and heat shocked at 42°C for 30 s. After incubation in SOC medium at 37°C for 1 h the bacteria was plated on LB medium containing 50  $\mu$ g/mL Kanamycin. The clones were screened by PCR, restriction

digestion and verified by sequencing before being transferred into pEXSG-CFP/pEXSG-YFP, pHellgate 8 and pXCSG-Strep vectors by LR reaction.

#### 2.7. Cloning of the pER8-AtREM1.2 and pER10-AtREM1.2 construct

An AtREM1.2-Strep fragment released from AtREM1.2-containing pXCSG-Strep construct by *Sall/XbaI* (Fermentas) double digest was ligated into *XhoI/SpeI*-digested (Fermentas) pER8 and pER10. The digestion site of *XbaI* is compatible with digestion site of *SpeI*; and the digestion site of *Sall* is compatible with the digestion site of *XhoI*. The ligation product was transferred to *E. coli* DH5 $\alpha$ .

#### 2.8. Cloning of AtREM1.2-RNAi into pCB302

The inverted repeat of AtREM1.2 from pHG8 construct was transferred to pCB302 (vector for BASTA selection) by first digesting the AtREM1.2-containing pHG8 using *NotI* (Fermentas). This releases the complete AtREM1.2-RNAi cassette, including 35S promoter and terminator and the DNA ends were filled in with dNTP using Klenow enzyme (Roche). This was ligated into *SmaI* –digested pCB302 with T4-DNA ligase.

#### 2.9. Cloning At2g20630 and At1g11650 into pENTR-TOPO vector

The ORFs of At2g20630 (PP2C) and At1g11650 (RNA BP) were PCR-amplified using specific primers with a CACC extension at the 5' ends of the forward primer. The PCR products were purified using PEG precipitation and cloned into pENTR-TOPO vectors (Invitrogen). Selection was performed on LB medium containing 50  $\mu$ g/mL Kanamycin, and DNA from the colonies was extracted using Qiagen miniprep (Qiagen) and analysed by *MluI* (Fermentas) digestion. Using LR recombination reaction the fragment was further transferred into pEarly101 and pGWB17 expression vectors.

#### 2.10. Agrobacterium transformation

Agrobacterium cultures were grown in LB containing the selection antibiotics at 28°C until OD<sub>600</sub> = 0.5 - 1. The cultures were harvested (centrifugation at 3,000 x g for 10 min at 4°C) and the pellet was resuspended in 1 mL of pre-cooled 20 mM CaCl<sub>2</sub>. One hundred microliter aliquot of the suspension was mixed with 1  $\mu$ g of plasmid DNA with the fragment-containing vector, incubated on ice for 5 - 30 min, frozen in liquid nitrogen for 1 min and immediately thawed at 37°C for 5 min. One milliliter of LB medium without selection antibiotics was added and the mixture was incubated at 28°C for 2 - 3 h with shaking.

Afterwards the mixture was plated on selection medium and incubated at 28°C for 2 - 4 d. After colonies were produced, they were picked and grown in the liquid medium containing the selection antibiotics. The cultures were pelleted and resuspended in solution containing 0.09 g glucose, 200 µL of 0.5 M EDTA, 200 µL of 1 M Tris HCl pH 8.0, and 0.04 g lysozyme in 10 mL solution. After incubation for 30 min (R.T.), the suspension was mixed with 200 µL of solution containing 1% SDS and 0.2 N NaOH. The solution was mixed gently and incubated for another 30 min (R.T.). Thirty microliter of alkaline phenol was added and mixed immediately, followed by addition of 150 µL of 3 M KAc. The solution was centrifuged at 15,000 x *g* for 5 min and the supernatant was mixed with 1 volume of phenol/chloroform/isoamylalcohol. After mixing and centrifugation, the aqueous phase was collected and added with 1 volume of chloroform. The aqueous phase was precipitated with isopropanol and the resulting DNA pellet was washed with 70% ethanol, air-dried, dissolved in EB buffer and analysed by restriction digest.

### 3. Plant growth, treatment and transformation

#### 3.1. Plant growth and treatment

The Col-0 *Arabidopsis* lines used in these experiments expressed AvrRpm1 under control of a dexamethasone-responsive promoter (Mackey et al., 2002). As a control, the same construct was expressed in the *rpm1-3* background (an allele of *RPM1* with a stop codon at amino acid 87) (Grant et al., 1995). Four-week-old plants were sprayed with 20 µM dexamethasone in 0.0075% silwet L-77. The leaves were harvested 2 and 6 h after spraying.

#### 3.2. *Arabidopsis* transformation using floral dip protocol

*Agrobacterium tumefaciens* strain carrying the gene of interest on a binary vector was grown in a LB medium liquid culture containing the appropriate antibiotics at 28°C. The cultures were centrifuged and the agrobacterium was resuspended to OD<sub>600</sub> = 0.8 in 5% sucrose solution. Silwet L-77 was added to a concentration of 0.05% before the dipping. The inflorescences were dipped in *Agrobacterium* solution for 2 - 3 s with gentle agitation. The dipped plants were placed under a cover for 16 - 24 h to maintain the humidity and prevented from excessive sunlight exposure. After 24 h the plants were transferred to greenhouse for seed production.

For the BASTA selection, *Arabidopsis* seeds were sowed on soil. After the secondary leaves appeared they were sprayed with BASTA solution (1:5000). This was repeated for 2 - 3 times at 2 - 3 d interval. For hygromycin or kanamycin selection, *Arabidopsis* seeds were

surface-sterilized by soaking them in 70% ethanol for 2 min and in 6% NaOCl solution containing 0.05% TritonX-100 for 15 min. The seed were rinsed with sterile distilled water for 5 times and sprinkled onto Murashige-Skoog medium plates containing the selective antibiotics. The seeds were stratified at 4°C for 2 d and transferred to growth cabinets. After 7 d, positive transformants which will be visible as green seedling with long roots were transferred to soil.

### 3.3. Trypan Blue staining

This staining method was adapted from (Peterhansel et al., 1997). The *Arabidopsis* leaves were boiled in trypan-blue solution containing 0.033% trypan-blue, 8% lactate, 8% glycerol, 8% phenol, 8% water and 67% ethanol, until the green color disappeared. After boiling, the leaves were washed with water and transferred to the saturated chloral hydrate solution (2.5 g chloral hydrate in 1 mL water) to remove unspecific staining. The leaves were stored in the 50% glycerol.

### 3.4. DAB staining

This staining method was adapted from (Thordal-Christensen et al., 1997). 3,3'-diaminobenzidine (pH 3.8, adjusted with HCl) was dissolved in water with a concentration of 1 mg/mL. The solution was kept in the dark to avoid oxidation by light. Leaves were incubated in freshly prepared DAB solution for 2 h before it was boiled with ethanol to remove the chlorophyll. Further destaining with chloral hydrate was performed as described above.

### 3.5. Bacterial growth curve assay

Bacteria were streaked out from a -80°C glycerol stock onto an LB medium plate with appropriate antibiotics and grown for 1 - 2 d at 28°C. Bacteria were transferred to LB liquid culture with appropriate antibiotics and grown with shaking at 28°C for 8 - 12 h and harvested (centrifugation at 3,000 x g, 10 min). The bacteria were washed and resuspended in 10 mM MgCl<sub>2</sub> to OD<sub>600</sub>=0.0002 (1 X 10<sup>5</sup> colony-forming units/mL). A 1-mL needleless syringe containing a bacterial suspension was used to pressure-infiltrate the leaf intercellular spaces from the abaxial side. The intercellular spaces of the infiltrated leaves were allowed to dry and then the plants were covered with a plastic dome to maintain high humidity. Leaves were harvested by excising leaf discs from two independent plants as a pool for a single tissue sample. The leaf discs were placed in a 1.5-mL microfuge tube and homogenized in Precellys

(Bertin Technologies) bead beater, in 1 mL of sterile water, until pieces of intact leaf tissue were no longer visible. The samples were thoroughly vortexed to distribute the bacteria within the water. A 10  $\mu$ L of sample is removed and diluted in 90  $\mu$ L of sterile water. A serial 1:10 dilution series was created for each sample by repeating this process. The samples were plated in LB medium with the appropriate antibiotics and incubated at 28°C for 2 d, and the colony-forming units for each dilution of each sample were counted.

### 3.6. Ion leakage assay

Eight leaf discs (8 mm diameter) were removed immediately following infiltration (t=0) and floated in 50 mL of water. After 30 min, the water was replaced with 10 mL of fresh water. Conductance of this 10 ml water was measured over time.

### 3.7. Agrobacterium transient expression in *Nicotiana benthamiana*

Agrobacterium cultures (2 mL) were grown overnight in LB medium with appropriate antibiotics and centrifuged to pellet the bacteria. The bacteria was resuspended in 1 mL of induction medium containing 1.05%  $K_2HPO_4$ , 0.45%  $KH_2PO_4$ , 0.1%  $(NH_4)_2SO_4$ , 0.05%  $C_6H_8O_7Na_3 \cdot 2H_2O$ , 0.012%  $MgSO_4$ , 0.1% glucose, 0.1% fructose, 0.4% glycerol and 0.145 % MES. The bacteria suspension was added with 3 – 5 mL of induction medium with antibiotics and grown for 5 – 6 h. The cultures were centrifuged; the pellet was resuspended in infiltration medium containing 10 mM MES pH 5.3 - 5.5, 10 mM  $MgCl_2$  and 150  $\mu$ g/mL acetosyringone to  $OD_{600}$  0.4 - 0.6. Fresh-looking leaves of young *Nicotiana benthamiana* were infiltrated using a needleless syringe on the underside.

## 4. Hormone analysis

### 4.1. JA and OPDA measurement

Ground leaves (0.5 g) were mixed with 100 ng of deuterated JA and OPDA each, as internal standards. Ten milliliter of methanol was added, and the sample was homogenized by 1 round of 1 min in a Polytron (Kinematica). The extract was cleared by filtration through Whatman paper and the eluate was applied to a DEAE-sephadex column and the first flow through was discarded. The column was washed with 3 mL of methanol, followed with 3 mL of methanol containing 0.1 N acetic acid. The JA and OPDA-containing fractions were eluted from the column using 3 mL of methanol containing 1 N acetic acid, followed by 3 mL methanol containing 1.5 N acetic acid. The flow through was collected and dried. The sample was dissolved in 100  $\mu$ L of methanol/water (1:1) and injected into the HPLC consisting of

Eurospher 100-C18, (5  $\mu\text{m}$ , 250 x 4 mm, Knauer, Germany). The eluent consists of solvent A – methanol, solvent B – 0.2% acetic acid in water; gradient 40%A to 100%A in 25 min. Fractions at  $R_t$  13 to 14.5 min (JA) and 21.75 to 22.50 min (OPDA) were combined and evaporated. The evaporated samples were dissolved in 200  $\mu\text{L}$  of  $\text{CHCl}_3/\text{N,N}$ -diisopropylethylamine (1:1) and derivatized using 10  $\mu\text{L}$  of pentafluorobenzylbromide at 20°C overnight. The samples were subsequently dissolved in 5 mL of n-hexane and passed through a Chromabond-SiOH-column (Machery-Nagel, Germany). The pentafluorobenzyl esters were eluted with 7 mL of n-hexane/diethylether (1:1). Elutes were evaporated, dissolved in 100  $\mu\text{L}$  of acetonitrile and analyzed by GC-MS.

GC-MS was performed on Polaris Q (Thermo-Finnigan), 100 eV, negative chemical ionization, ionization gas  $\text{NH}_3$ , ion source temperature 140°C, column Rtx-5w/Integra Guard (Restek, Germany) (5 m inert precolumn connected with column 15 m x 0.25 mm, 0.25  $\mu\text{m}$  film thickness, crossbond 5% diphenyl – 95% dimethyl polysiloxane, injection temperature 220°C, interface temperature 250°C; helium 1 mL  $\text{min}^{-1}$ ; splitless injection of 1  $\mu\text{L}$  sample. Column temperature program: 1 min 60°C, 25°C  $\text{min}^{-1}$  to 180°C, 5°C  $\text{min}^{-1}$  to 270°C, 10°C  $\text{min}^{-1}$  to 300°C, 10 min 300°C;  $R_t$  of pentafluorobenzyl esters: ( $^2\text{H}_6$ )JA 11.80 min, ( $^2\text{H}_6$ )-7-iso-JA 12.24 min, JA 11.86 min, 7-iso-JA 12.32 min, *trans*-( $^2\text{H}_5$ )OPDA 21.29 min, *cis*-( $^2\text{H}_5$ )OPDA 21.93 min, *trans*-OPDA 21.35 min, *cis*-OPDA 21.98 min.

#### 4.2. SA measurement

Ground leaves (0.5 g) were extracted with 0.5 mL of 90% methanol, sonicated for 5 min and centrifuged at 14,200 x g for 5 min. The supernatant was collected and the pellet was re-extracted with 0.5 mL of 100% methanol, sonicated and centrifuged. The supernatant was collected and combined, and subsequently mixed with 20  $\mu\text{L}$  of 2 M NaOH. The mixtures was dried in a speedvac for 2 h using heating, and then re-suspended in 250  $\mu\text{L}$  of 5% TCA solution. The extract was partitioned twice with ethyl acetate/cyclohexane (1:1), 800  $\mu\text{L}$  each. The organic phase was collected and mixed with 20  $\mu\text{L}$  of HPLC mobile phase, while the TCA phase was kept for SA glycoside analysis. The mixture was dried in a speedvac for 15 min until the organic phase was evaporated and only the mobile phase was left. Two hundreds microliter of HPLC mobile phase was added, and the mixture was centrifuged at 14,200 x g for 5 min. The supernatant was ready for HPLC analysis to determine the free SA content. To measure the SA glycoside levels, the TCA phase was mixed with 20  $\mu\text{L}$  of 8 M HCl and incubated at 80°C for 1 h. This mixture was then partitioned twice with ethyl acetate/cyclohexane (1:1) and processed according to the procedure for free SA analysis.

The HPLC system consisted of Phenomenex column type Luna 3  $\mu\text{m}$  C18(2) 150 x 4.6 mm. The eluent contained 60% acidified water (adjusted to pH 2.8 using acetic acid) and 40% methanol. The flow rate was 0.7 mL/min. Twenty microliter of extracts were injected. Salicylic acid was detected with a Jasco FP-920 spectrofluorometer detector, using an excitation wavelength of 300 nm and an emission wavelength of 410 nm.

#### 4.3. ET measurement

ET emissions were measured with a photo-acoustic spectrometer (INVIVO, University of Florida, Gainesville). The light source consisted of a line-tuneable CO<sub>2</sub> laser, and the detection device was a resonant photo-acoustic cell. The “fingerprint” spectrum of ET in the infra-red spectral region allows for a highly sensitive analysis by alternating measurement of the photo-acoustic signal on the CO<sub>2</sub> laser lines 10p14 and 10p16. The detection device consisted of 2 acoustic cells. One cell was filled with a known ET concentration (516 ppb) from a calibration gas reservoir, which was used to calibrate and continuously adjust the laser line. The sampling cell was calibrated with the gas (516 ppb) before the start of each experiment. To remove hydrocarbons, air was cleaned by oxidizing all organics: air was passed through a platinum catalyst at 540°C (Sylatech, <http://www.sylatech.de/>) before being directed to the sampling devices. The leaves of *Arabidopsis* were treated and detached. Excised leaves were transferred to 250 mL cuvettes, and ET was allowed to accumulate in the headspace for 6 h. The cuvettes were flushed with a flow of purified air at 130 – 150 mL min<sup>-1</sup>, which has also passed through a cooling trap to remove CO<sub>2</sub> and H<sub>2</sub>O.

### III. Results

#### 1. Proteomics analysis of differentially regulated proteins during *avrRpm1*-RPM1 interaction

The aim of this proteomics study was to find proteins potentially involved in early regulatory events during *avrRpm1*-RPM1 interaction. An inducible system that allows for conditional expression of the bacterial type III effector protein, *avrRpm1*, following dexamethasone treatment of the transgenic plants (Mackey et al., 2002), was used. Changes in cellular proteins were detected by comparing expression patterns in two isogenic *Arabidopsis* lines that each carries the same conditional *avrRpm1* transgene, but differs in the absence or presence of the *RPM1* gene (Andersson et al., 2006; Mackey et al., 2002).

Two representative time points were chosen for the analysis. The “early” sample was taken two hours after dexamethasone treatment, which is shortly after *avrRpm1* mRNA was detectable (Fig. 4B, 5). The “late” sample was taken six hours after dexamethasone treatment, when the HR, in the form of tissue collapse, was macroscopically visible (Fig. 4A, 5).

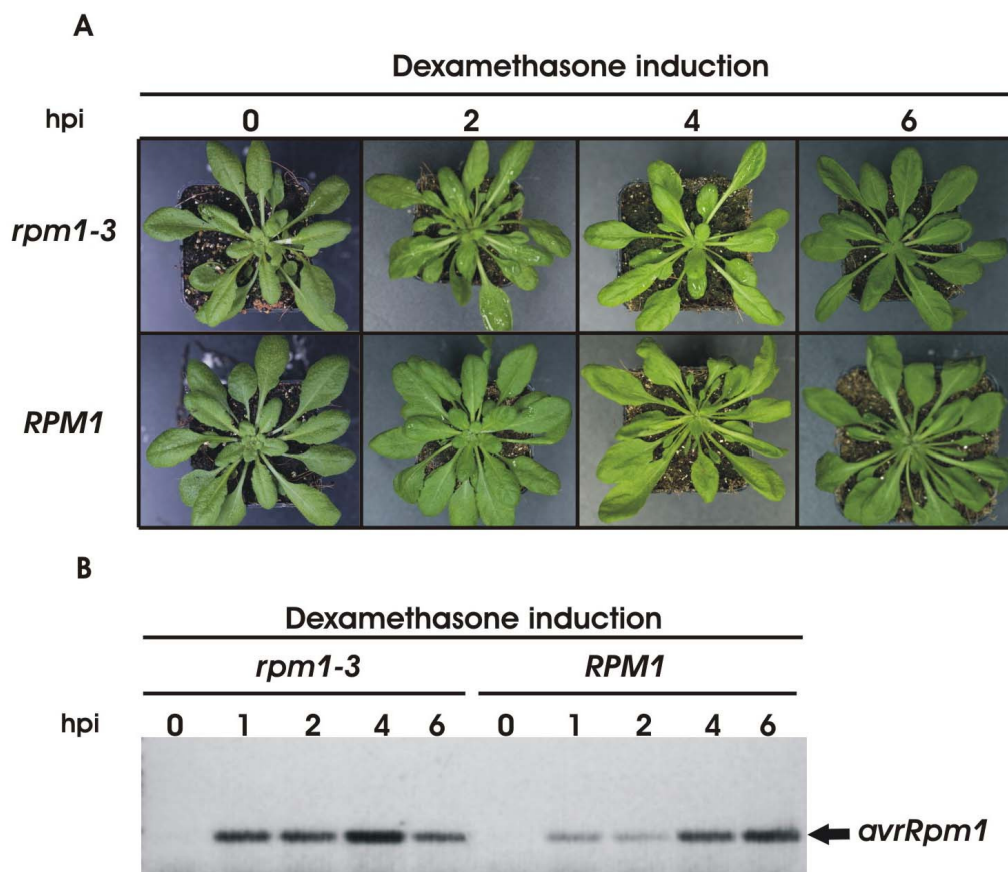


**Fig. 4** Two isogenic *Arabidopsis* lines that carry the same conditional *avrRpm1* transgene, but differ in the absence (*rpm1-3*) or presence (*RPM1*) of the *RPM1* gene during dexamethasone induction. (A) The *RPM1* line, but not the *rpm1-3* line developed HR, which is visible as tissue collapse (between 5-6 hpi). (B) RT-PCR showing that both lines expressed *avrRpm1* mRNA as early as 1 hpi.

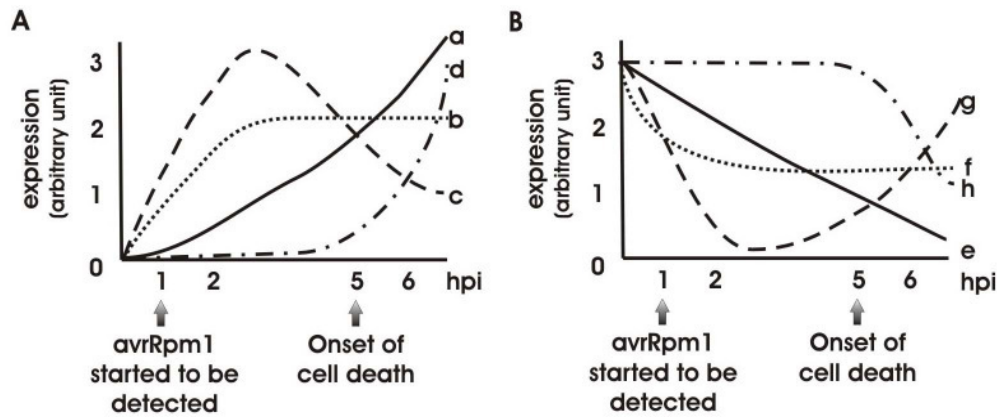


**Fig. 5** Hypothetical expression profiles of proteins involved in specific recognition events in plant-pathogen interactions. (A) Proteins can be up-regulated at an early time point (2 hpi) with a continuous increase (a) or steady state (b), transiently up-regulated at the early time point (c), or up-regulated at the late time point (6 hpi, d). (B) Protein can be down-regulated at an early time point with continuous decrease (e) or steady state (f), transiently down-regulated at an early time point (g), or down-regulated at late time point (h).

Figure 5 illustrates the various expression profiles that can be expected. Proteins involved in signaling may be transiently up-regulated at an early time point (profile c), up-regulated at early time point and maintained at a steady state (profile b) or continuously increasing (profile a, Fig 5A). Secondary stress reactions are expected for up-regulation at late time points (profile d, Fig. 5A). The reciprocal profiles might also be expected with protein down-regulation during the response (Fig 5B). To capture all these events, different filters were applied in the image analysis software. A protein was considered up- or down-regulated at specific time points when it differs  $\geq 1.5$  or  $\leq 0.75$  fold in spot intensities compared to the preceding time point. Only changes in abundance with a  $P$  value  $< 0.05$  (student's t-test) and reproduced in at least three independent biological experiments were considered.

### 1.1. Differential regulation of proteins in total protein extract

2-DE of total protein extract showed an excellent resolution (Fig. 6A), thus enabling roughly 1500 protein spots to be visualized (see comparison in Fig. 8), which is twice the number of protein spots that could be resolved in similar experiments with *Arabidopsis* leaf material (Jones et al., 2006; Jones et al., 2004). The high abundance of the large subunit of Rubisco in this extract masked proteins spots near its vicinity (50kDa region).

After performing image analysis and filtering all protein spots with a change in expression levels, 16 candidates were picked and identified by MS (first three columns in Table 1). Detailed information regarding statistical significance of expression profiles within the investigated time course and protein identification are presented in the table A2 in the appendix. These candidates include proteins with putative functions in general metabolism or

defense (Table 1); some were known from previous studies (Jones et al., 2006; Jones et al., 2004). They were mostly up-regulated at early time point with continuous increase (profiles a, Fig. 5A) or up-regulated at late time point (profiles d, Fig. 5A). Signaling proteins, presumably of low abundance, were not found.

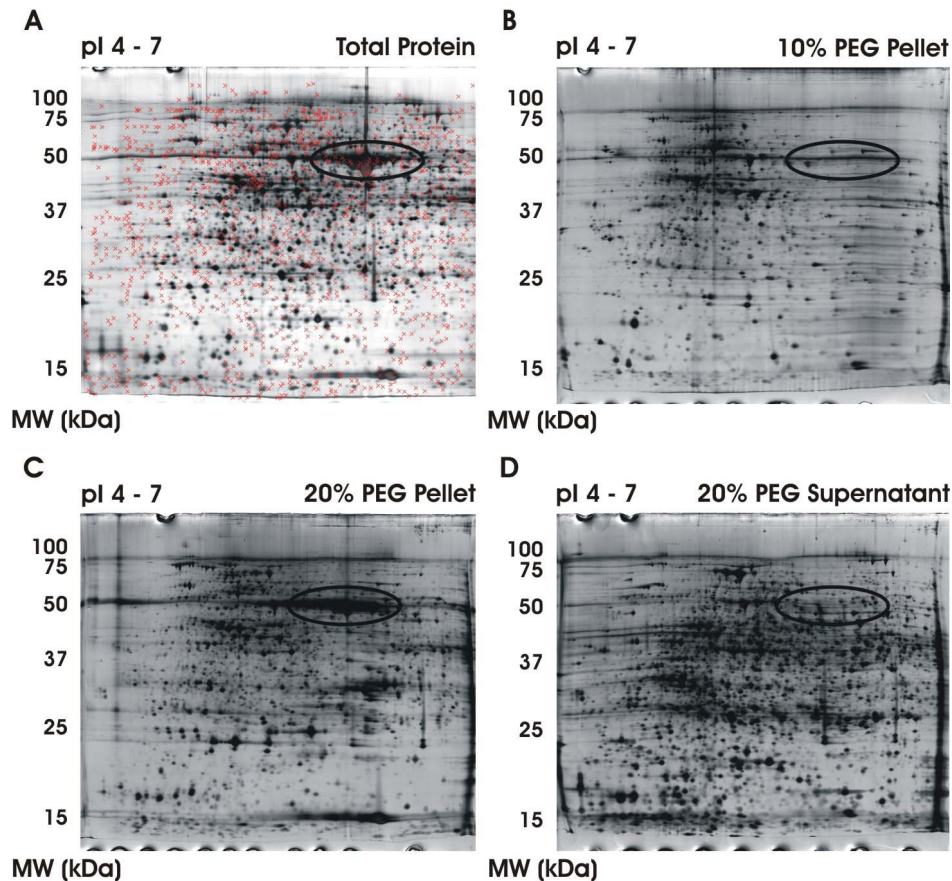


**Fig. 6** Silver-stained 2D gels of total proteins and Rubisco-depleted total proteins. (A) Total protein, (B) 10% PEG pellet, (C) 20% PEG pellet, (D) 20% PEG supernatant. The circled area indicates the location of the abundant Rubisco large subunit. The crosses in “A” indicate positions of protein spots that are newly present or more than three fold increased in spot intensity, both in 10% PEG pellet and supernatant fractions compared to total protein.

## 1.2. Differential regulation of proteins in microsomal protein extract

One strategy to enhance the sensitivity of 2-DE analysis is to analyze sub-proteomes. Microsomal proteins were chosen since several components of AvrRpm1-RPM1 signaling are membrane-associated. RPM1 itself has been shown to be a peripheral plasma membrane protein (Boyes et al., 1998), and AvrRpm1 is also localized there *via* N-terminal myristoylation (Nimchuk et al., 2000). RIN4, a protein that is required for RPM1-mediated resistance, is also localized to membranes *via* C-terminal acylation (Kim et al., 2005; Mackey et al., 2002).

Microsomal protein extract was obtained by ultracentrifugation, and the microsomal pellet was subjected to 2-DE. The 2D gel from microsomal fractions showed good resolution

(Fig. 7A) and enabled roughly 1500 protein spots to be resolved (Fig. 8). However, comparison between figures 6A and 7A showed that both large and small subunits of Rubisco were even more abundant in microsomal than in total protein fractions. One possibility is that Rubisco was trapped in the microsomal vesicles. Nine candidate proteins were obtained from microsomal fractions, some of them overlapped with candidates from total protein extract, including phenylalanine ammonia-lyase (PAL) and glutathione transferase (GST), which are not classified as membrane proteins; hence supporting the hypothesis that abundant proteins were trapped in vesicles during the microsomal protein preparation.

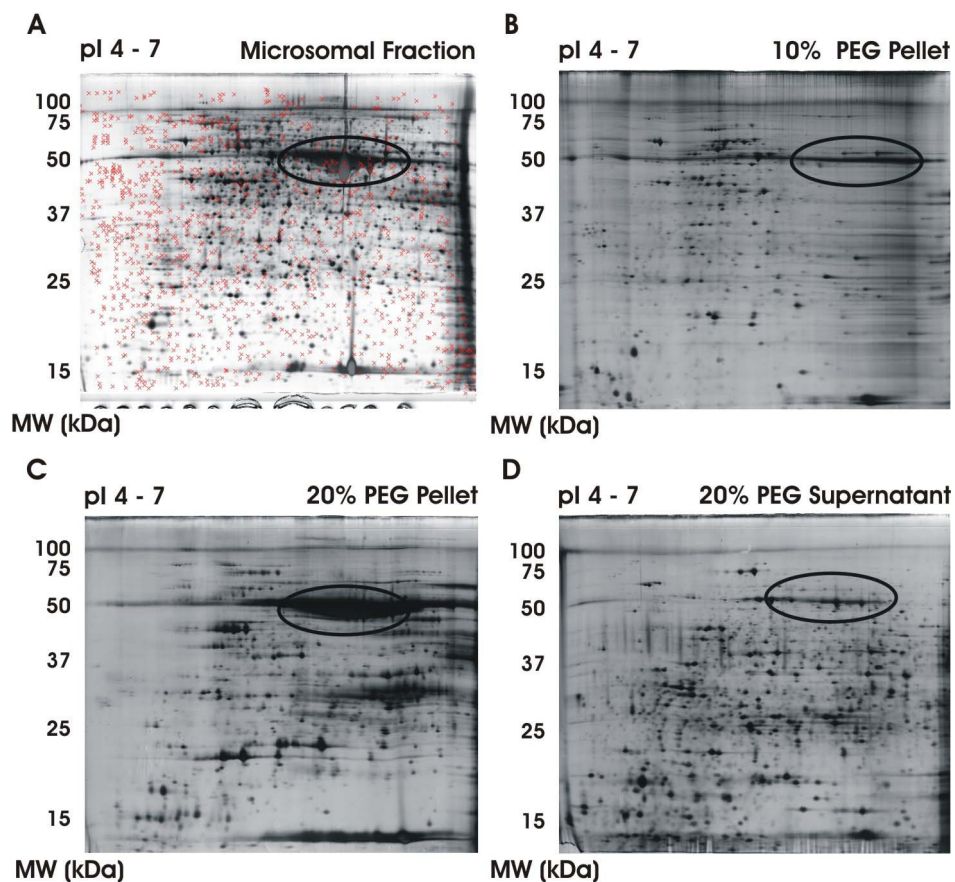


**Fig. 7** Silver-stained 2D gels of microsomal proteins and Rubisco-depleted microsomal proteins. (A) Microsomal proteins, (B) 10% PEG pellet, (C) 20% PEG pellet, (D) 20% PEG supernatant. The circled area indicates the location of Rubisco. The crosses in “A” indicate the positions of protein spots that are newly present or more than three fold increased in spot intensity, both in 10% PEG pellet and supernatant fractions compared to microsomal proteins.

The results from microsomal fraction analysis confirmed the findings from total protein with two additional candidates - myrosinase-associated protein (At3g14210) and a member of the remorin family, AtREM1.2 (At3g61260) (Raffaele et al., 2007). Each of these proteins was present as two isoforms; both isoforms of myrosinase-associated protein and one isoform of AtREM1.2 were up-regulated (Table 1). With the exception of AtREM1.2, potential signaling proteins with early up-regulation were not yet detected both in total protein

and microsomal fractions. The fact that both fractions contained highly abundant Rubisco suggested that low abundant signaling proteins could be severely masked by Rubisco, therefore Rubisco depletion was applied for further analysis.

### 1.3. Rubisco depletion from total protein and microsomal fractions

To deplete Rubisco from total and microsomal protein extracts, protocols from Kim et al. (2001) using PEG precipitation was adapted (Kim et al., 2001). Rubisco is highly enriched in the 20% PEG pellet, strongly reduced in the 10% PEG pellet and almost absent from the 20% PEG supernatant (Fig. 6 and 7). Therefore, the 10% PEG pellet and 20% PEG supernatant fractions were chosen for 2-DE analysis. Since the number of gels for each sample escalates after PEG fractionation, analysis was restricted to the early time point.

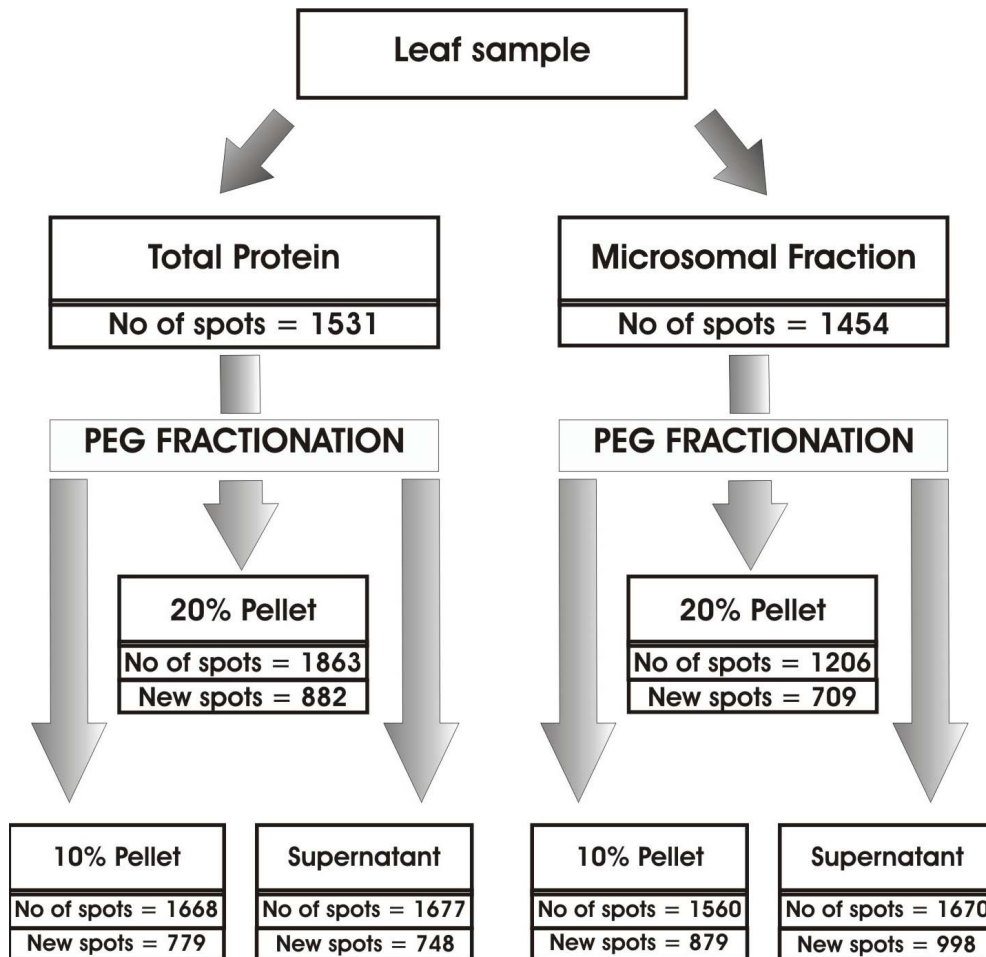


**Fig. 8** Schematic diagram depicting the fractionation steps applied to the protein samples. The number of protein spots recovered on 2D gels from each fraction and the number of protein spots newly present in each fraction compared to the unfractionated samples are indicated below each fraction. Representative gels of the fractionation procedure are shown in Fig. 3 and 4.

The relative complexity of total and microsomal proteins is revealed by the increment in proteins detected after fractionation (~700-1000 new spots per fraction, Fig. 8). When a

composite gel of the Rubisco-depleted fractions (i.e. 10% PEG pellet and 20% PEG supernatant fraction) was compared to the corresponding unfractionated sample, many new or protein spots with increased abundance were detected (marked as crosses in Fig. 6A and 7A). Thus, the coverage of the proteome is highly enhanced through the fractionation and Rubisco depletion.

After Rubisco depletion from total protein, new sets of proteins were found to be differentially regulated at the early time point. Only one candidate (PSII-P) from Rubisco-depleted total protein overlapped with candidates from total protein. Proteins involved in metabolism/photosynthesis are still predominant (Table 1). Rubisco depletion enhanced the detection of three new metabolism proteins which were not observed in total/microsomal protein. New candidates potentially involved in signaling include a protein phosphatase 2C (PP2C, At3g20630) and a protein with similarity to RNA-binding protein 45 (At1g11650). A third isoform of AtREM1.2 was detected, but the levels of this isoform were constant. Two proteins with unknown functions (At5g48930 and At4g39260) were found to be down-regulated.

The absolute number of candidates from Rubisco-depleted microsomal protein fraction was limited, but all candidates found were potentially involved in signaling (Table 1). No protein from metabolism or defense-related group was observed. Besides PP2C (At3g20630) and AtREM1.2, a C2-domain containing protein (At4g34150) and two more isoforms of AtREM1.2 were identified as new candidates.

#### **1.4. Comparison between Rubisco depletion using PEG fractionation and commercial Rubisco-removal spin column**

To evaluate the Rubisco-depletion strategy, total protein extract was also subjected to immunocapture using commercial Seppro® IgY-Rubisco spin column, which very effectively removed Rubisco (Fig. 9). The 2-DE pattern from the spin column FT (Fig. 9B) was similar to the supernatant fractions from total extracts after PEG fractionation (Fig. 6D). In an overlay of proteins obtained from the two methods, most of the spots matched well but the number of spots or the intensities for some spots were increased after PEG fractionation (visualized as orange-colored spots in Fig. 9C). The three candidates detected in Rubisco-depleted total proteins after PEG fractionation (RNA-binding protein 45, AtREM1.2 and PP2C, Fig. 10) were not detected in the sample based on the Seppro® IgY-Rubisco spin column.

**Table 1** Classification of differentially expressed proteins according to their presumed biological function and expression pattern in different fraction.

	T <sup>a</sup>			MF <sup>b</sup>			TPEG <sup>c</sup>		MFPEG <sup>d</sup>	
	0 <sup>e</sup>	2 <sup>f</sup>	6 <sup>g</sup>	0	2	6	0	2	0	2 (h)
<b>DEFENSE</b>										
1	+	++	+++	+	++	++				
2	+	++	++							
3	+	+	++							
4	+	+	++							
5	+	++	+++							
6				-	-	+				
7				-	-	+				
<b>RNA PROCESSING</b>										
1	+	+	++							
2							-	+		
<b>METABOLISM &amp; PHOTOSYNTHESIS</b>										
1	+	+	++	+	+	++				
2				+	+	++				
3	+	+	++							
4				-	-	+				
5				-	-	+				
6	+	+	++							
7	+	++	+++							
8	+	+	++							
9	+	+	++				-	+		
10	+	++	+++							
11	+	++	++							
12	-	-	+							
13							-	+		
14							-	+		
15							-	+		
<b>SIGNALING</b>										
1				+	+	+	+	+	+	+
2				+	++	++	+	++	+	++
3							+	+	+	+
4									+	++
5									-	+
6							+	++	+	++
7									+	++
<b>UNKNOWN FUNCTIONS</b>										
1	+	+	++							
2							++	+		
3							++	+		
Number of proteins										
16			9			11		7		

a) Total protein; b) Microsomal protein; c) Rubisco-depleted total protein; d) Rubisco-depleted microsomal protein; e) 0, f) 2, g) 6 hrs after dexamethasone treatment. 1), 2), 3), 4), 5): Superscript number beside the protein ID refer to protein isoforms observed on 2D gels

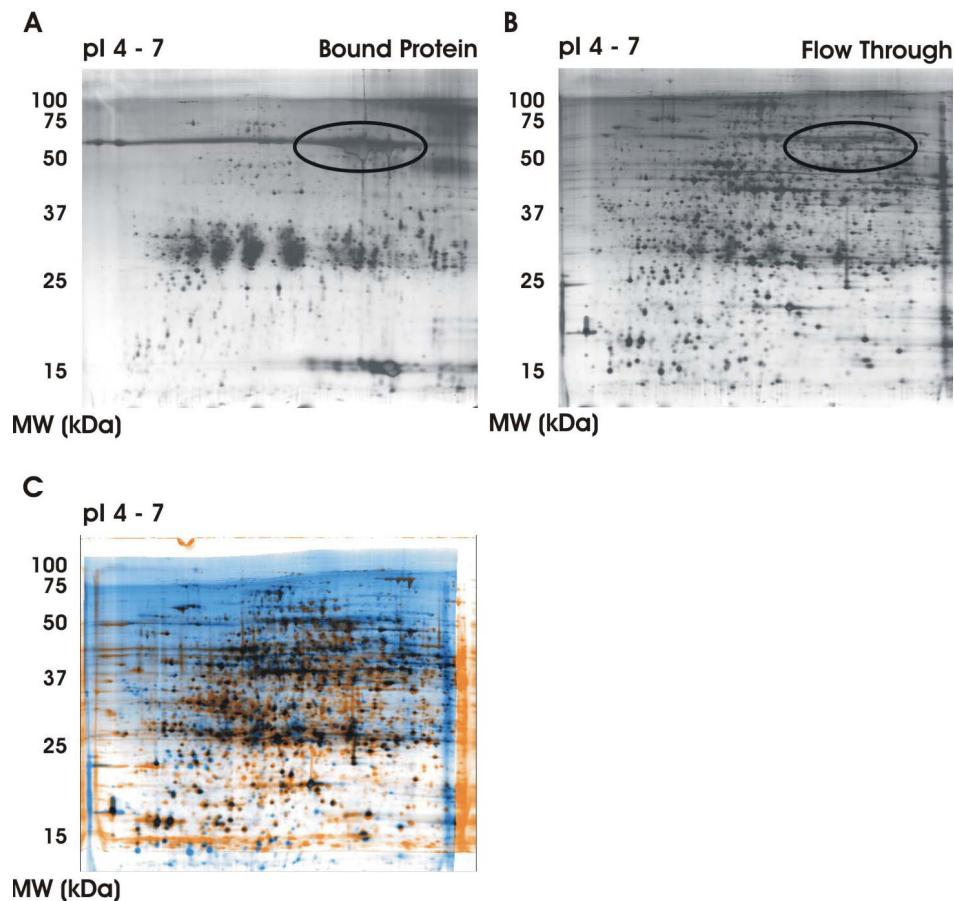


**Fig. 9** Silver-stained 2D gels from Rubisco depletion using Seppro<sup>®</sup> IgY Rubisco Spin Column. Proteins that bound to the IgY column (A) and the flow through fraction (B) were analyzed by 2-DE. (C) An overlay image between Flow Through from Seppro<sup>®</sup> IgY Rubisco Spin Column and supernatant from total protein after PEG fractionation. Image analysis software was used to compare the protein patterns. Orange-colored spots represent proteins from 20% PEG supernatant fraction, whereas blue-colored spots represent proteins from the Flow Through IgY Rubisco Spin Column.

### 1.5. Differential regulation of proteins of different biological functions

The biggest group of up-regulated proteins during the investigated “avrRpm1-RPM1” interaction is metabolism-related protein. These are either involved in carbon metabolism or photosynthesis (Table 1). Rubisco activase and three components of photosystem II were already up-regulated at the early time point, even long before HR formation. Two proteins with sequential function in carbon metabolism were enhanced in expression: one protein similar to malate dehydrogenase and the malic enzyme. In general, most of these metabolism proteins were already turned on early and kept at steady levels (profile b, Fig. 5A) or increased levels until the occurrence of HR (profiles a, Fig. 5A).

The second biggest group of up-regulated proteins is defense-related proteins, and among them are enzymes for redox regulation dominating this group (Table 1). Two expression patterns were observed for the defense proteins. Expression of GSTF7, peroxiredoxin and PAL were turned on at the early time point and preserved until HR

formation (profile a and b, Fig. 5A); while GSTF6 and myrosinase-associated protein were up-regulated at the occurrence of HR (profile d, Fig. 5A; and hence probably due to secondary stress).

All proteins with potential signaling function (protein with a similarity to RNA-binding protein 45, AtREM1.2, PP2C and C2-domain containing protein) involved in this interaction were up-regulated at the early time point, and in the case of AtREM1.2, it was continuously up-regulated until HR occurs (see Fig. 28).

### 1.6. Candidate signaling proteins are post-transcriptionally or post-translationally regulated

Transcript abundance for signaling protein candidates were analyzed by semi-quantitative RT-PCR (Fig. 10B). Transcript levels of the PP2C and C2-domain-containing proteins were elevated in an RPM1-dependent manner, as were their protein levels (Fig. 10A). AtREM1.2, however, showed decreased transcript levels, while RNA-binding protein 45 transcript levels remained constant during the analyzed time course (Fig 10B).

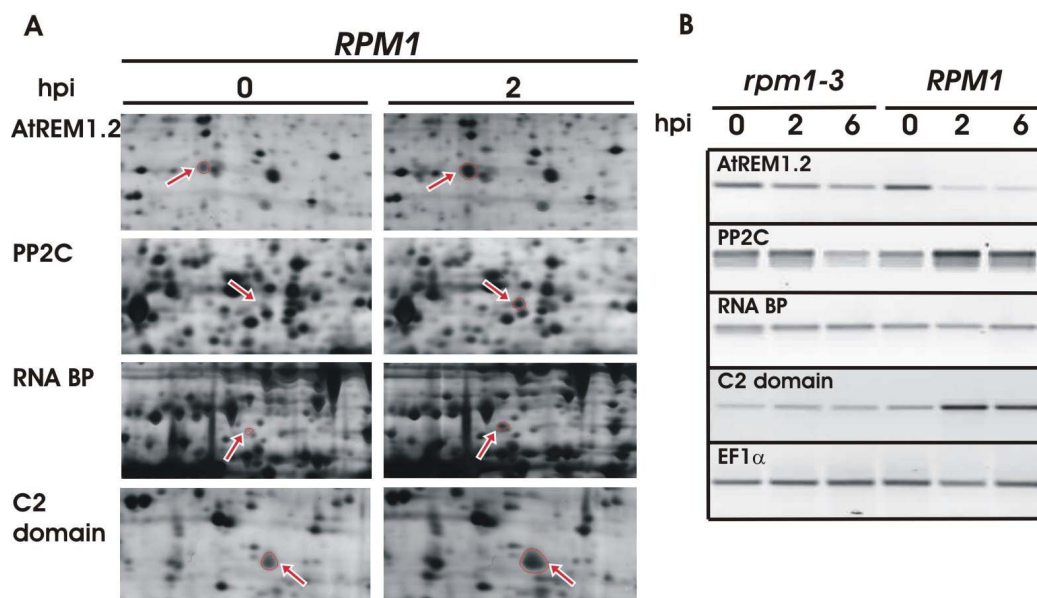


**Fig. 10** Correlation between the protein and transcript levels of four candidate proteins that were found to be up-regulated at the early time point. (A) Panels of selected regions of 2D gels showing protein levels (indicated by arrows) before and two hours after dexamethasone treatment. (B) Semi-quantitative RT-PCR analysis of the mRNA levels with EF1 $\alpha$  as a constitutive control at different time points after dexamethasone treatment is shown.

Two isoforms of AtREM1.2 were initially identified in microsomal fractions - both with very low spot intensity on 2D gels (Fig 11B). As more extensive fractionation was performed, more AtREM1.2 isoforms were uncovered.

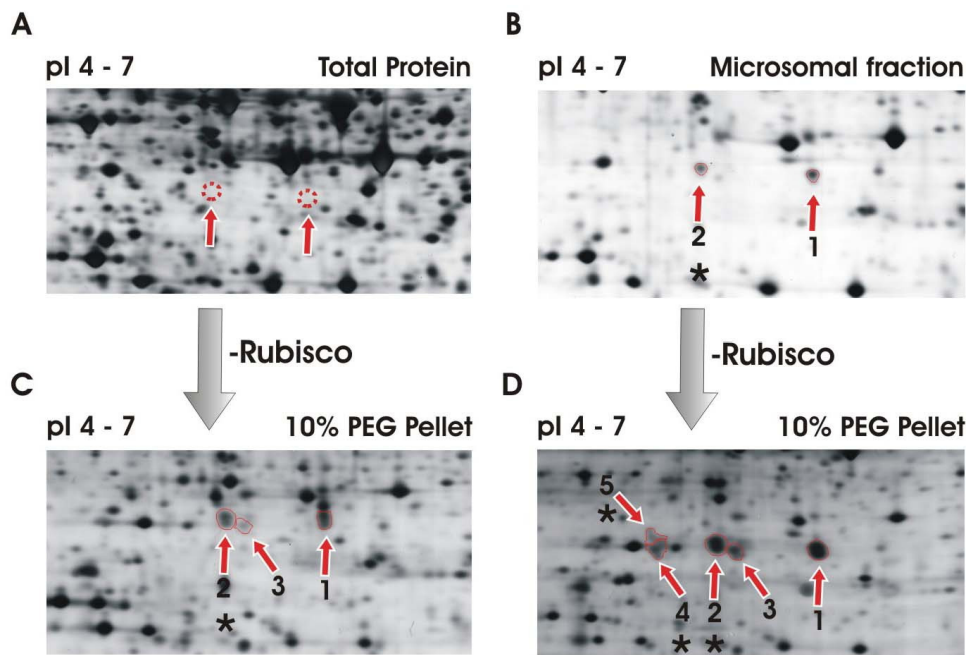


**Fig. 11** Increasing numbers of remorin isoforms were recovered after pre-fractionation. Remorin isoforms were not detected in total protein but their positions relative to other proteins are indicated (A). Two isoforms of remorin were detected in the microsomal protein fraction (B). After Rubisco depletion from total protein extract, a third isoform was detected in addition to the two isoforms found in B (10% PEG pellet, C). In the Rubisco-depleted microsomal protein fraction, a total of five isoforms were detectable (10% PEG pellet, D) “\*” indicates the isoforms that were up-regulated after dexamethasone induction.

In Rubisco-depleted total protein, three isoforms were identified with higher spot intensities than in the non-depleted sample (Fig. 11C); and in Rubisco-depleted microsomal protein, five isoforms were identified (Fig. 11D). Changes in abundance were only detected for some of the isoforms and these changes were RPM1-dependent. The pattern of these isoforms with a shift towards acidic pI indicated possible phosphorylation events during the AvrRpm1-RPM1 interaction.

The Protein Modification Screening Tool (ProMoST) was used to calculate the effect of single or multiple posttranslational modifications on the AtREM1.2 pI (Halligan et al., 2004). The theoretical phosphorylation patterns of AtREM1.2 predicted by ProMoST matched the pattern observed on 2D gels (Fig. 12). Furthermore, isoforms 4 and 5, as well as 2 and 3, have similar pIs but show minor differences in the second dimensions of 2-DE (Fig. 12), which might suggest additional modifications.

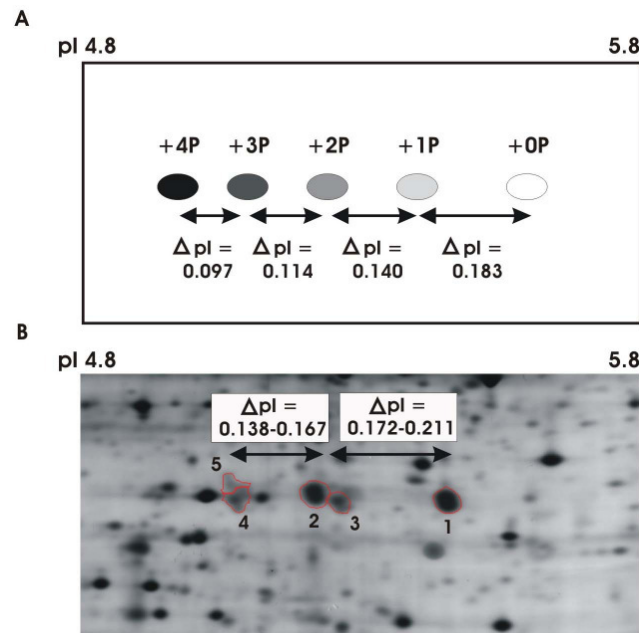


**Fig. 12** Theoretical pattern of phosphorylated remorin on 2D gels predicted by ProMoST matches the observed pattern. (A) The pI shift ( $\Delta pI$ ) on 2D gels resulting from single or multiple phosphorylation was calculated by ProMoST. The non-modified remorin is located at the most basic pI, while addition of phosphate groups shifts the pI towards the acidic region. (B) Selected region of a 2D gel of the 10% PEG pellet of microsomal protein showing remorin isoforms. The pI shift between isoform 1 and isoform 2/3 fits the theoretical value for single phosphorylation, while the pI shift between isoforms 2/3 and 4/5 fits the theoretical value for double phosphorylation. The disparity between theoretical and observed  $\Delta pI$  shifts might be due to the inaccuracy in pI calibration on 2D gels, which was determined by the ProteomWeaver software on the basis of the pI range of the IPG strips used.

In summary, screening for putative regulatory proteins in *avrRpm1*-RPM1 interaction resulted in four potential candidates: AtREM1.2, PP2C, RNA binding protein 45 and C2-domain containing protein. Functional analysis using gain-of-function and loss-of function approaches were carried out to study the role of each candidate in RPM1-mediated disease resistance. The collection of T-DNA insertion *Arabidopsis* mutants from publicly available database provide mutants for AtREM1.2, PP2C and RNA BP 45. Using these mutants, a preliminary analysis on altered disease resistance against *Pto* DC3000(*avrRpm1*) was performed, and changes were observed in plants with mutation in *AtREM1.2* and *PP2C*, which will be the focus of the following sections.

## 2. Functional analysis of the putative Protein Phosphatase 2C (At2g20630)

The PP2C, At2g20630, is up-regulated two hours after dexamethasone induction in RPM1-dependent manner, and is of low abundance since it was only detectable after PEG fractionation to deplete Rubisco from total and microsomal protein fractions (Fig. 13A, B).

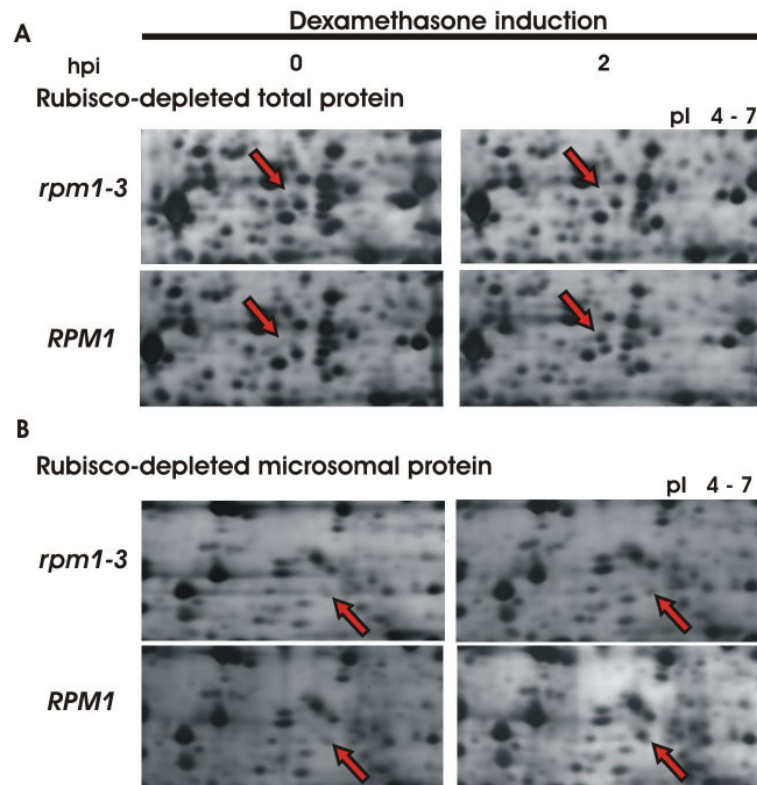


**Fig. 13** The PP2C up-regulation after dexamethasone induction. The PP2C was up-regulated 2 hpi only in the *RPM1* line, but not in the *rpm1-3* line. Panels of selected regions of 2D gels showing protein levels of the PP2C (indicated by arrow) before and after dexamethasone treatment in Rubisco-depleted total protein (A) and Rubisco-depleted microsomal protein (B).

The statistical significance of the PP2C up-regulation is indicated by student's t-test ( $P$  value  $< 0.01$  in Rubisco-depleted total protein and  $P$  value  $< 0.05$  in Rubisco-depleted microsomal protein, Table A2 Appendix).

### 2.1. PP2C up-regulation is specific for *avrRpm1*

Upon infiltration of wild type *Arabidopsis* (Col-0) with *Pto* DC3000(*avrRpm1*) the up-regulation of the PP2C can be seen at 2 hpi (Fig. 14), thus reproducing the finding from the transgenic DEX-inducible system. To check whether PP2C up-regulation can be induced by other effector proteins, *Arabidopsis* Col-0 plants were infiltrated with *Pto* DC3000 containing *AvrB*, another effector protein that also induces RPM1-mediated resistance (Mackey et al., 2002), or *avrRpt2*, the effector protein that induces RPS2-mediated resistance (Mackey et al., 2003). Virulent strain *Pto* DC3000, *Pto* DC3000(*hrpA*<sup>-</sup>) and flg22 were included to check the PP2C up-regulation by the whole arsenal of type three effectors, TTSS mutant and PAMP, respectively. Two hours after treatment with different bacterial strains, this PP2C was up-regulated exclusively by the infiltration of bacteria with *avrRpm1*.

Surprisingly, no up-regulation was seen with the *avrB*-containing strain, although *avrB* is considered to act similarly like *avrRpm1* (Fig. 14).

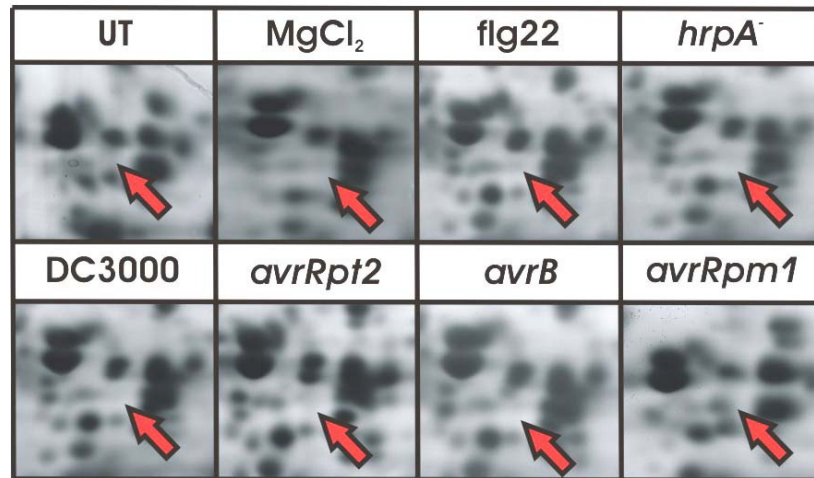


**Fig. 14** The PP2C up-regulation in *Arabidopsis* (Col-0) after infiltration with the indicated bacterial strains/treatments. Selected regions from 2D gels showing the presence of the PP2C (indicated by arrow) before (UT=untreated) and 2 hours after infiltration with MgCl<sub>2</sub>, flg22 (10 μM), *Pto* DC3000(*hrpA*<sup>-</sup>) (from left to right, upper panel), *Pto* DC3000, *Pto* DC3000(*avrRpt2*), *Pto* DC3000(*avrB*), *Pto* DC3000(*avrRpm1*) at 10<sup>8</sup> cfu/ml (from left to right, lower panel).

Since this PP2C (At2g20630) was only induced by *avrRpm1*, it is renamed to PIA1 (PP2C induced by *avrRpm1*-1) for easier reference.

## 2.2. At2g20630 T-DNA insertion mutants do not express PIA1

Induction of PIA1 may potentially regulate protein phosphorylation and hence signaling events in RPM1-mediated defense response. To investigate the role of PIA1 in RPM1-defense response by a loss-of-function approach, the SALK mutant collection was screened for At2g20630 mutants.

Two T-DNA insertion mutants for At2g20630 were identified for homozygosity of the insertion and these lines were subsequently sequenced to determine the position of the T-DNA inserts. The T-DNA insert is located in the second exon of At2g20630 fragment in the first T-DNA mutant (N519305) and at the border between the third exon and adjacent intron of At2g20630 fragment in the second T-DNA mutant (N605978) (Fig. 15A). Both mutants showed no accumulation of *PIA1* mRNA by RT-PCR analysis (Fig. 15B), and neither N519305 nor N605978 showed accumulation of PIA1 proteins two hours after infiltration with *Pto* DC3000(*avrRpm1*) (Fig. 15C). Altogether, these data showed that the *pial* mutants are null mutants that do not accumulate At2g20630 mRNA and protein.

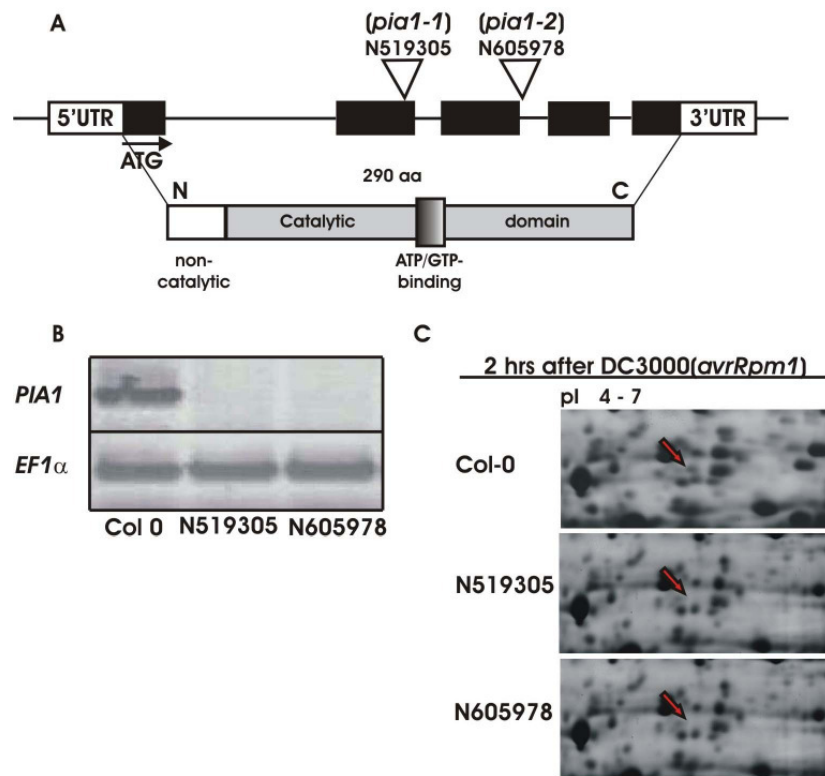


**Fig. 15** Two *Arabidopsis pial* null mutants from SALK Institute insertion database do not express *PIA1* mRNA and protein. (A) Schematic diagram depicting the gene structure and protein motifs of *PIA1*. The gene contains five exons, which encode a 290-amino acid protein consisting of non-catalytic and catalytic domains with ATP/GTP binding site. The position of T-DNA insert of the two mutants (N519305 and N605978) in the At2g20630 DNA fragment is indicated by triangles. (B) *PIA1* mRNAs were absent in the two mutants. (C) No *PIA1* protein was accumulated 2 hpi in the two mutants compared to Col-0.

### 2.3. The *pial* mutants showed enhanced resistance to *Pto* DC3000(*avrRpm1*), but not to *Pto* DC3000

“Gene-for-Gene” defense responses are normally accompanied by HR, which is considered as a programmed cell death mechanism by host plants to halt pathogen colonization (Hammond-Kosack and Jones, 1996). The mechanism of HR formation is still not clear, but production of ROS is believed as one trigger of HR besides its toxic effect to kill the pathogen (Hammond-Kosack and Jones, 1996). HR and ROS production can be checked easily using specific staining methods. Trypan blue staining is widely used to visualize HR formation in the form of cell death, since physiological changes in cells committed to die results in the uptake of the dye (Peterhansel et al., 1997). 3,3-diaminobenzidine (DAB) polymerizes with  $H_2O_2$  in the presence of peroxidase and produces reddish brown polymer (Thordal-Christensen et al., 1997).

To check whether *PIA1* regulates components of programmed cell death or acts in the pathway of ROS production, Col-0 and the *pial* mutants were infiltrated with *Pto*

DC3000(*avrRpm1*) and the infiltrated leaves were harvested seven hours after infiltration and subjected to trypan blue and DAB staining. Figure 16 shows representative leaves from Col-0 and the *pial* mutants after infiltration and staining. The uptake of trypan blue dye and the production of brown-colored DAB polymer in Col-0 and the *pial* mutants can not be distinguished, suggesting that neither HR formation nor ROS production are affected by the loss of *PIA1*.

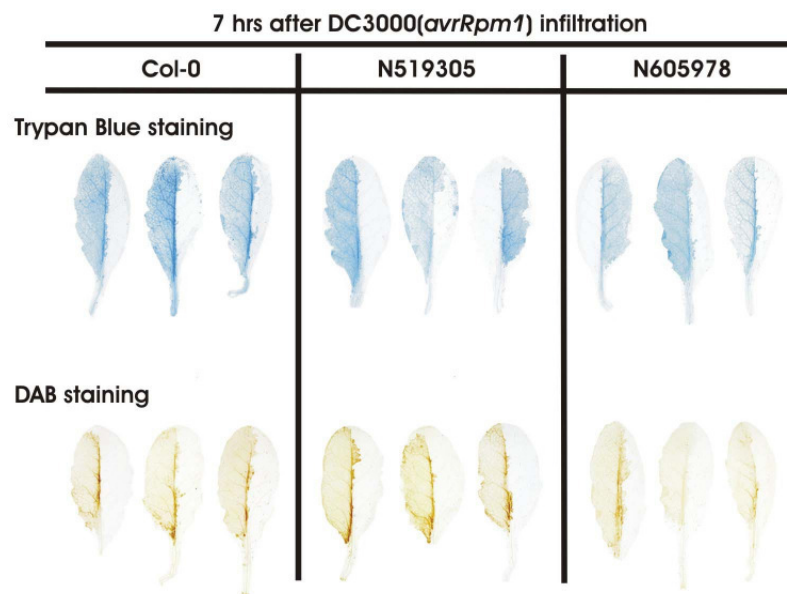


**Fig. 16** HR and ROS production in Col-0 and the *pial* mutants after *Pto* DC3000(*avrRpm1*) infiltration. One half of the leaves were infiltrated with bacteria resuspended to  $10^8$  cfu/mL. No difference was seen between Col-0 and the two *pial* lines in cell death (trypan blue staining) or ROS accumulation (DAB staining).

Resistance to pathogen colonization is not necessarily achieved by HR formation; there is evidence that in some cases *R-Avr* gene-mediated resistance appears not to involve HR (Hammond-Kosack and Jones, 1996). Therefore, the resistance against bacterial colonization in the *pial* mutants compared to Col-0 using virulent and avirulent strain of *P. syringae* was analyzed. The growth of the virulent strain *Pto* DC3000 was not different between Col-0 and the *pial* mutants (Fig. 17).

Contrarily, bacterial growth of *Pto* DC3000(*avrRpm1*) was reduced about five fold in the *pial* mutants compared to Col-0 two days after inoculation (Fig. 17). Statistical analysis using student's t-test estimates a *P* value < 0.05 for line N519305 and a *P* value < 0.01 for line N605978, indicating that the difference is significant. Four days after inoculation, the *pial* mutants still exhibited reduced bacterial growth about five fold compared to Col-0 with a *P* value < 0.05 for line N519305 and a *P* value < 0.1 for line N605978. Even though the

difference in bacterial growth is not enormous, it still indicates that loss of *PIA1* increases a certain degree of resistance specifically against the avirulent strain *Pto* DC3000(*avrRpm1*).

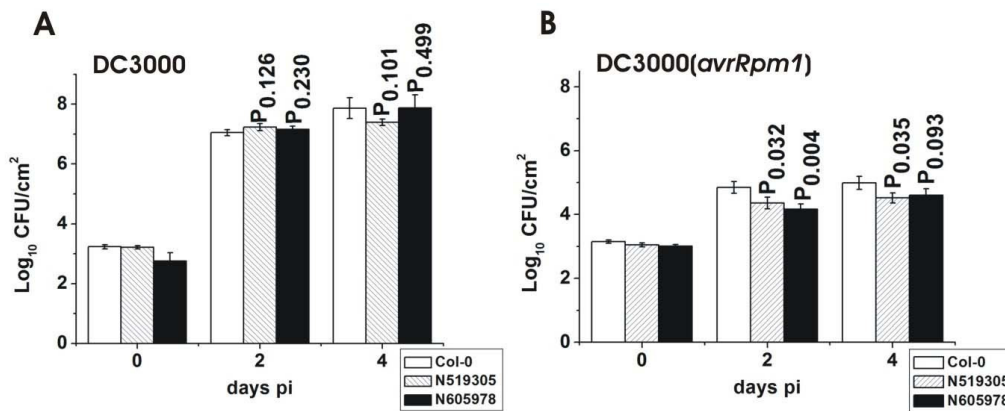


**Fig. 17** Loss of *PIA1* did not change the susceptibility to the virulent strain *Pto* DC3000, but increased the resistance to the avirulent strain *Pto* DC3000(*avrRpm1*). Plants were syringe-infiltrated with bacteria resuspended to 10<sup>5</sup> cfu/mL and bacterial growth was monitored *in planta* by assaying infiltrated leaves at 0, 2 and 4 days after inoculation. Col-0 and the *pia1* mutants showed similar susceptibility to *Pto* DC3000, but the mutants showed increased resistance to *Pto* DC3000(*avrRpm1*). Points are means of 18 plants  $\pm$  SE (DC3000) and 28 plants  $\pm$  SE (DC3000(*avrRpm1*)), sampling two leaves/plant for each time point, the experiment was repeated four times (*Pto* DC3000) and five times (*Pto* DC3000 (*avrRpm1*)).

#### 2.4. Expression of the RPM1-responsive gene, *MMP2*, is enhanced in the *pia1* mutants.

The observation that the loss of *PIA1* did not affect HR formation, but increased a certain degree of resistance against *Pto* DC3000(*avrRpm1*) suggests that *PIA1* might participate in the RPM1-mediated defense signaling. To test this hypothesis, the induction of several marker genes for the RPM1-mediated defense response in the *pia1* mutants compared to Col-0 was analyzed. Three RPM1-responsive genes were chosen for the analysis: the RPM1-induced protein kinase (*RIPK*; At2g05940), a matrix metalloprotease (*MMP2*; At1g70170) and a gene encoding a product of unknown function predicted to localize to the chloroplast (*TonB*; At2g32190) (de Torres et al., 2003).

Upon infiltration with *Pto* DC3000(*avrRpm1*), *MMP2* showed slightly enhanced transcript levels in the *pia1* mutants compared to Col-0, while *RIPK* and *TonB* were not affected (Fig.18). Peculiarly, transcript levels of *RIPK*, *MMP2* and *EF1 $\alpha$*  in the line N605978 were completely suppressed at 6 hpi (“\*” sign, Fig. 18). This suppression is not due to technical errors since it is observed in three independent biological experiments, and suggests the possibility of secondary insertions or mutations in the line N605978. Altogether, this data indicates that loss of *PIA1* alters the regulation of RPM1-mediated signaling leading to enhanced expression of a gene (*MMP2*) activated during the response.

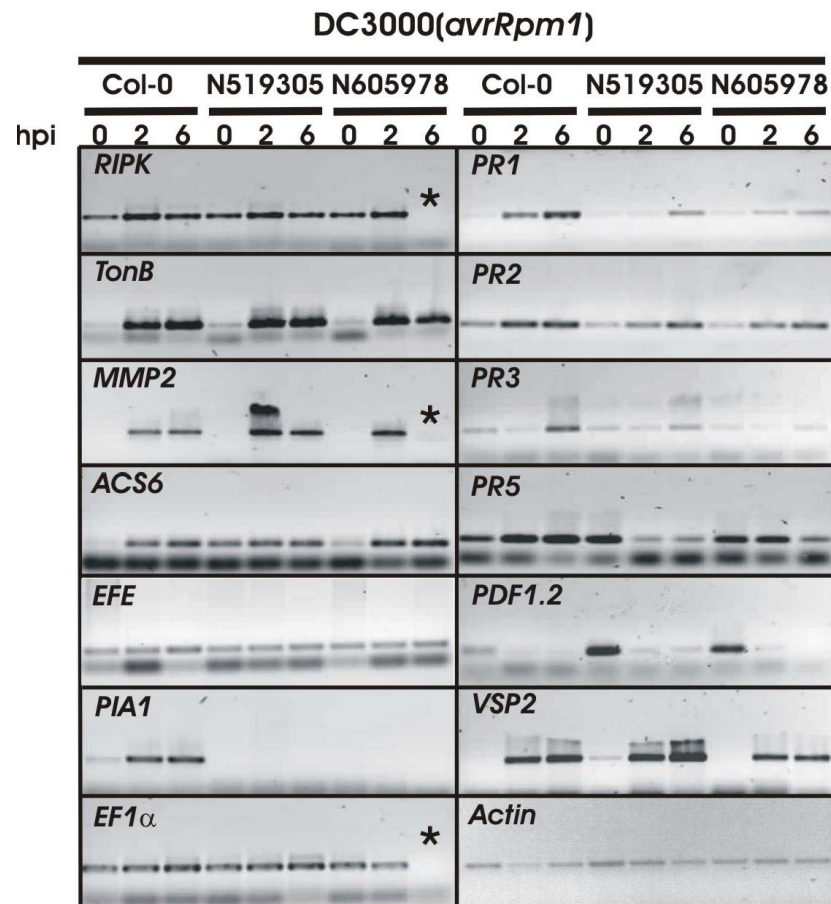


**Fig. 18** Loss of *PIA1* changed the expression pattern of several defense- and stress-related marker genes after infiltration with *Pto* DC3000(*avrRpm1*). Plants were syringe-infiltrated with *Pto* DC3000(*avrRpm1*) resuspended to  $10^8$  cfu/mL and the transcript levels of each gene were monitored *via* RT-PCR by sampling the infiltrated leaves at 0, 2 and 6 hpi. *EF1 $\alpha$*  and actin as constitutive controls were shown for every time point after infiltration. “\*” showed the missing expression of several genes at 6 hpi only in the line N605978. The experiment was repeated thrice with similar results.

## 2.5. *PIA1* regulates the induction of pathogenesis- and stress-related genes.

To examine whether *PIA1* also regulates other defense-related genes, RT-PCR for some pathogenesis- and stress-related genes was performed. Activation of pathogenesis-related (*PR*) genes was often associated with resistance in incompatible interactions; among them are *PR1*, *PR2* and *PR5* that are regulated by SA, and *PR3* that is regulated by JA and ET (Van Loon and Van Strien, 1999). Two stress responsive genes: *PDF1.2* (antimicrobial defensin), whose expression is prevented by mutations that block JA or ET signaling (Penninckx et al., 1996; Penninckx et al., 1998), and *VSP2* (vegetable storage protein) that is induced by JA (Rojo et al., 1998) were also included.

After infiltration with *Pto* DC3000(*avrRpm1*), transcript levels of all *PR* genes were continuously up-regulated until HR formation at 6 hpi in Col-0, but to a lesser extent in the *pial* mutants, and this observation is consistent for all *PR* genes (Fig. 18). Moreover *PR5*

basal transcript levels were higher in the *pial* mutants compared to Col-0, and the expression was down-regulated instead of being up-regulated during RPM1-mediated responses.

Increased basal levels were also observed for *PDF1.2* in both *pial* mutants, while *VSP2* transcript levels were similar between the *pial* mutants and Col-0 (Fig. 18). Since *PDF1.2* is JA- and ET-regulated, while *VSP2* is JA-regulated, it is likely that PIA1 regulation on *PDF1.2* occurred *via* ET pathway, instead of JA pathway. To test whether the ET pathway is also affected, two genes involved in ET biosynthesis were analyzed. *ACS6* basal levels were higher in the *pial* mutants prior to bacteria infiltration, while *EFE* (Ethylene forming enzyme/ACC oxidase) had similar expression pattern as Col-0 (Fig. 18).

Altogether, these results suggest that PIA1 negatively regulates the expression of *PR5*, *PDF1.2* and *ACS6* prior to infection, and during RPM1-mediated resistance it negatively regulates *MMP2* expression, but positively regulates the expression of *PR1*, *PR2*, *PR3*, and *PR5*. Of particular interest here is the opposite effects of *PIA1* on *PR5* before and after infection.

## **2.6. Differential regulation of pathogenesis- and stress-related genes in the *pial* mutants corresponds to changes in plant hormones involved in defense**

Two major hormonal pathways control plant defense responses: the SA- and JA/ET-dependent signaling pathways, which are important for the activation of stress-related genes (Dong, 1998; Kunkel and Brooks, 2002). Differential *PR* and stress marker gene expression described above may be related to the changes in SA, JA or ET production; or changes in perception of these phytohormones in defense signaling. To evaluate which hormone contributes to the altered gene expression in the *pial* mutants, quantification for SA, JA and ET levels were performed.

There was, generally, no significant difference in the JA and OPDA levels between the lines before or after infiltration with *Pto* DC3000(*avrRpm1*); JA was, however, lower in one of the *pial* mutants compared to Col-0 at 6 hrs pi ( $P$  value < 0.05, Fig. 19A,B).

ET levels were similar in Col-0 and the *pial* mutants under basal (untreated) conditions, as well as upon infiltration with *Pto* DC3000(*avrRpm1*) (Fig. 20). Infiltration with  $MgCl_2$  served as a control for the wounding effect on ET production when plants were infiltrated. The ET levels after  $MgCl_2$  infiltration were much lower compared to bacterial infiltration, thus the wounding effect during infiltration is negligible. However, the ET levels in the *pial* mutants appears to be lower compared to Col-0 after  $MgCl_2$  treatment, and these

are significant for both mutants (student's t test with  $P$  value  $< 0.05$  for line N519305 and  $P$  value  $< 0.01$  for line N605978).

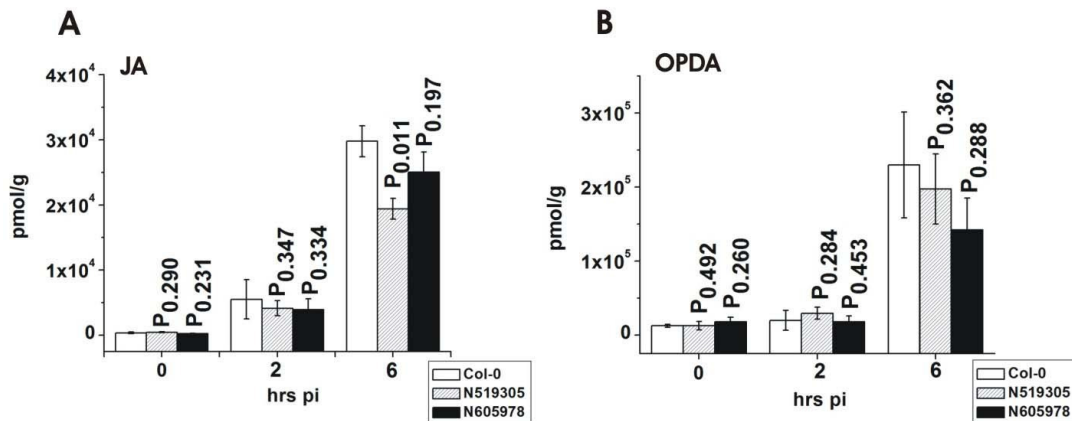


**Fig. 19** JA and OPDA levels in the *pial* mutants were not statistically different from Col-0 after *Pto* DC3000(*avrRpm1*) infiltration. Plants were infiltrated with *Pto* DC3000(*avrRpm1*) resuspended to 10<sup>8</sup> cfu/mL and the levels of JA and OPDA were measured after 0, 2 and 6 hpi from infiltrated leaves. At 6 hpi the JA and OPDA levels in the mutants were lower compared to Col-0, but only line N519305 showed significantly lower JA compared to Col-0. Points are means of three biological replicates  $\pm$  SE.

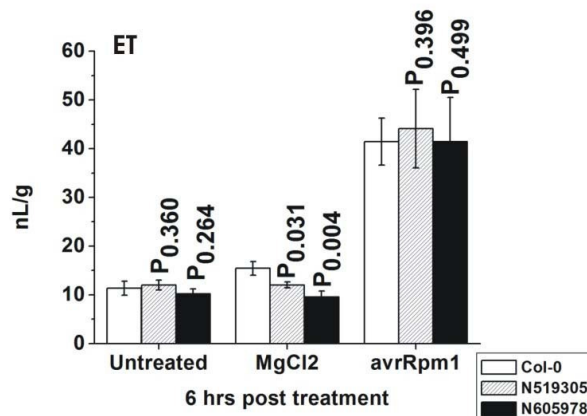


**Fig. 20** ET levels in the *pial* mutants and Col-0 were similar at basal condition and after *Pto* DC3000(*avrRpm1*) infiltration, but lower after MgCl<sub>2</sub> treatment. Leaves with no treatment or infiltrated with MgCl<sub>2</sub> and *Pto* DC3000(*avrRpm1*) resuspended to 10<sup>8</sup> cfu/mL were excised, and the ET production was accumulated for six hours after treatment and measured. Points are means of five to seven plants  $\pm$  SE; sampling four leaves/plant; the experiment was repeated twice.

The levels of free SA, SA glycoside (SAG) and total SA levels in the *pial* mutants were generally lower at 2 and 6 hpi compared to Col-0 (Fig. 21A, B, C), but only at 6 hpi both *pial* mutants accumulated significantly lower SA compared to Col-0 (student's t-test with  $P$  value  $< 0.05$ ), which indicates that the accumulation of SA is affected in the *pial* mutants.

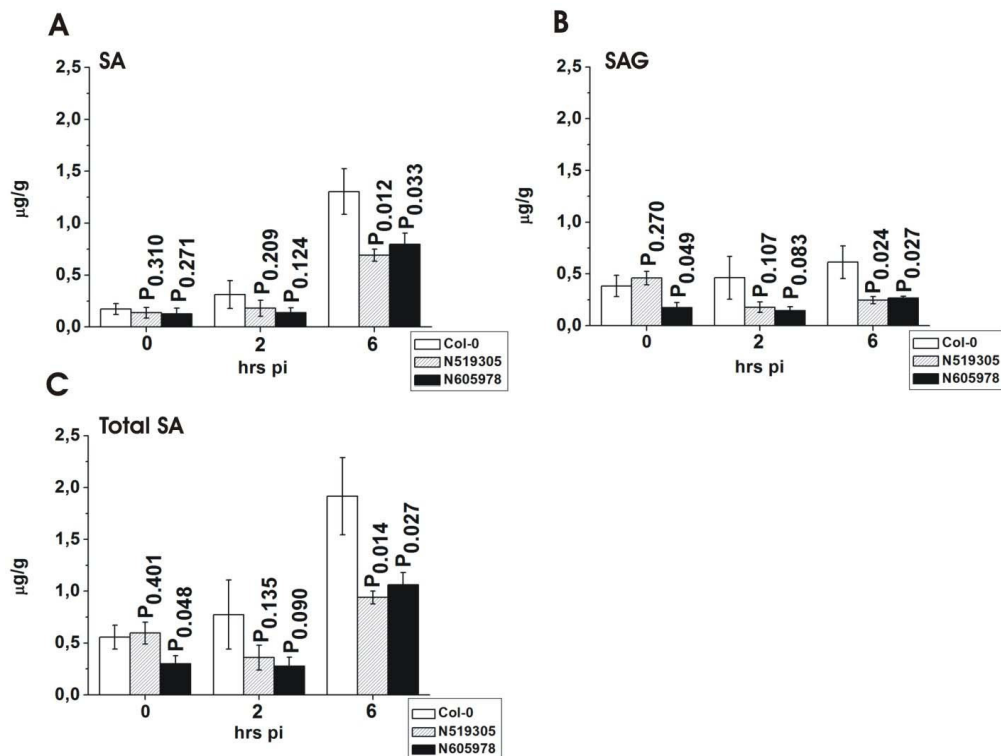


**Fig. 21** SA, SAG and total SA levels in the *pial1* mutants were significantly reduced compared to *Col-0*. Plants were infiltrated with *Pto* DC3000(*avrRpm1*) resuspended to  $10^8$  cfu/mL and the levels of SA (A), SAG (B) and total SA (C) were measured at 0, 2 and 6 hpi from infiltrated leaves. Points are means of 3 technical and 3 biological replicates  $\pm$  SE.

## 2.7. PIA1 does not regulate phosphorylation of RIN4 and AtREM1.2

Results from previous experiments have shown that PIA1 plays a role in resistance against *Pto* DC3000(*avrRpm1*), either by regulating a component of RPM1-mediated signaling or other defense-related genes *via* SA-dependent pathway. PIA1 can be assumed to function as phosphatase involved in phosphorylation events that occur after pathogen recognition and contribute to the establishment of resistance; hence it would be interesting to identify its direct or indirect target protein. The simplest approach to find PIA1 target is to look at proteins that are already known to be phosphorylated in the RPM1-mediated resistance. RIN4, a protein interacting with *avrRpm1* and required for RPM1-mediated signaling, is phosphorylated by introduction of *AvrRpm1* and *AvrB* (Mackey et al., 2002). Remorin (AtREM1.2) is also potentially phosphorylated after introduction of *AvrRpm1* (see Fig 24). This protein was found within this work as a candidate protein potentially involved in RPM1-mediated resistance *via* 2-DE, but its function is still unknown.

RIN4 phosphorylation can be observed as an increase of molecular weight on one dimensional gel (1-DE) after immunodetection by  $\alpha$ -RIN4 (Mackey et al., 2002). Two hours after infiltration with *Pto* DC3000(*avrRpm1*), RIN4 was phosphorylated and the

phosphorylation was lost six hours after infiltration (Fig 22A). The phosphorylation pattern in Col-0 was not changed in the *pial* mutants.

In contrast to the RIN4, AtREM1.2 phosphorylation does not cause a visible mobility shift in 1-DE. It was visualized as a shift towards the acidic pI range in 2-DE (see Fig. 12). AtREM1.2 phosphorylation on 2D gel was still observed in the *pial* mutants (Fig. 22B). Taken together, phosphorylation of RIN4 and AtREM1.2 are either not regulated by PIA1 or alternatively, there are other PP2Cs that can redundantly control the phosphorylation.

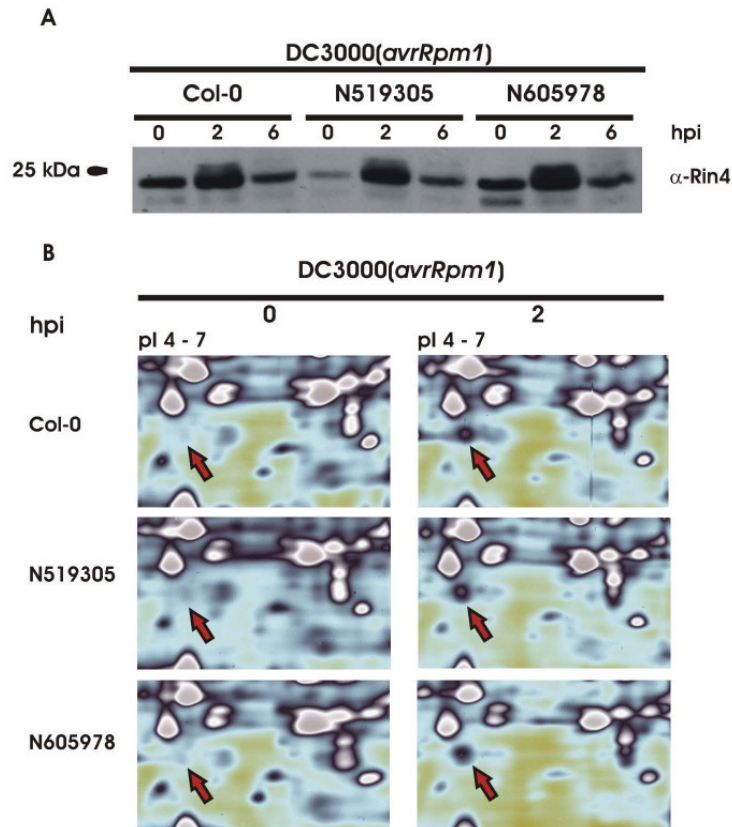


**Fig. 22** RIN4 and AtREM1.2 phosphorylation was not affected by loss of *PIA1*. Plants were infiltrated with *Pto* DC3000(*avrRpm1*) resuspended to  $10^8$  cfu/mL and harvested at 0, 2 and 6 hpi. Protein was extracted and subjected to 1-DE and western blot followed by immunodetection by α-RIN4 (A); or subjected to 2-DE and stained using silver (B). The panels of selected regions of 2D gels showing the presence of phosphorylated AtREM1.2 (indicated by arrow) at 2 hpi; the 2D gels were shown in pseudo color to enhance the visualization of AtREM1.2 spots.

## 2.8. Screening for putative *PIA1* targets by Proteomics analysis of the *pial* mutants.

One strategy to find a putative target is to search for differential regulation of proteins in the *pial* mutants compared to wild type plants during RPM1-mediated resistance. When *PIA1* is present and active in wild type plants, its putative targets would be dephosphorylated, shifting them to a more basic pI. This dephosphorylation event would be repressed in the absence of *PIA1*. Consequently, it would be possible to find a putative target by looking for proteins with a shift towards the acidic side in the *pial* mutants compared to wild type plants

as a result of hyperphosphorylation due to the absence of *PIA1* (Fig. 23A, upper panels). This approach may identify a direct target of PIA1. PIA1 may also regulate its target *via* another protein causing up/down-regulation of its putative target. Loss of *PIA1* would then prevent this up/down-regulation; subsequently one can look for proteins that are up/down-regulated in wild type plants, but not in the *pia1* mutants (Fig. 23A, lower panels). Proteins from such a screen will represent indirect targets of PIA1.

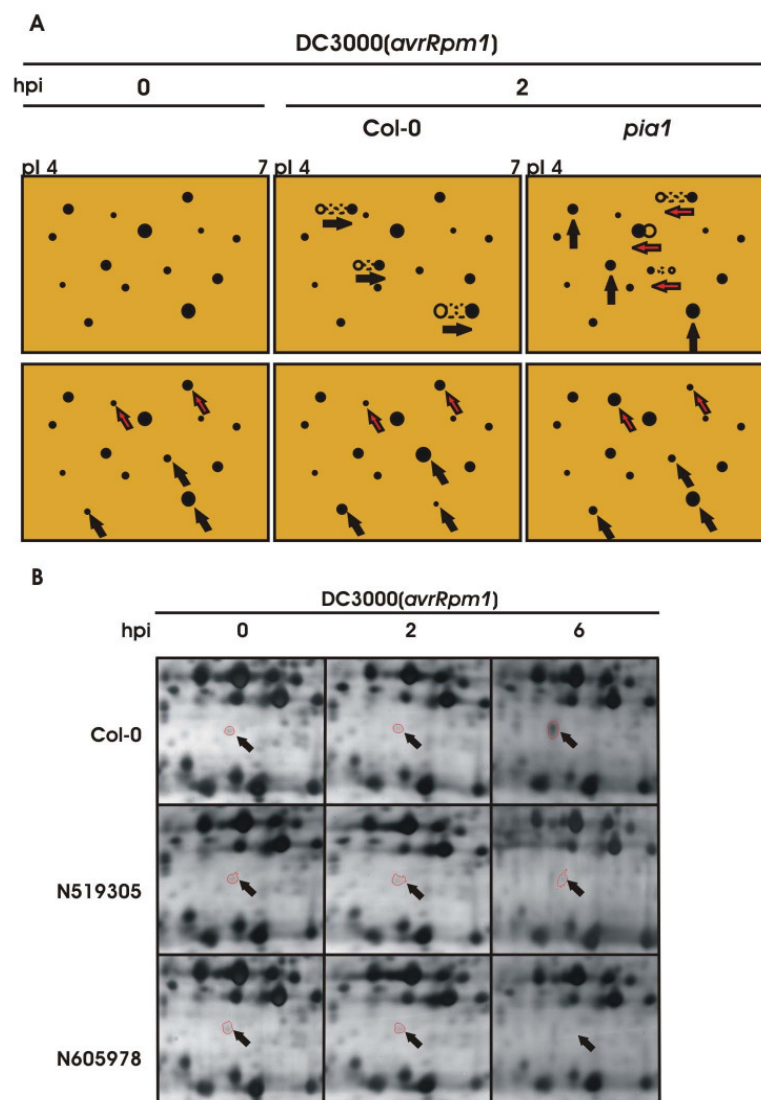


**Fig. 23** Theoretical and experimental 2D gels showing the differential expression of putative PIA1 targets in Col-0 and the *pia1* mutants after infiltration with *Pto* DC3000(*avrRpm1*). Putative targets were dephosphorylated to a more basic pI in Col-0 (indicated by black arrow), but not in the *pia1* mutants; or hyperphosphorylated to a more acidic pI in the mutants (indicated by red arrows), but not in Col-0 (upper panels, A). Putative targets can also be up-/down-regulated in Col-0, but not in the mutants; and some targets were up-/down-regulated in the mutants, but not in Col-0 (lower panels, A). One example of a potential PIA1 target that is up-regulated in Col-0 but not in the *pia1* mutants (B).

Screening for direct/indirect targets of PIA1 was performed on Rubisco-depleted total protein extract (10%PEG pellet and 20%PEG supernatant) after infiltration of wild type Col-0

and the *pial* mutants with *Pto* DC3000(*avrRpm1*). No direct target of PIA1 was detected in these fractions, but three proteins that were up-regulated in Col-0 but not in the *pial* mutants were found. These were very faint protein spots, suggesting that they are of low abundance even in the Rubisco-depleted fraction (Fig. 23B). One of them could be identified as the chloroplast-encoded gene for  $\beta$  subunit ATP synthase (ATPB) by LC-MS/MS, making it a putative indirect target of PIA1. The protein identification of two other candidates was not successful, probably due to the very low abundance of these proteins.

### 3. Functional analysis of AtREM1.2 (At3g61260)

AtREM1.2 (At3g61260), a protein belonging to the remorin family, was initially found to be up-regulated 2 hours post dexamethasone treatment. During more extensive fractionation to enrich for low abundance proteins, more AtREM1.2 isoforms were uncovered, some of which were differentially regulated during *avrRpm1*-RPM1 interaction. Figure 24 shows the presence of AtREM1.2 isoforms in different fractions. Two AtREM1.2 isoforms were detected in the microsomal protein fractions, where only isoform 2 showed increased expression (Fig. 24A). In Rubisco-depleted total protein, three isoforms were detected, and isoform 2 was again found to be up-regulated (Fig. 24B). Five isoforms were present in the Rubisco-depleted microsomal protein fraction, among which three of them (isoforms 2, 4 and 5) showed increased expression after dexamethasone treatment (Fig. 24C). This up-regulation is RPM1-dependent, since it was not detected in the *rpm1-3* line.

#### 3.1. $\alpha$ -Remorin recognized protein spots identified as AtREM1.2

A specific fragment from AtREM1.2 amino acid sequence was chosen and used to generate a peptide antibody (Fig. 25A). This peptide antibody was tested on the 2D Western blot of Rubisco-depleted microsomal protein. Three isoforms (isoforms 1, 2 and 3), which have been identified as AtREM1.2 by PMF MALDI-TOF/MS from silver-stained 2D gels (Fig. 25B) were detected by  $\alpha$ -Remorin, indicating that the protein identification was accurate (Fig. 25B). Isoforms 4 and 5, which are very low abundant, were not detected by  $\alpha$ -Remorin; even though they were visible after silver staining. This reduced sensitivity of  $\alpha$ -Remorin in detecting proteins on 2D Western blots was likely due to the difficulty to transfer proteins from 2D gels to the membrane. The blotting procedure of 2D gels required lengthened transfer time, yet the blotted gel still contained a lot of proteins after the transfer (data not shown).

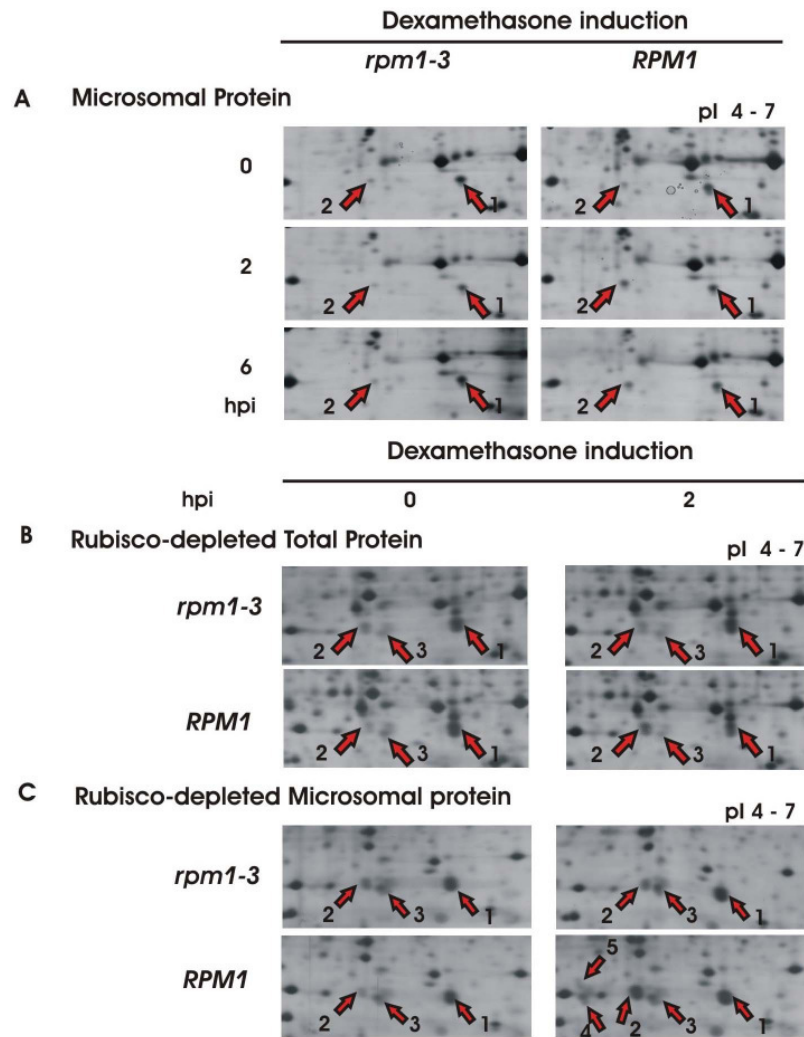


**Fig. 24** AtREM1.2 up-regulation after dexamethasone induction. AtREM1.2 isoforms 2, 4 and 5 were up-regulated 2 hpi only in the *RPM1* line, but not in the *rpm1-3* line. Panels of selected regions of 2D gels showing protein levels of different isoforms of AtREM1.2 (indicated by arrow) before and after dexamethasone treatment. In microsomal protein isoform 2 was up-regulated (A); in Rubisco-depleted total protein isoform 2 was up-regulated (B); in Rubisco-depleted microsomal protein isoforms 2, 4 and 5 were up-regulated (C).

Additionally,  $\alpha$ -Remorin also cross-reacted with proteins other than those that have been identified as AtREM1.2 (protein spots in green-colored circle; Fig. 25B). Protein identification by PMF MALDI-TOF/MS revealed that all of those proteins neither belonged to remorin family nor contained the specific peptide sequence used to generate  $\alpha$ -Remorin. To increase the specificity of  $\alpha$ -Remorin, antibody purification based on the peptide affinity was performed. The purified fractions still contained the antibodies that resulted in non-specific cross reaction. Furthermore, the unspecific immunoreactions could also be competed with AtREM1.2 specific peptide, thus the peptide affinity-based purification would not result in purified  $\alpha$ -Remorin. Even though this  $\alpha$ -Remorin suffered from rather low specificity and

sensitivity in recognizing AtREM1.2, it is still useful for immunodetection on 1D/2D western since AtREM1.2 is resolved at distinct pI and MW.

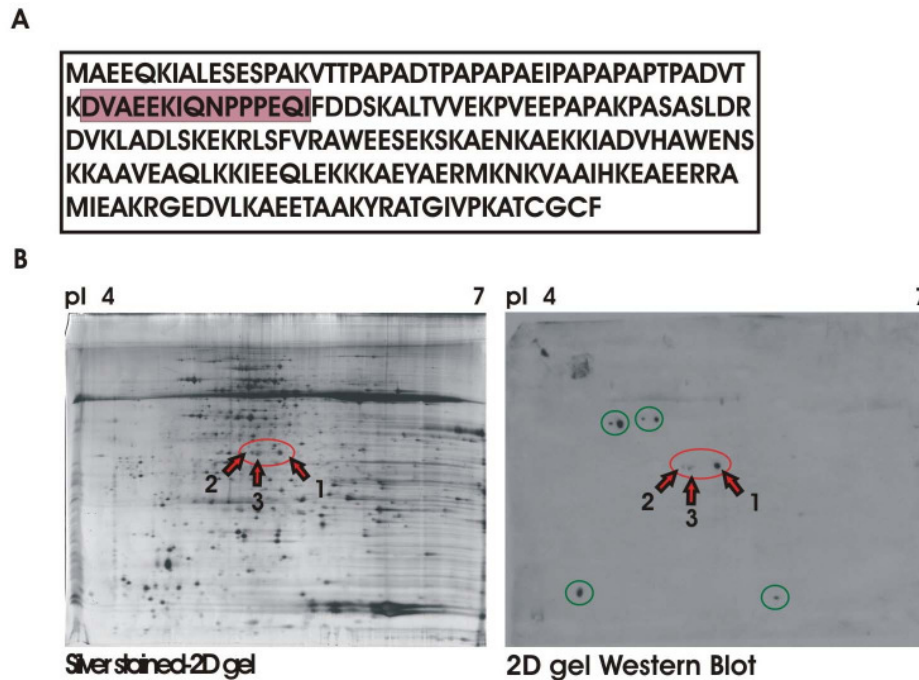


**Fig. 25**  $\alpha$ -Remorin detected the protein spots identified as AtREM1.2. A complete amino acid sequence of AtREM1.2; the highlighted peptide sequence was used to generate peptide antibodies (A). Silver-stained 2D gels from Rubisco-depleted microsomal protein and corresponding 2D Western with  $\alpha$ -Remorin (B). The protein spots that have been identified by PMF MALDI-TOF/MS and confirmed by  $\alpha$ -Remorin are indicated by arrows. The protein spots in green-colored circled resulted from non-specific reaction

### 3.2. Up-regulation of AtREM1.2 observed on silver-stained 2D gels was confirmed by 2D-Western using $\alpha$ -Remorin

The  $\alpha$ -Remorin was used to confirm the up-regulation of AtREM1.2 observed on the silver-stained 2D gels. Rubisco-depleted microsomal protein from dexamethasone-induced *RPM1* plants was subjected to 2D-PAGE, transferred to the membrane and detected using  $\alpha$ -Remorin.

Isoforms 1 and 2 were detected by  $\alpha$ -Remorin in untreated and treated plants (Fig. 26). Overlay between the “t=0 hpi” and “t=2 hpi” samples (Fig. 26) showed higher intensity of isoform 2 in “t=2 hpi” sample (represented by blue color) compared to “t=0 hpi” sample (represented by orange color); which is in agreement with the result from silver-stained gels. Isoform 3 showed higher intensities in the untreated sample, which was also observed in the silver stained-gels, but this observation was not reproducible for all biological replicates.

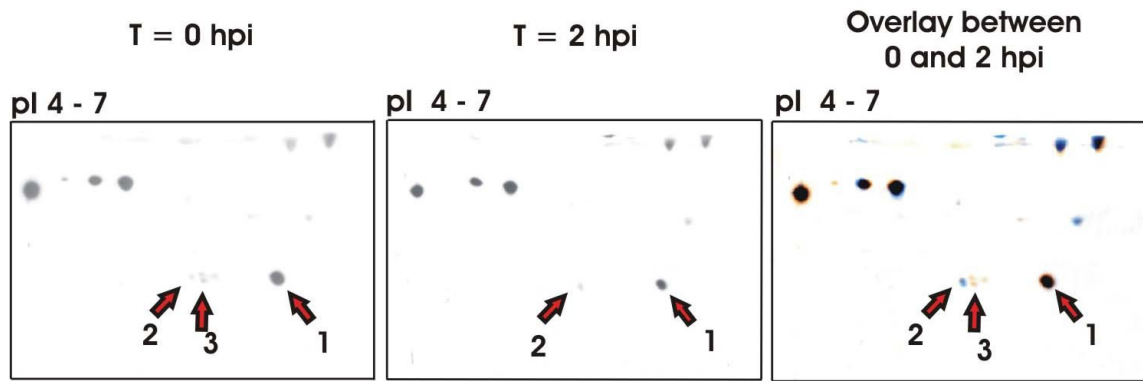


**Fig. 26** AtREM1.2 up-regulation was also observed on 2D Western immunodetected by  $\alpha$ -Remorin. Panels with selected regions of 2D Westerns showing the protein levels of AtREM1.2 isoforms (indicated by arrow). Three isoforms (left panel) and two isoforms (middle panel) were present before and 2 hours after dexamethasone treatment. The overlay between two samples showed increased expression of isoform 2 at 2 hpi (represented by blue color).

### 3.3. AtREM1.2 is up-regulated by *avrRpm1* and *AvrB*, but not by *AvrRpt2*

The AtREM1.2 up-regulation was further tested on wild type *Arabidopsis* (Col-0) upon infiltration with different bacterial strains.

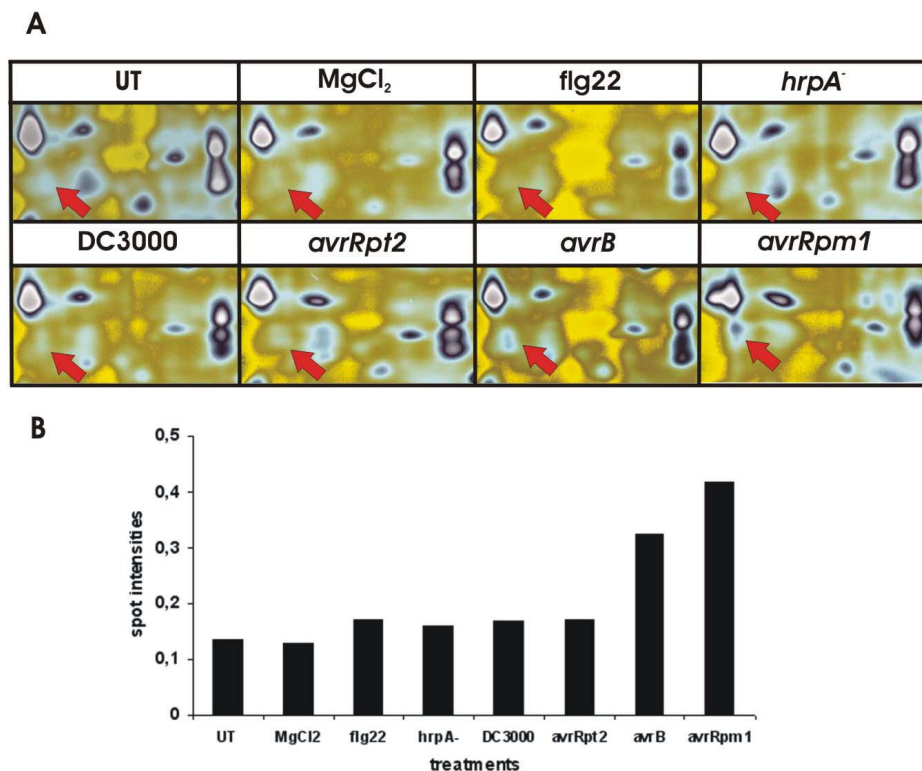


**Fig. 27** AtREM1.2 up-regulation in wild type Col-0 after infiltration with indicated bacterial strains/treatments. Panels with selected regions of silver-stained 2D gels in pseudo colour showing the protein levels of AtREM1.2 isoform 2 (indicated by arrow) before and after infiltration with MgCl<sub>2</sub>, flg22 (10  $\mu$ M), *Pto* DC3000(*hrpA*<sup>-</sup>) (from left to right, upper panel), *Pto* DC3000, *Pto* DC3000(*avrRpt2*), *Pto* DC3000(*avrB*), *Pto* DC3000(*avrRpm1*) at 10<sup>8</sup> cfu/mL (left to right, lower panel) (A). Diagram bar chart showing the spot intensities of AtREM1.2 isoform 2 calculated by image analysis software after different treatments (B).

Figure 27A shows 2D gels of Rubisco-depleted total protein from the untreated sample and samples infiltrated with  $MgCl_2$ , flg22, virulent strain *Pto* DC3000, *Pto* DC3000 containing *hrpA* mutation, *avrRpm1*, *avrB* or *avrRpt2*. Image analysis software was used to calculate the spot intensities of AtREM1.2 isoform 2, and the value after normalization was depicted in the bar chart (Fig. 27B). Corresponding to the results from the dexamethasone system, up-regulation of AtREM1.2 isoform 2 can be observed at two hpi with *Pto* DC3000(*avrRpm1*). It was also up-regulated after infiltration with *Pto* DC3000(*avrB*), but not with other bacterial strains or treatments.

### 3.4. Up-regulation of AtREM1.2 was continued until 6 hpi when HR occurred, and the expression went back to basal levels at 10 hpi

To follow the regulation of AtREM1.2 during AvrRpm1-RPM1 interaction, its expression was observed during later time points after dexamethasone induction. AtREM1.2 isoform 2 was up-regulated at two and six hpi, but at ten hpi it went back to basal levels (Fig. 28). The AtREM1.2 up-regulation was specific for RPM1-mediated response, since the *rpm1-3* line did not show any increase in AtREM1.2 expression even until 10 hpi.

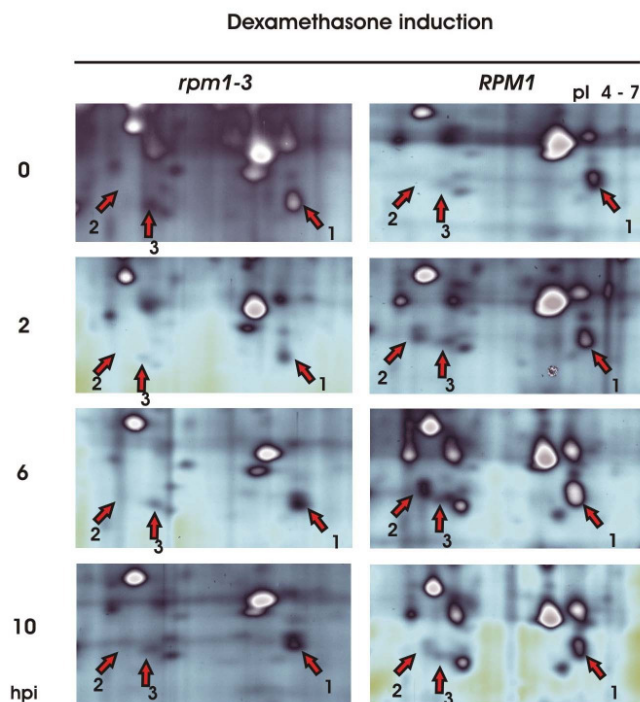


**Fig. 28** Up-regulation of AtREM1.2 continued until HR formation and returned to the basal levels afterwards. The *RPM1* and *rpm1-3* lines were treated with 20  $\mu$ M dexamethasone and leaf samples were collected at 0, 2, 6 and 10 hpi, and subjected to total protein extraction with Rubisco depletion. Panels with selected regions of silver-stained 2D gels in pseudo colour showing the protein levels of AtREM1.2 isoforms. Protein levels of isoform 2 were enhanced at 2 and 6 hpi, but went down at 10 hpi (right panels). The up-regulation of AtREM1.2 was only observed in the *RPM1*, but not in the *rpm1-3* line (left panels).

### 3.5. AtREM1.2 is present in the detergent resistant membrane (lipid raft membrane) fraction

Proteins from the remorin family have been frequently identified in the lipid raft preparation (Bhat and Panstruga, 2005; Lefebvre et al., 2007; Mongrand et al., 2004; Morel et al., 2006). To check whether AtREM1.2 is also localized to lipid raft membranes, we analysed the detergent-resistant membrane fraction (DRM) from wild type *Arabidopsis* Col-0. A DRM preparation protocol from Borner et al. (2005) was adapted. Microsomal protein fraction (TM) was obtained from total protein extract by ultracentrifugation and subsequently solubilized in the Tris buffer containing 2% Triton X-100 at 4°C, and separated in a sucrose gradient by ultracentrifugation. The lipid raft fraction (DRM) was isolated as a floating layer in the sucrose gradient due its high lipid composition, while the soluble fraction (DSM) was precipitated from the total sucrose gradient. The DRM fraction, DSM fraction and TM were subjected to 1-DE and proteins immunodetected using  $\alpha$ -Remorin and  $\alpha$ -BiP (Fig. 29).

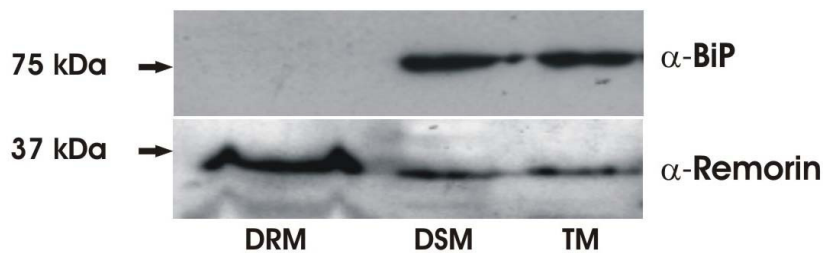


**Fig. 29** AtREM1.2 was present in Detergent Resistant Membrane (DRM; lipid raft fraction). *Arabidopsis* Col-0 was subjected to microsomal protein isolation (TM) and lipid raft isolation by separation in sucrose gradient with ultracentrifugation. The same amount of the DRM, DSM (detergent soluble membrane) and TM were loaded in each lane and subjected to western blot with  $\alpha$ -Remorin and  $\alpha$ -BiP.

While some AtREM1.2 is solubilized (i.e. in the DSM fraction), it is also found in the DRM fraction.  $\alpha$ -BiP was used to check whether there is contamination from DSM in the DRM fraction during the preparation. BiP is a luminal endoplasmic reticulum protein that is released during TritonX-100 treatment. BiP was exclusively present in TM and DSM, but not in DRM fraction, indicating that the DRM preparation was not contaminated with DSM protein.

### 3.6. Dephosphorylation assay confirms AtREM1.2 phosphorylation during RPM1-mediated resistance

AtREM1.2 was detected as several isoforms. Three of the five detected isoforms in the Rubisco-depleted microsomal fraction (isoform 2, 4 and 5) showed up-regulation during *avrRpm1*-RPM1 interaction (Fig. 24C). The acidic shift of isoform 2/3 from isoform 1

suggested single phosphorylation, while the acidic shift of isoform 4/5 from isoform 1 suggested double phosphorylation, which was predicted by ProMoST (see Fig. 12).

To confirm the AtREM1.2 phosphorylation, a dephosphorylation assay was performed. The microsomal protein fraction was isolated, treated with and without  $\lambda$ -phosphatase and subsequently precipitated by PEG to obtain the 10% PEG pellet that enriches most of the AtREM1.2 isoforms. 2D gels of the 10% PEG pellet with and without  $\lambda$ -phosphatase treatment is depicted in figure 30. Spot intensities of isoforms 2, 4 and 5 were reduced after  $\lambda$ -phosphatase treatment, while isoform 1 and 3 seem to have the same intensity before and after  $\lambda$ -phosphatase treatment. This data demonstrates that isoform 2, 4 and 5 are likely phosphorylated, while isoform 1 and 3 are not. The small difference in migration between isoforms 2-3 and isoforms 4-5 suggest another modification.

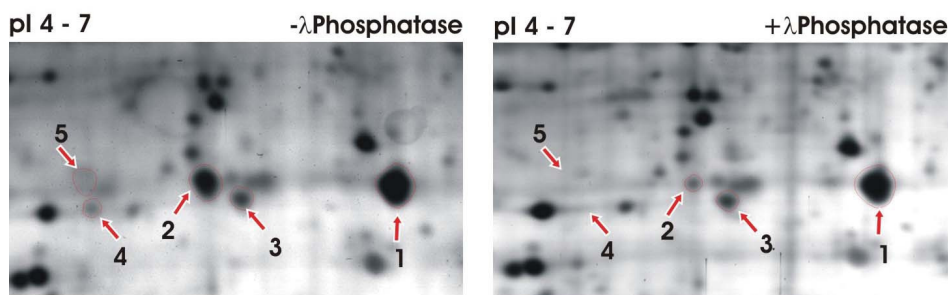


**Fig. 30** Isoforms of AtREM1.2 underwent phosphorylation. Dexamethasone-induced *Arabidopsis* samples were subjected to microsomal protein extraction and treated with (right panel) and without (left panel)  $\lambda$ -Phosphatase, followed by Rubisco depletion. Isoforms 2, 4 and 5 were disappeared after phosphatase treatment, indicating they were phosphorylated.

### 3.7. Interaction between AtREM1.2 and RIN4 was not detected

To check the possibility of direct interaction between AtREM1.2 and RIN4, co-immunoprecipitation using  $\alpha$ -Remorin and  $\alpha$ -RIN4 was performed.

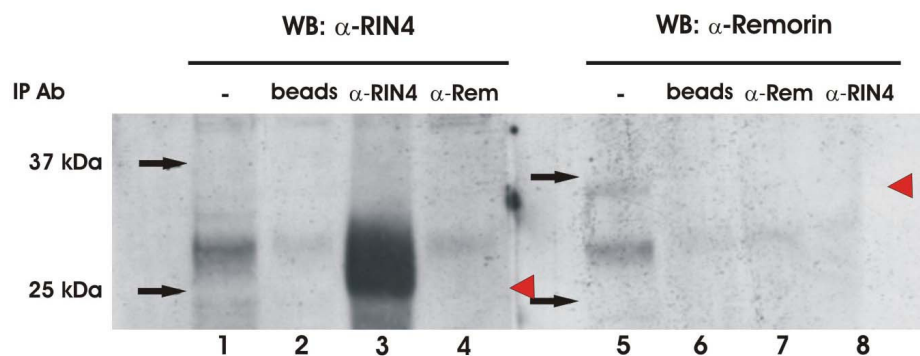


**Fig. 31** Interaction between AtREM1.2 and RIN4 was not detected. Co-IP with  $\alpha$ -RIN4 showed that RIN4 did not associate with AtREM1.2. Reciprocal co-IP with  $\alpha$ -Remorin did not show clear result since AtREM1.2 itself was not immunoprecipitated by  $\alpha$ -Remorin. The positions of RIN4 (MW = 24 kDa) and AtREM1.2 (MW = 32 kDa) are indicated by red arrows.

RIN4 was undetectable in the microsomal protein fraction (Fig. 31, lane 1), but showed an intense band at MW = 25 kDa after immunoprecipitation using  $\alpha$ -RIN4 (Fig. 31, lane 3). Even though RIN4 was immunoprecipitated, AtREM1.2 was not co-immunoprecipitated by  $\alpha$ -RIN4 (Fig. 31, lane 8). AtREM1.2 was detected in the microsomal fraction as a faint band at 35 kDa (Fig. 31, lane 5), but it was not immunoprecipitated by  $\alpha$ -Remorin (Fig. 31, lane 7), and consequently the co-immunoprecipitation of RIN4 using  $\alpha$ -Remorin was not possible (Fig. 31, lane 4). IgG beads with addition of pre-immune serum of the antibodies was used as a negative control (Fig. 31, lane 2 and 6). A faint band at molecular weight above 25 kDa, which was present in almost all lanes, is likely an unspecific reaction. The results from Co-IP can only imply that physical interaction between RIN4 and AtREM1.2 was not detected.

### **3.8. Over expression of *AtREM1.2* did not cause necrosis, but silencing of *AtREM1.2* produced subtle necrosis during the *Agrobacterium*-mediated transient expression**

To study the role of AtREM1.2 in the plant defense response mediated by avrRpm1-RPM1 interaction, loss-of-function and gain-of-function approaches were used. Two SALK T-DNA insertion mutants of At3g61260 were obtained. The first insertion line was screened for homozygosity but sequencing analysis showed that the T-DNA insert is located after the stop codon. Only heterozygous plants were found for the second line, and southern blot analysis revealed that the T-DNA insert in the putative knock out line was not within the At3g61260 gene. Both of these T-DNA insertion mutants were not used for further analysis.

Using Gateway cloning, over-expressing, knockdown and inducible lines were generated. The over-expressing lines were generated from full-length *AtREM1.2* under control of 35S promoter and tagged with CFP, YFP or Strep tag. The inducible lines were driven by an estradiol inducible promoter, while the knockdown line was based on RNA-interference silencing by introducing inverted repeats of *AtREM1.2*. All the constructs were transformed into wild type Col-0 as well as the transgenic Dex:avrRpm1 plants (with *rpm1-3* or *RPM1* background) used in the Proteomics screen. The over-expressing, inducible and RNAi lines were screened at DNA levels to check for the presence of the constructs in the putative transformed plants and at the protein levels to check the effect of over/induced expression and silencing at the proteins levels.

From 27 over-expressing lines that passed screening at the DNA levels, only two lines showed positive phenotype at the protein levels. The rest did not show increased protein levels, contrarily they showed co-suppression of endogenous and transgene *AtREM1.2*. This

observation suggested the possibility that over-expression of *AtREM1.2* may lead to lethality. To test this possibility, Agrobacterium-mediated transient expression using *AtREM1.2* constructs for over/induced expression and silencing was performed.

Three different constructs with 35S-promoter, one construct with inducible promoter and one construct with RNAi silencing were expressed transiently in *N. benthamiana* (Fig. 32). As a positive and negative control, PcMKK5<sup>DD</sup> and PcMKK5<sup>KR</sup> were also included. PcMKK5<sup>DD</sup> is capable of eliciting an HR-like cell death when expressed transiently in tobacco, while PcMKK5<sup>KR</sup> is not (Lee et al., 2004).

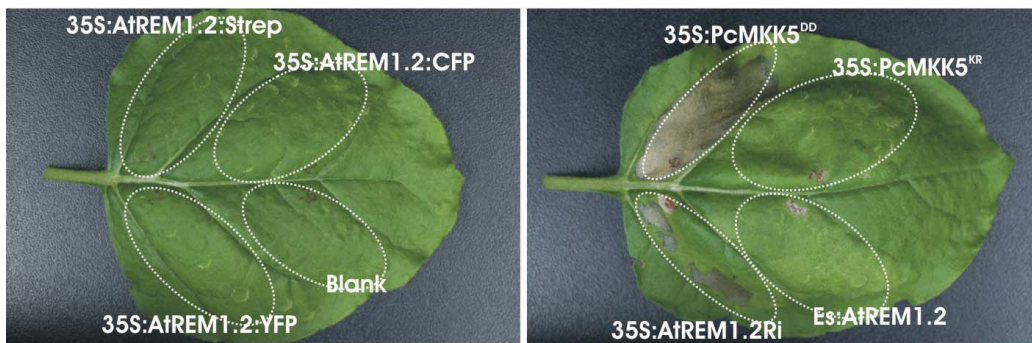


**Fig. 32** Over/induced expression of *AtREM1.2* did not cause necrosis, while silencing of *AtREM1.2* cause subtle necrosis after Agrobacterium-mediated transient expression. *N. benthamiana* was syringe-infiltrated with induction medium (blank), Agrobacterium containing 35S:*AtREM1.2*:YFP, 35S:*AtREM1.2*:Strep, 35S:*AtREM1.2*:CFP, 35S:PcMKK5<sup>DD</sup>, 35S:PcMKK5<sup>KR</sup>, Est:*AtREM1.2* and 35S:*AtREM1.2*Ri. Five days after infiltration massive necrosis was developed by expression of 35S:PcMKK5<sup>DD</sup> and weak necrosis by expression of 35S:*AtREM1.2*Ri. The experiment was repeated once with similar results.

The expression of PcMKK5<sup>DD</sup> produced necrosis several days after infiltration of tobacco leaves, while PcMKK5<sup>KR</sup> did not (Fig. 32). None of the constructs over expressing *AtREM1.2* under the 35S promoter, as well as *AtREM1.2* construct with inducible promoter developed necrosis (Fig. 32). Expression of the RNAi construct produced necrosis, which was less severe compared to the one produced by PcMKK5<sup>DD</sup> (Fig. 32). Repetition of the assay on *N. tabacum* also showed minor necrosis upon silencing of *AtREM1.2*, but to a lesser extent.

### 3.9. Inducible expression and silencing of *AtREM1.2* did not cause any change in HR formation

Further analysis was performed on the DEX:*avrRpm1* transgenic plants in *rpm1-3* and *RPM1* background that now additionally carried different *AtREM1.2* constructs. These are denoted as Es*AtREM1.2/rpm1-3* and Es*AtREM1.2/RPM1* for the estradiol-inducible *AtREM1.2*, and as *AtREM1.2Ri/rpm1-3* and *AtREM1.2Ri/RPM1* for the RNAi lines.

Regulation of HR formation in RPM1-mediated resistance by *AtREM1.2* was analysed by conditional expression of *avrRpm1* in *AtREM1.2Ri/RPM1* and

EsAtREM1.2/*RPM1* after dexamethasone treatment. The RNAi and inducible AtREM1.2 lines did not show any difference in HR formation compared to the *RPM1* plants (Fig. 33A, B), with HR developing 5-6 hpi (seen as leaf curling) and collapse at 24 hpi.

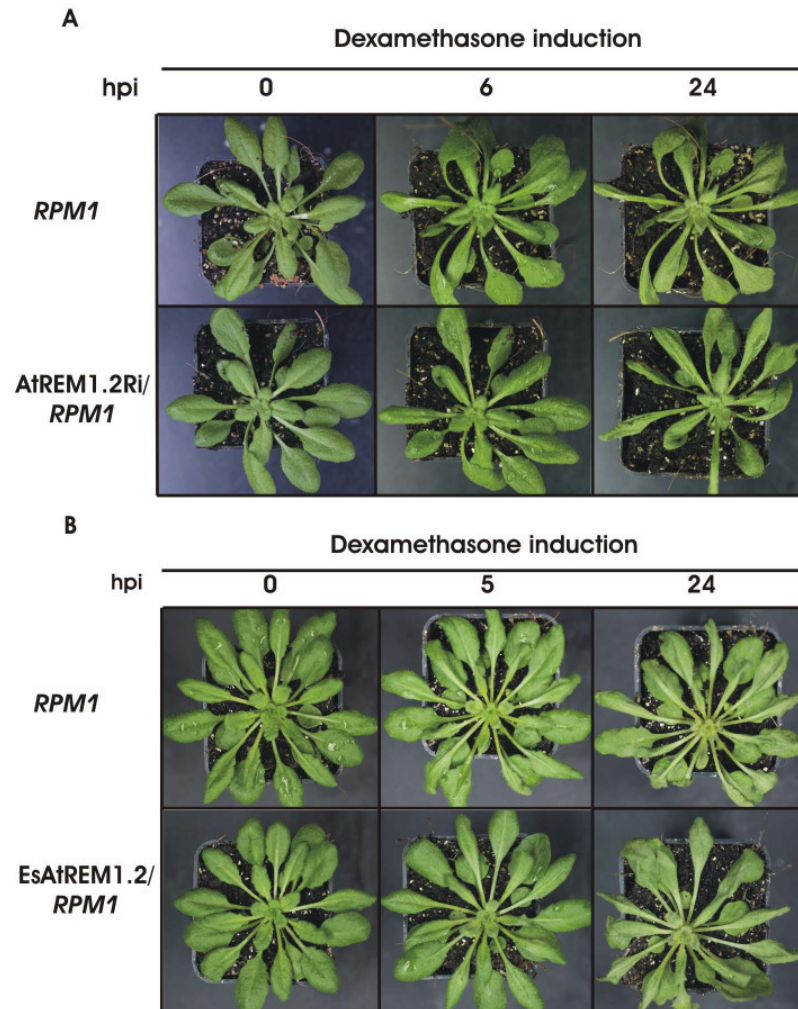


**Fig. 33** Silencing and induced expression of *AtREM1.2* did not cause any changes in HR formation. The *EsAtREM1.2/RPM1* plants were sprayed with 20  $\mu$ M Estradiol one day prior dexamethasone treatment. The *RPM1*, *AtREM1.2Ri/RPM1* and *EsAtREM1.2/RPM1* plants were sprayed with 20  $\mu$ M dexamethasone and HR formation was observed as early as 5 hpi in all lines. HR, in the form of tissue collapse, was not different between the *RPM1* and *AtREM1.2Ri/RPM1* lines (A); as well as between the *RPM1* and *EsAtREM1.2/RPM1* lines (B).

The HR formation is accompanied by ion leakage from the plant cells leading to the increased conductivity of medium (Baker et al., 1991). This phenotype is more quantifiable compared to the HR itself. Therefore, ion leakage assay was also performed to see if there is a quantitative change in HR formation. Neither *AtREM1.2Ri/RPM1* nor *EsAtREM1.2/RPM1* lines showed significant difference in conductivity compared to the *RPM1* plants during the development of HR (Fig. 34A). The dexamethasone concentration was reduced to 1  $\mu$ M to induce a slower HR reaction, but this also did not result in reproducible differences. Two

independent RNAi lines and three independent inducible lines were used in this experiment. To correlate the expression levels of *AtREM1.2* transgene in inducible lines to the observed conductivity in ion leakage assay, the inducible plants were grouped from 1 - 4 according to the weak - strong expression (Fig. 34B). In general, there is no clear correlation between level of *AtREM1.2* expression and conductivity.

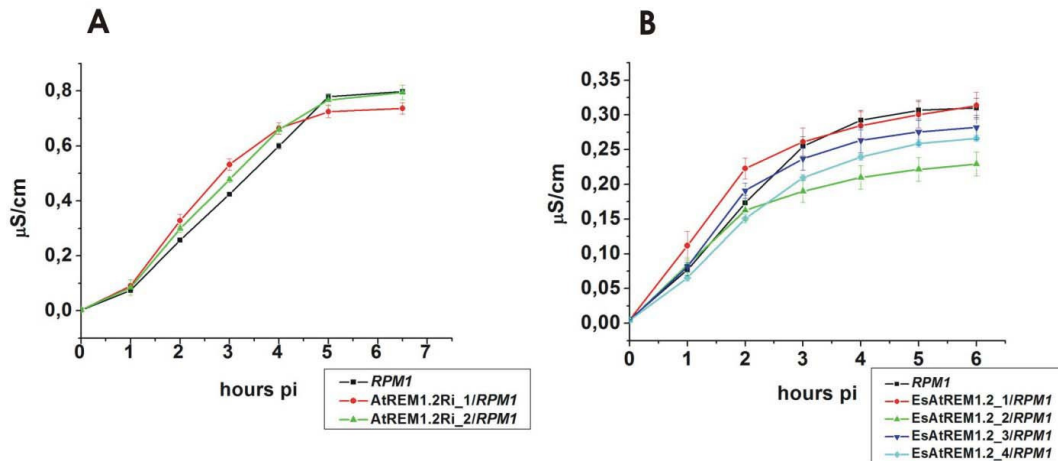


**Fig. 34** Ion leakage during HR development is similar in the *AtREM1.2Ri/RPM1* and *EsAtREM1.2/RPM1* lines compared to the *RPM1* lines. The *EsAtREM1.2/RPM1* plants were sprayed with 20  $\mu$ M estradiol one day prior the assay. Leaves from the *RPM1*, *AtREM1.2Ri/RPM1* and *EsAtREM1.2/RPM1* plants were syringe-infiltrated with 1  $\mu$ M dexamethasone and the conductivity of dexamethasone-treated leaf discs was measured over time. Two independent RNAi lines did not show significant difference in conductivity compared to the *RPM1* plants (A). Independent inducible lines were grouped according to the level of *AtREM1.2* transgene expression (1-4 = weak-strong). There was no correlation between the expression level and the difference in conductivity compared to the *RPM1* plants (B). Points are means of three replicates  $\pm$  SE. The experiments were repeated at least twice with similar results.

### 3.10. Inducible expression and silencing of *AtREM1.2* did not change the susceptibility against virulent strain *Pto* DC3000

Bacterial growth assays were conducted to evaluate resistance upon silencing or induced expression of *AtREM1.2*. Reproducible changes in susceptibility against *Pto* DC3000 was not observed upon silencing of *AtREM1.2*. Only one of the two *AtREM1.2/rpm1-3* lines showed significantly reduced bacterial growth ( $P$  value < 0.05) at four dpi compared to the *rpm1-3* line (Fig. 35A); and only one of the two *AtREM1.2Ri\_2/RPM1* lines showed significantly reduced bacterial growth ( $P$  value < 0.05) compared to the *RPM1* line at two and four dpi (Fig. 35B).

The estradiol-inducible *AtREM1.2* plants were grouped according to the transgene expression (Strong: *EsAtREM1.2+tg/RPM1*; Weak: *EsAtREM1.2-tg/RPM1*). Although there seems to be less bacterial growth at 2 dpi compared to the *RPM1* lines, this was not seen at 4 dpi. Moreover, there was no correlation between the transgene expression level and the

resistance level (Fig 35C). Hence, estradiol-induced expression of *AtREM1.2* in three independent lines did not result in altered susceptibility to *Pto* DC3000.

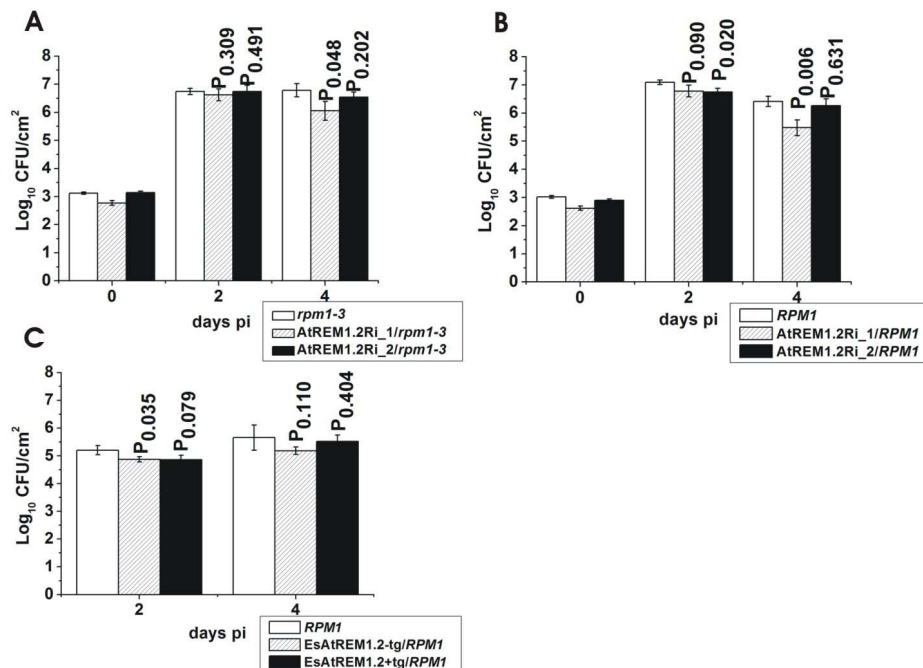


**Fig. 35** Silencing and induced expression of *AtREM1.2* did not change the susceptibility to the virulent strain *Pto* DC3000. Plants were syringe-infiltrated with bacteria resuspended to  $10^5$  cfu/mL and bacterial growth was monitored *in planta* by assaying infiltrated leaves at 0, 2 and 4 days after inoculation. Silencing *AtREM1.2* in the *rpm1-3* (A) and *RPM1* (B) plants did not reproducibly change the susceptibility to *Pto* DC3000. Induced expression of *AtREM1.2* did not affect susceptibility to *Pto* DC3000 (C). Points are means of 7-18 plants  $\pm$  SE; sampling two leaves/plants, the experiment was repeated at least twice.

### 3.11. Silencing of *AtREM1.2* increased resistance against *Pto* DC3000(*avrRpm1*), but induced expression of *AtREM1.2* did not influence the resistance against the avirulent strain

*Pto* DC3000(*avrRpm1*) grew to higher levels in the *rpm1-3* (Fig. 36A) compared to the *RPM1* plants (Fig. 36B). Silencing *AtREM1.2* did not affect the susceptibility of the *rpm1-3* plants, but increased the resistance of the *RPM1* plants to *Pto* DC3000(*avrRpm1*) (Fig. 36B). Two independent RNAi lines were used in this experiment (AtREM1.2Ri\_1/*RPM1* and AtREM1.2Ri\_2/*RPM1*), and both of them showed a significant *P* value < 0.05 at two and four dpi.

Increased resistance upon silencing *AtREM1.2* was not accompanied by decreased resistance after its induced expression. The bacterial growth in three independent inducible lines with high *AtREM1.2* transgene expression (collectively named EsAtREM1.2+tg/*RPM1*) and with low *AtREM1.2* transgene expression (EsAtREM1.2-tg/*RPM1*) was similar to the *RPM1* plants (Fig. 36C).

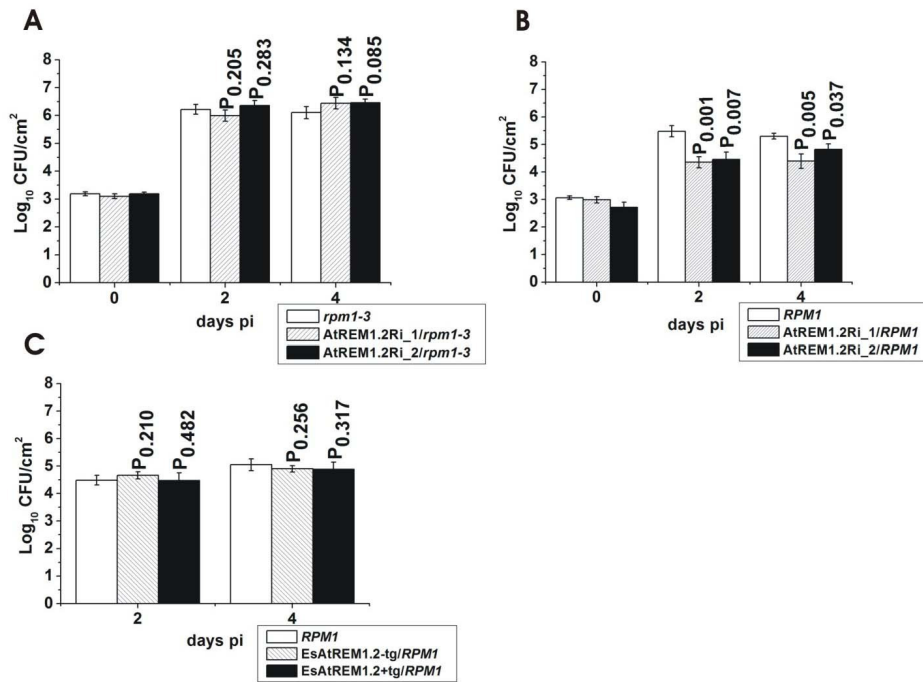


**Fig. 36** Silencing *AtREM1.2* in the *RPM1* plants increased resistance to *Pto* DC3000(*avrRpm1*) compared to the *RPM1* plants. Plants were syringe-infiltrated with bacteria resuspended to  $10^5$  cfu/mL and bacterial growth was monitored *in planta* by assaying infiltrated leaves at 0, 2 and 4 days after inoculation. Silencing *AtREM1.2* in the *rpm1-3* plants did not change susceptibility to *Pto* DC3000(*avrRpm1*) (A), but silencing *AtREM1.2* in the *RPM1* plants increased resistance to *Pto* DC3000(*avrRpm1*) compared to the *RPM1* plants (B). Induced expression of *AtREM1.2* did not compromise resistance to *Pto* DC3000(*avrRpm1*) (C). The EsAtREM1.2+tg/*RPM1* lines are a pool of 3 independent transgenic lines that show higher level of transgene expression (compared to the EsAtREM1.2-tg/*RPM1*). Points are means of 7-18 plants  $\pm$  SE; sampling two leaves/plant; the experiment was repeated at least twice.

### 3.12. Silencing of *AtREM1.2* did not change the RIN4 phosphorylation

Since silencing *AtREM1.2* affected resistance against *Pto* DC3000(*avrRpm1*), components of RPM1-mediated signaling may also be affected. RIN4, which is important for RPM1-mediated resistance and phosphorylated by *avrRpm1* (Mackey et al., 2002) was checked in the RNAi plants. RIN4 phosphorylation pattern was not changed after silencing *AtREM1.2* in the *rpm1-3* and *RPM1* plants (Fig 37). Two hours after dexamethasone induction, RIN4 was already phosphorylated, and the phosphorylation continued until ten hours post induction. RIN4 phosphorylation in the *RPM1* and *rpm1-3* lines after dexamethasone treatment showed a different pattern in comparison to *Pto* DC3000(*avrRpm1*)-infiltrated Col-0 that demonstrated induced phosphorylation at two hpi but already returned to basal level at six hpi (see Fig. 22). This difference might be caused by sustained induction of *avrRpm1* in the transgenic system compared to bacteria-delivered *avrRpm1*. One representative of the RNAi lines is shown (Fig. 37), but the experiment with another independent line gave similar results.

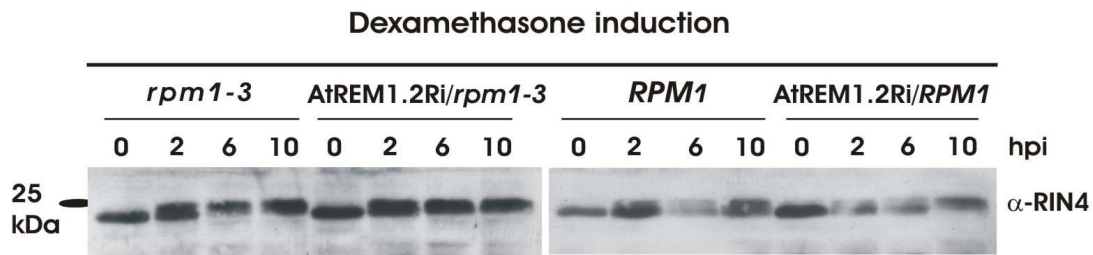


**Fig. 37** RIN4 phosphorylation was not affected by silencing *AtREM1.2*. Plants were treated with 20  $\mu$ M dexamethasone and harvested at 0, 2, 6 and 10 hpi. Protein was extracted and subjected to 1-DE and western blot followed by immunodetection by  $\alpha$ -RIN4

### 3.13. Silencing of *AtREM1.2* did not change the expression of selected *RPM1*-marker genes

To check whether silencing *AtREM1.2* changes the expression of *RPM1*-marker genes, semi quantitative RT-PCR was conducted.

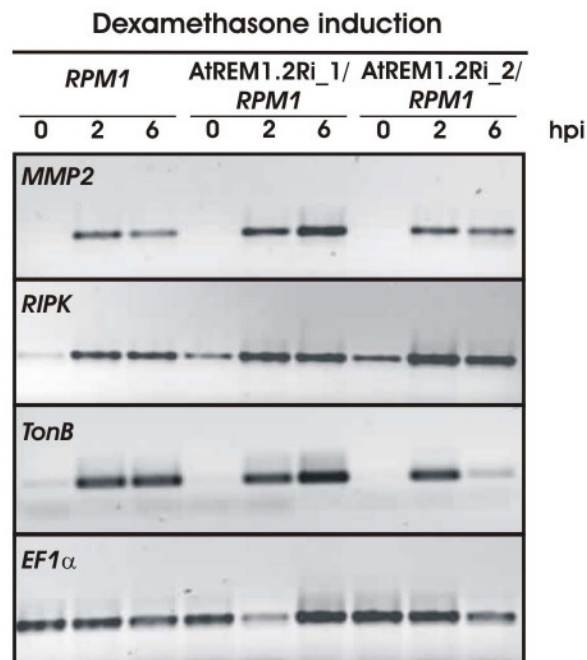


**Fig. 38** Silencing of *AtREM1.2* did not change the expression pattern of the *RPM1*-marker genes after dexamethasone induction. Plants were treated with 20  $\mu$ M dexamethasone and the transcript levels of each gene were monitored *via* RT-PCR by sampling the infiltrated leaves at 0, 2 and 6 hpi. *EF1α* as a constitutive control was shown for every time point after infiltration. The experiment was repeated twice with similar results. The enhanced *RIPK* basal transcript levels in the AtREM1.2Ri/*RPM1* lines were only seen in this experiment.

Three marker genes were checked: *MMP2*, *RIPK* and *TonB*, and none of them showed reproducible changes in expression after silencing *AtREM1.2* (Fig. 38).

### 3. 14. *AtREM1.2* transgene could not be induced in the *rpm1-3* line

During the functional analysis using inducible lines, the expression of *AtREM1.2* transgene in the *rpm1-3* background (*EsAtREM1.2/rpm1-3*) was very rarely observed. Since the *EsAtREM1.2/RPM1* lines were able to express *AtREM1.2* transgene after estradiol induction and both the *RPM1* and *rpm1-3* lines were transformed using the same *Est:AtREM1.2* construct, it is very unlikely that defects of the transgene expression in the *EsAtREM1.2/rpm1-3* line was caused by errors in the binary construct. Using specific primers for the *Est:AtREM1.2* construct, a DNA product with the correct size was obtained from both the *EsAtREM1.2/rpm1-3* and *EsAtREM1.2/RPM1* lines (Fig. 39). This indicates that the *Est:AtREM1.2* construct was still present in the *EsAtREM1.2/rpm1-3* line. Semi quantitative RT-PCR using specific primers that amplify transgene mRNA showed that in both *EsAtREM1.2/rpm1-3* and *EsAtREM1.2/RPM1* lines the transgenes were transcribed and correctly spliced, but the mRNA levels of the transgene in *EsAtREM1.2/rpm1-3* lines were severely reduced compared to the *EsAtREM1.2/RPM1* line (Fig. 39). At the protein level, the transgene could only be detected in the *EsAtREM1.2/RPM1* line (Fig. 39).

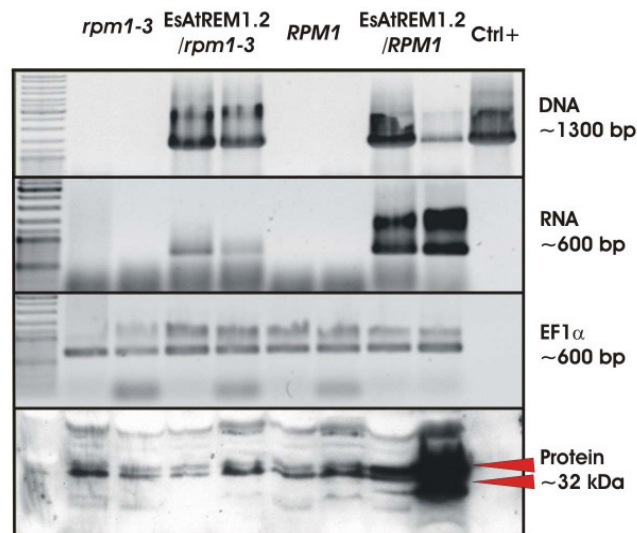


**Fig. 39** Expression of *AtREM1.2* transgene was not observed at protein levels in the *rpm1-3* background. The *rpm1-3*, two independent *EsAtREM1.2/rpm1-3*, *RPM1* and two independent *EsAtREM1.2/RPM1* lines were analysed for the presence of *Est:AtREM1.2* constructs that produced a product at 1300 bp. Semi quantitative RT PCR showing the mRNA levels of *AtREM1.2* transgene after estradiol treatment, with *EF1α* as a constitutive control. Western blot using  $\alpha$ -Remorin to detect the endogenous *AtREM1.2* (indicated by lower arrow) and *AtREM1.2* transgene (indicated by upper arrow).

This observation leads to the assumption that the expression of *AtREM1.2* may require the expression of *RPM1*. To rule out this possibility, the *EsAtREM1.2/rpm1-3* line was crossed to the *RPM1* line. The progenies will contain *EsAtREM1.2/RPM1* genotype and the expression of the *AtREM1.2* transgene will be rescued if the assumption above is true. The

seeds obtained from the crossing between the *EsAtREM1.2/rpm1-3* (as pollen donor) and the *RPM1* line were screened for the presence of *Est:AtREM1.2* constructs, and those that showed the presence of the right construct were checked at the mRNA and protein levels. However, the mRNA levels of *AtREM1.2* transgene were again very low and no protein could be detected in this *EsAtREM1.2/RPM1* genotype (data not shown). Hence, the assumption that *AtREM1.2* transgene expression requires *RPM1* is probably not true, and the cause for the lower *AtREM1.2* transgene mRNA level in *EsAtREM1.2/rpm1-3* line needs further investigation.

## IV. Discussions

### 1. Proteomics analysis of differentially regulated proteins during *avrRpm1*-RPM1 interaction

It has been shown that there is a significant overlap in genes that are differentially regulated during responses to challenge by *Pseudomonas syringae* DC3000 (*Pto* DC3000), *hrp* mutant and *Pto* DC3000 containing *avrRpm1* (*Pto* DC3000(*avrRpm1*)), both at RNA and protein levels (Jones et al., 2006; Truman et al., 2006). So far, the effort to identify genes specifically responding to effectors was done by comparing responses to *Pto* DC3000(*avrRpm1*) and to *hrp* mutants (Jones et al., 2006; Truman et al., 2006). Using this approach, genes that are common in both signaling pathways will be overlooked. To look for protein candidates with a possible role in early signaling of RPM1-mediated resistance, an inducible system for the expression of *avrRpm1* was used. Compared to infection with bacteria expressing *avrRpm1*, this system has an advantage in avoiding the confounding effects of signaling *via* PAMPs and other type III effectors. Therefore, this inducible system can provide complementary information to the bacterial system.

Two representative time points were chosen: the early time point after *avrRpm1* transcripts were detectable and the late time point when HR was proceeding (Fig 4). The timing of *avrRpm1* transcript appearance and HR development in the inducible system is comparable to that following inoculation with *Pto* DC3000(*avrRpm1*), where *avrRpm1* transcript accumulation was first detected 30 - 60 minutes after bacterial challenge and initial signs of tissue collapse occurred five hours post-challenge (de Torres et al., 2003).

The analysis was focused on early responses, which enhances the chance of finding candidates with regulatory or signaling roles. By contrast, late responses are likely HR-related secondary effects. Using bacterial inoculation, Truman et al. (2006) found an extensive transcriptional reprogramming four hours after challenge with *Pto* DC3000(*avrRpm1*). Based on the similarity in timing of *avrRpm1* transcripts accumulation and HR development between the inducible system and bacterial infection, it is likely that sampling at two hours post induction would represent early changes after recognition of *avrRpm1*-RPM1 and when defense reactions are just being initiated.

#### 1.1. Combination of microsomal enrichment and fractionation-based Rubisco depletion reveals novel candidates with potential signaling roles in RPM1-mediated resistance

Since proteins with regulatory or signaling roles are presumably of low abundance, different pre-fractionation approaches were applied to enrich for them. The candidates from

total protein fractions clearly showed that only highly abundant proteins were detected in this fraction. Enrichment of microsomal fractions did not improve the detection of putative signaling proteins, which is most probably caused by the presence of high abundant Rubisco. Depletion of Rubisco can improve the detection of low abundant proteins by increasing their relative abundance. This is evident from the candidates obtained after Rubisco depletion from total and microsomal protein using PEG precipitation. Rubisco-depleted total protein results in completely different protein candidates from those obtained from total protein. More importantly, several putative signaling proteins were found in this fraction (PP2C, RNA BP 45 and AtREM1.2). Combination of microsomal enrichment and Rubisco depletion is even more effective in detecting low abundant proteins. All the candidates from Rubisco-depleted microsomal fraction are proteins potentially involved in signaling (PP2C, C2-domain containing protein and AtREM1.2), and only in this fraction, the highest number of AtREM1.2 isoforms can be detected. Nevertheless, the yield in terms of identified candidates is comparatively low. The complicated procedure during the fractionation may account for this problem, since every additional step in the procedure can contribute to variability of the end results.

Comparison between Rubisco depletion using PEG precipitation and Rubisco depletion using IgY-Rubisco spin column showed that the two methods result in similar protein pattern. Nevertheless the low abundant candidate proteins observed after PEG precipitation could not be found in preparations using the commercial Rubisco spin column. This suggests that abundant proteins still predominate in the spin column-based protein sample and impede detection of low abundant proteins. The superiority of PEG precipitation over the Rubisco spin column is that it does not only deplete Rubisco but also further sub-fractionate proteins *via* physicochemical properties. The 10% PEG pellet recovered weakly stained proteins with horizontal streaking at basic region, which may represent low abundant membrane proteins that are generally alkaline (15), while the 20% PEG supernatant fraction recovered low-molecular weight, hydrophilic proteins (12). Furthermore, samples from the IgY-Rubisco spin column were frequently contaminated with IgY fragments, which interfered with the protein identification by PMF MALDI-TOF/MS.

Two of the putative signaling candidate proteins showed post-translational regulation. AtREM1.2 showed decreased transcript levels, while putative RNA binding protein transcript levels remained unchanged during the analyzed time course (Fig. 10). This highlights the necessity of analyzing post-transcriptional events for plant defense responses as a complement to global transcriptional changes that has been reported by several earlier studies (de Torres et

al., 2003; Truman et al., 2006). Besides post-transcriptional regulation, post-translational regulation is also important, but is often impeded by the availability of suitable analytical tools. AtREM1.2 was present in several isoforms, some of which were differentially regulated in this system. Due to the low abundance of these remorin isoforms and the technical challenges in identifying phosphorylation or other post-translational modifications, it is very unlikely that such a target would have been identified through LC-based approaches - hence emphasizing the superiority of the combination between fractionation and enrichment in 2-DE for such analysis.

## 1.2. Potential functions/roles of the candidates

Metabolism proteins comprise the largest group of up-regulated proteins identified. Most of them are either involved in carbon metabolism or photosynthesis (Table 1). Plant defense carries out a number of NADPH-consuming actions, requiring pathways to replenish the depleted-NADPH. In the regulation of redox in plant defense, NADPH also acts as electron donor to oxygen, leading to the formation of reactive oxygen species (ROS) during the oxidative burst (Pugin et al., 1997). Two proteins (At5g09660 and At5g11670) that contribute to NADPH production were up-regulated, which may account for the NADPH supply. Besides NADPH production, they also provide CO<sub>2</sub> for carbon fixation by Rubisco. Up-regulation of photosystem II components were also described previously and may serve as an additional source of ROS (Jones et al., 2006). In general, most of the metabolism proteins were already turned on very early and kept at steady levels or increased levels until the occurrence of the HR. It can be difficult to define the difference between metabolic changes as part of the defense mechanism and metabolic changes that result from the action of pathogen effectors. The early up-regulation and maintenance of metabolic proteins in this system is more likely to function as energy supply for plant defense, therefore they can be important for the defense response. De Torres et al. (2003) also showed that transcript levels of genes involved in metabolic processes were induced at two different phases: early phase (0.5-1 hour post inoculation) and late phase (3-4 hour post inoculation); the latter probably reflects the subversion of host metabolism by *avrRpm1*.

The second largest group of up-regulated proteins encompasses defense-related proteins. Some of them were turned on earlier and lasting until HR formation (GSTF7, peroxiredoxin and PAL) and some of them were up-regulated at the occurrence of HR (GSTF6 and myrosinase-associated protein) (Table 1). PAL catalyses the conversion of phenylalanine to trans-cinnamic acid which is the first step in the biosynthesis of

phenylpropanoids leading to diverse plant metabolites, some of which are involved in plant defense reactions (Hahlbrock and Scheel, 1989). Truman et al. (2007) already detected the induction of PAL transcript systemically four hours after infiltration with *Pto* DC3000(*avrRpm1*) and this is in agreement with the finding of early up-regulation of PAL in this system. The up-regulation of redox regulation enzymes before and concomitantly with HR may have protective function in that it prevents plant cells from damage by toxic ROS produced to kill the invading pathogen (Sutherland, 1991). Conceivably, this may allow survival of neighboring cells and restrict the extent of cell death to a localized area in a typical HR initiated by avirulent pathogens.

Some of the differentially regulated proteins in this system were also observed in the study using bacterial inoculation by Jones et al. (2006). For example GSTF7, GSTF6, PrxIII were considered as PAMP responsive proteins by comparing between *hrp* mutant challenge and mock inoculation. Rubisco activase and carbonic anhydrase were considered as PAMP and type III effector responsive by the comparison described above and between *hrp* mutant and *Pto* DC3000 challenge, respectively. The data here that represents *avrRpm1*-responsive proteins indicates that common genes were activated by PAMPs, a collection of type III effectors and the single effector, *avrRpm1*. It appears that the plant immune system activates a general defense response upon attack by different pathogens, instead of activating a distinct pathway for each challenge. Alternatively, these candidates are simply responsive to general stress.

The number of up-regulated proteins in this system covers 94% of differentially regulated protein, while only two (i.e. 6%) are down-regulated proteins. The suppression of type III effectors on host protein to promote pathogen virulence has been known from bacterial inoculation studies and is evident at transcript and protein levels (Jones et al., 2006; Truman et al., 2006). The low number of down-regulated proteins found here compared to the previous study might be due to the lack of other bacterial components in this system. Truman et al. (2006) showed that the number of down-regulated proteins after *Pto* DC3000(*avrRpm1*) infection compared to MgCl<sub>2</sub> treatment covered 50% of total differential proteins, but the number went down to roughly 10% when it is compared to inoculation with *Pto* DC3000 and *hrp* mutant.

Signaling proteins were the focus in this study. Four candidate proteins were considered to have potential early signaling roles: A protein with similarity to RNA-binding protein 45 (At1g11650), a PP2C (At2g20630), a C2-domain-containing protein (At4g34150) and AtREM1.2 (At3g61260).

While RNA-binding proteins are generally not ascribed with signaling roles, they could be potentially interesting since their involvement in plant immunity has been implicated. For instance, expression of an RNA-binding protein is regulated during TMV-induced HR (Naqvi et al., 1998). Recently, five RNA-binding proteins were found to be ADP-ribosylated by the type III effector, HopU1, and a null mutant of one of them, *grp7*, was more susceptible to *P. syringae* (Fu et al., 2007). Interestingly, one of these ADP-ribosylated RNA-binding proteins, At2g37220, was also found to be up-regulated in the total extract at the six hours time point (Table 1).

C2-domains are conserved modules that bind phospholipids in a calcium-dependent manner, resulting in the activation of the adjacent kinase domains (Newton and Johnson, 1998). In some proteins, C2-domains mediate protein-protein interaction (Dekker and Parker, 1997; Gray et al., 1997; Ron et al., 1995) and in coordination with lipid binding this could permit recruitment of the C2-domain-containing proteins to specific membrane compartments (Mellor and Parker, 1998). Recent studies by Benes et al. (2005) demonstrated that a C2-domain within a Ser/Thr kinase constitutes a novel phosphotyrosine binding domain.

PP2C is particularly interesting since the timing of its up-regulation coincides with RIN4 phosphorylation. Additionally, this PP2C was recovered from microsomal fractions and hence is possibly membrane-associated. Therefore, it may be properly localized to regulate RIN4 phosphorylation. AtREM1.2 is a plant-specific lipid-raft-associated protein with unknown function (Bhat and Panstruga, 2005; Mongrand et al., 2004; Morel et al., 2006). Its similarity to the cell-to-cell movement protein of tobacco mosaic virus (TMV-MP) suggests a potential role in mediating *avrRpm1* signaling (Reymond et al., 1996). Further investigation on these two candidates was pursued to study their role in the RPM1-mediated defense response, which will provide a better understanding of signaling events in this process.

## 2. Functional analysis of PIA1 for RPM1-mediated defense response

The rapid induction of PP2C (At2g20630) suggests potential roles in early signaling of RPM1-mediated defense response. There are 76 members of *Arabidopsis* PP2C family, which are clustered into ten groups based on amino acid sequence homology (Schweighofer et al., 2004). During the screening for putative signaling proteins in RPM1-mediated resistance, only one PP2C was detected as a candidate, but this does not exclude that other PP2Cs might also be regulated since only limited pH range (4-7) was used in 2D-PAGE during the screening. This PP2C, renamed as PIA1 (PP2C induced by *avrRpm1-1*), is presumably of low

abundance since it is not observed in total protein extract, but in the Rubisco-depleted total and microsomal protein.

Biological functions have been assigned only for several PP2C groups, such as the well-studied PP2Cs associated with abscisic acid (ABA) signal transduction or PP2Cs that share homology to MP2C, an alfalfa PP2C regulating MAPK signaling (Schweighofer et al., 2004). PIA1 belongs to a group that has not been characterized. Recent studies identified one member of the group (At4g31750) as HopW1-1-interacting protein, highlighting the possible role for members of this group in plant defense (Lee et al., 2008).

The PIA1 protein consists of a non-catalytic domain at the N terminus, a catalytic domain at the C-terminus and an ATP/GTP-binding site motif (Fig. 15A). It does not contain any putative mitogen-activated protein kinase (MAPK) interaction motif (KIM) or any transmembrane spanning region (Schweighofer et al., 2004). Despite the absence of a transmembrane domain in PIA1, it was fractionated in the microsomal fraction. Post translational modification motifs for membrane anchor such as acylation, prenylation, GPI-anchor and palmitoylation (Bijlmakers and Marsh, 2003) were not present in PIA1, thus its association to membranes may happen *via* protein-protein interaction; or it may well be that the microsomal preparation did not specifically enrich membrane proteins and still contain many soluble proteins.

### **2.1. PIA1 does not regulate cell death formation and ROS production, but negatively regulates disease resistance mediated by RPM1**

Two T-DNA insertion mutants of *PIA1* were obtained to perform functional analysis; both of them are homozygous null mutants. These *pial* mutants did not show any obvious visible phenotype under unchallenged conditions. They show normal development and have no defect in flower development.

The requirement of phosphatases in mediating programmed cell death in plants has been shown previously. TMV elicits the *N* gene-mediated programmed cell death in tobacco. Addition of okadaic acid, a specific inhibitor of serine/threonine protein phosphatase type 1 and 2A, causes significantly fewer cell death lesions in TMV-infected tobacco (Dunigan and Madlener, 1995). Bax-mediated cell death was also blocked by okadaic acid. Bax is a death promoting member of the Bcl-2 family, and able to trigger cell death in tobacco when it is expressed from a TMV vector. Treatment of TMV.Bax-infected leaves with okadaic acid completely blocked formation of Bax-induced cell lesions (Lacomme and Santa Cruz, 1999). In both cases, a phosphatase is required in the signaling pathway to initiate the cell death

program. However, He et al. (2004) showed that a phosphatase acts as a negative, instead of a positive regulator of cell death. When *PP2Ac* (catalytic subunit of *PP2A*) was silenced in *N. benthamiana*, the plants formed necrotic lesions, a form of localized cell death, on leaves and stems (He et al., 2004).

Loss of *PIA1* did not show any influence on HR formation as to the timing and the extent of cell death. Lower bacterial inoculation to evoke weaker reactions in order to detect more subtle phenotype did not result in altered HR formation between the *pial* mutants and wild type plants (Col-0). Moreover the oxidative burst was not affected in the *pial* mutants. It is still not clear what actually causes cell death in plants, it could be a programmed cell death initiated by the plant upon pathogen recognition, or production of toxic compounds, such as ROS, that kill the pathogen and host cells, or a combination of both (Dangl et al., 1996). Since loss of *PIA1* does not cause any effect on both phenotypes, it does not seem to play a role in signaling leading to cell death and ROS production.

Even though HR is considered to be involved in pathogen arrest, recent evidence shows that HR is not required to stop pathogen growth in some cases (Hammond-Kosack and Jones, 1996). The *Arabidopsis dnd* (*defense no death*) mutant still retained effective “gene-for-gene” resistance against *Pto* DC3000(*avrRpt2*) and *Pto* DC3000(*avrRpm1*) but lacks the occurrence of HR (Yu et al., 1998). Even though *PIA1* has no role in HR formation, loss of *PIA1* results in plants with increased resistance against the avirulent strain, *Pto* DC3000(*avrRpm1*), but similar susceptibility to the virulent strain, *Pto* DC3000 (Fig. 17). The increase in resistance was only minor, but reproducible in several independent experiments with many biological replicates. The redundancy effect from other PP2Cs may account for the marginal difference observed in bacterial growth assays. Similar results were reported before, for example, silencing of *PP2Ac* in *N. benthamiana* produced increased resistance to a virulent strain of *P. syringae* pv. *tabaci* (He et al., 2004), and *Arabidopsis* with increased levels of AP2C1, an *Arabidopsis* MAPK-interacting PP2C, compromised innate immunity against the necrotrophic pathogen *Botrytis cinerea* (Schweighofer et al., 2007). In both cases, phosphatases act as negative regulators of plant defense responses, which reinforces the finding that loss of *PIA1* increases resistance against *Pto* DC3000(*avrRpm1*).

Loss of *PIA1* also modified the transcriptional reprogramming specific for RPM1-mediated resistance. *RIPK*, *MMP2* and *TonB* are induced by AvrRpm1 and AvrB, but not by *Pto* DC3000(*hrpA*<sup>-</sup>) and *Pto* DC3000, and are thus considered as *RPM1*-specific marker genes (de Torres et al., 2003). Even though there is no clear evidence for the function of these genes in RPM1 defense response, their induction can be used as an indicator for RPM1-defense

activation. Induction of *MMP2* was more pronounced in the *pia1* mutants compared to Col-0 after challenge with *Pto* DC3000(*avrRpm1*), suggesting the positive regulation of the *avrRpm1*-mediated response by loss of *PIA1*. This enhanced regulation of *RPM1*-signaling would fit the enhanced resistance against *Pto* DC3000(*avrRpm1*). Interestingly, not all of *RPM1*-responsive marker genes were affected; *RIPK* and *TonB* showed similar induction to Col-0. Thus, *PIA1* might regulate distinct pathways of *RPM1*-mediated resistance involving *MMP2*.

In animals, matrix metalloproteinases (MMPs) are the major group of proteinases that degrade the extracellular cell matrix, and play a role in development, embryogenesis, organ morphogenesis and wound healing, while in plants, MMPs have been implicated in plant development and senescence (Golldack et al., 2002), as well as in programmed cell death (Delorme et al., 2000).

The involvement of MMPs in plant defense was discovered by Liu et al. (2001), who demonstrated that transcript levels of *Glycine max* *MMP2* (GmMMP2) was increased in soybean tissue following infection with the oomycete, *Phytophthora sojae*, and the bacterium *P. syringae* pv. *glycinea* (*Psg*), as well as treatment with yeast extract elicitor (YE) (Liu et al., 2001). The increased *MMP2* transcript levels did not correlate with cell death, since both *Psg* and YE induced the expression of *MMP2*, but only *Psg* produced cell death. The authors proposed the role of *MMP2* in defense as a regulator of plant enzymes that digest microbial cell walls to release elicitors. This is based on the similarity to the MMPs in animal system, such as the metalloproteinase matrilysin in mouse, which activates the  $\alpha$ -defensin cryptidin by cleaving the propeptide from the cryptidin precursor, thus activating antibacterial activities. This was then proven by co-culturing the mature GmMMP2 with *Psg* and *P. sojae* that resulted in strong inhibition of bacterial and oomycete growth. It is likely that GmMMP2 releases an antimicrobial compound to halt the pathogen growth (Liu et al., 2001).

The relation between loss of *PIA1* and enhanced expression of *MMP2* is unclear, but there are several evidences from animal systems, which demonstrate regulation of MMPs by phosphorylation. For example, mutation in the SH2 domain of protein tyrosine phosphatase impaired the production, secretion and proteolytic activation of *MMP2* in response to Concanavalin-A (Ruhul Amin et al., 2003). Inhibition of protein tyrosine phosphatase also block the HIV-tat-induced expression of *MMP9* (Kumar et al., 1999). These data suggest that *MMP2* may play a role in *RPM1*-mediated defense response, and it is regulated/mediated by the activity of *PIA1*.

## 2.2. PIA1 regulates pathogenesis- and stress-related gene expression

Besides *MMP2*, several genes associated with defense and stress responses were also differentially regulated upon loss of *PIA1*. *PR1*, *PR2* and *PR5* transcript levels were suppressed in the *pia1* mutants compared to Col-0 during RPM1-mediated resistance. In *Arabidopsis*, expression of these PR proteins is induced by SA and usually correlated with increased resistance to a wide range of pathogens (Uknes et al., 1992). Suppression of *PR* gene expression corresponds to decreased SA levels in the *pia1* mutants compared to Col-0. SA reduction in the *pia1* mutants was only prominent after infiltration with *Pto* DC3000(*avrRpm1*). This might suggest that PIA1 does not regulate the SA biosynthesis itself, but rather regulate the signal transduction leading to SA accumulation upon activation of defense responses.

Interestingly, *PR3*, which is JA/ET-regulated, displayed suppression similar to the SA-regulated *PR* genes. JA and OPDA levels in the *pia1* mutants exhibited the tendency of lower production compared to Col-0, but this was only statistically significant for one of the two *pia1* mutants (Fig. 19). The suppression of SA- and JA/ET-responsive genes in the *pia1* mutants is inconsistent with antagonistic cross-talk between SA- and JA/ET-dependent pathways in *Arabidopsis*. However, several mutants display a phenotype that does not follow this general assumption. The *hrr1* (*hypersensitive response-like lesion 1*) of *Arabidopsis* produced spontaneous necrotic lesions and ROS, constitutive expression of the SA-responsive genes, *PR-1*, *PR-2* and *GST1*, as well as the JA/ET-responsive gene, *PDF1.2* (Devadas et al., 2002). Additionally, analysis of *Arabidopsis cpr* (*constitutive expressor of PR genes*) revealed that components of JA/ET-dependent pathway are required for SA-mediated, NPR1-independent resistance (Clarke et al., 2000) and SA is required for the expression of *PDF1.2* in the *ssi1* (*suppressor of SA insensitivity 1*) (Shah et al., 1999).

The enhanced resistance against *Pto* DC3000(*avrRpm1*) and decreased *PR* gene expression and SA levels in the *pia1* mutants seems to be contradictory since *PR* gene expression and SA induction are commonly associated with HR and SAR (systemic acquired resistance) in incompatible interaction. Nevertheless, there are also defense responses that do not require SA. Induced systemic resistance (ISR) from nonpathogenic rhizobacteria, which is phenotypically similar to SAR, does not require SA production or *PR* gene activation (van Loon et al., 1998). Colonization of the rhizosphere with *P. fluorescence* resulted in induced-resistance against *Fusarium oxysporum* f. sp. *raphani* and *Pto* DC3000. This enhanced-resistance mediated by rhizosphere is not affected in *NahG* plants, which are unable to accumulate SA, and does not coincide with the accumulation of *PR* gene transcripts (Pieterse

et al., 1996). Inhibition of *PR-1* expression in the *Arabidopsis* double mutant, *cpr5npr1*, did not affect the resistance against *Pma* ES4326 and *H. parasitica* Noco2 (Clarke et al., 2000). This could mean that the residual amount of *PR* gene expression in these mutants is sufficient to confer resistance.

The regulation of *PR* gene expression is not completely understood, but evidence for phosphorylation events in this regulation is accumulating. Raz and Fluhr (1993) demonstrated the induced accumulation of *PR-1*, *PRB-1b*, *PR-2* and *PR-3* in tobacco leaves after application of phosphatase inhibitor. This is supported by Després et al. (1995) who showed phosphorylation of PBF-1, a nuclear factor that binds and activates the potato *PR-10a* promoter, and treatment with okadaic acid resulted in an increase accumulation of the *PR-10a* transcripts (Despres et al., 1995). However, Conrath et al. (1997) showed an opposite effect of phosphatase inhibitor application on *PR* gene expression. Okadaic acid blocked SA-mediated induction of *PR-1* genes, implying the involvement of phosphoproteins downstream of SA. The authors also found that kinase inhibitors could induce *PR-1* gene expression, and this induction was suppressed in *NahG* tobacco plants, suggesting that another phosphoprotein acts upstream of SA (Conrath et al., 1997). Since both *PR* gene expression and SA accumulation are affected in the *pial* mutants, the PIA1 regulation of *PR* gene expression may be upstream of SA (Fig.40).

In contrast to *PR-1*, *PR-2* and *PR-3* expression, *PR-5* showed a slightly different pattern. The basal levels of *PR-5* in the *pial* mutants were higher than in Col-0, but during the defense response its expression was strongly repressed (Fig. 18). Since the basal SA levels in the *pial* mutants and Col-0 is indistinguishable, the enhanced constitutive expression of *PR5* seems to be regulated by PIA1 *via* a pathway independent of SA. It could mean that in the non-challenged condition, *PR-5* is negatively regulated by PIA1, but during RPM1-defense response, another pathway, in which PIA1 exerts positive regulation, takes over. In summary, PIA1 positively regulates *PR* gene expression and this may be *via* a SA-dependent pathway.

*PDF1.2* is activated after pathogen attack and wounding *via* JA- and ET-dependent signaling pathways. Expression of the *PDF1.2* gene is prevented by mutations that block JA (i.e. *coronatine insensitive 1*, *coi1*) or ET (i.e. *ethylene insensitive 2*, *ein2*) signaling. JA- and ET-signaling seem to be required simultaneously, as *PDF1.2* expression is not activated by either ET treatment of *coi1* plants or JA treatment of *ein2* plants (Penninckx et al., 1996; Penninckx et al., 1998). Constitutive expression of *PDF1.2* in the *pial* mutants was higher compared to Col-0, but JA-regulated *VSP2* (*vegetable storage protein 2*) expression was not affected, which leads to the assumption that the increased levels of *PDF1.2* in the *pial*

mutants might be ET- instead of JA-regulated. The analysis of the ET biosynthesis gene, *ACS6* (1-aminocyclopropane-1-carboxylic acid (ACC) synthase-6), showed enhanced basal transcript levels. However, the increase in *ACS6* transcript levels was not accompanied by increase in ET production (Fig. 18 & 20). It is known that *ACS* transcripts are short-lived and negatively regulated by unknown repressor(s) (Liang et al., 1992; Wang et al., 2002). Protein phosphorylation has been implicated in the regulation of *ACS*, not by regulating the catalytic activity itself but by controlling the protein turnover rate. Mutation of potential phosphorylation sites in *ACS6* from Ser(S) to Asp(D) residues to mimic phosphorylated form of *ACS6* increased the ET production in *ACS6<sup>DDD</sup>* transgenic plants, even though the mutant *ACS6* protein showed similar activities to wild type protein (Liu and Zhang, 2004). In contrast to the known regulation of *ACS6* protein by phosphorylation, the effect of phosphorylation on the *ACS6* gene expression is not known. The enhanced expression of *ACS6* transcripts in the *pial* mutants might be due to the release of *ACS6* suppressor upon elimination of *PIA1*.

Mutants carrying a T-DNA insertion in the *AP2C1* gene already expressed *PDF1.2* at low levels prior to wounding and this increased *PDF1.2* levels correlated with the increase of wound-induced levels of JA in *AP2C1* knockout plants. In addition, the *AP2C1* over-expressing plants showed reduced ET production, even though the *AP2C1* knockout plants did not show significantly increased ET production (Schweighofer et al., 2007). The *pial* mutants, which showed enhanced *PDF1.2* but not ET accumulation, might be affected in ET signaling rather than its biosynthesis. The model for the ET signal transduction pathway proposes that the ET receptor activates the Raf-like kinase, CTR1 in the absence of ET. This CTR1 in turn negatively regulates the downstream ET pathway, possibly through a MAPK cascade (Wang et al., 2002). *PIA1* might regulate the phosphorylation events in this cascade, leading to the enhanced *PDF1.2* expression. It may also directly regulate *PDF1.2* expression by releasing the repressor or activating the promoter of *PDF1.2*.

### 2.3. Searching for *PIA1* target proteins

Many studies showed that phosphatases regulate defense responses in plants against biotic or abiotic stress, but it is still not clear which phosphatase is involved in mediating specific defense responses since inhibitors that target phosphatases collectively were used. Phosphatases also demonstrate opposite regulatory functions, as positive and negative regulator in defense, which might be determined by their target proteins. Therefore, finding

the phosphatase protein target would be valuable to clarify the mechanism of defense regulation.

Phosphorylation of RIN4, a protein with unknown biochemical function that interacts with *avrRpm1* and RPM1, is critical for the RPM1-defence response (Mackey et al., 2002). So far, it is not known which kinases and phosphatases regulate RIN4 phosphorylation. Loss of *PIA1* did not influence RIN4 phosphorylation, suggesting that RIN4 is not the target of PIA1. Remorin, a protein that is also phosphorylated during the RPM1-defense response, was not affected in the *pial* mutants either. Since PIA1 does not have putative MAPK interaction motif in its amino acid sequence, it most likely targets other phosphoproteins. Comparison of protein patterns between the *pial* mutants and Col-0 after challenge with *Pto* DC3000(*avrRpm1*) via 2-DE may provide a tool to look for putative direct or indirect targets of PIA1. The superiority of this approach is the ability to directly depict posttranslational modification as pI or MW shift on 2D gels, thus enabling the immediate identification of differential phosphorylations between Col-0 and the *pial* mutants. The candidate proteins that were identified from Rubisco-depleted protein were limited. Only three candidates were found and all of them showed very low spot intensities. One of them is ATPB (chloroplast-encoded gene for  $\beta$ -subunit ATP synthase), which was suppressed in the *pial* mutants compared to Col-0. The result from candidate screening indicates that the putative targets of PIA1 might be very low abundance proteins, which are presumably involved in signaling. Alternatively, the conditions tested did not contain these phosphotargets. Efforts to identify the putative PIA1 target could be achieved by applying different fractionation strategies to enrich low abundance proteins. The most plausible approach for future experiments would be phosphoprotein enrichment.

#### **2.4. PIA1 regulates an *avrB*-independent pathway in RPM1-mediated defense response**

PIA1 was only up-regulated by introduction of *avrRpm1*, but not by *avrB*, a type III effector with no sequence similarity to *avrRpm1* that also interacts with RIN4 and induces its phosphorylation, presumably leading to the activation of RPM1 (Mackey et al., 2002) (Fig. 14). Since both *avrRpm1* and *avrB* can trigger the same action during the defense response, they are often considered to act similarly in RPM1-mediated disease resistance. However, there are now data that indicates separable disease resistance responses to *avrB* and *avrRpm1*. *Pma* M6C $\Delta$ E(*avrRpm1*) grew 10-fold more than *Pma* M6C $\Delta$ E(vector) in the *rpm1* plants, but *Pma* M6C $\Delta$ E(*avrB*) failed to promote more bacterial growth in the *rpm1* plants. This implies that another RPM1-independent pathway, which is responsive to *avrB* but not to *avrRpm1*,

exists (Belkhadir et al., 2004). Recently, Eitas et al. (2008) identified TAO1, a TIR-NB-LRR protein, that contributes to disease resistance against *Pto* DC3000(*avrB*), but not to *Pto* DC3000(*avrRpm1*). TAO1 is required for *avrB*-induced chlorosis in the *rpm1* plants, and its activation results in *PR1* expression. In *RPM1* but not in *rpm1* plants, loss of TAO1 reduced disease resistance to *Pto* DC3000(*avrB*) about 10 fold, which suggests that TAO1 is a weak disease resistance protein that can not induce sufficient defense responses in the absence of *RPM1*, and that the activation of both *RPM1* and TAO1 can additively generate full disease resistance to *Pto* DC3000(*avrB*) (Eitas et al., 2008).

Since *avrB*-induced chlorosis is independent of *RIN4*, TAO1 perception of *avrB* is likely to occur *via* another protein target(s) (Eitas et al., 2008). Belkhadir et al. (2004) also showed that *RIN4* is not the only target for *avrRpm1*, *avrRpt2* and *avrB* (Belkhadir et al., 2004). The *PIA1* up-regulation in this study found to be specific to *avrRpm1*, but not *avrB*, provides additional evidence that supports the existence of separable pathways between *avrB* and *avrRpm1*. However, *MMP2*, which is responsive to *avrRpm1* and *avrB*, is affected in the *pial* mutants. Thus, these two separable pathways may converge on *MMP2* in mediating resistance, or alternatively, *MMP2* is responsive to several effectors.

In summary the data demonstrate that *PIA1* (At2g20630) may act as a negative regulator of the *RPM1*-mediated defense response by directly or indirectly modulating the *avrRpm1*-responsive gene, *MMP2*. On the other hand it exerts positive regulation on the expression of *PR* proteins possibly *via* a *SA*-dependent pathway. *PIA1* also regulates the expression of *PDF1.2*, *ACS6* and *PR5* in the absence of pathogens, either by releasing the repressors or activating the promoters of these genes. The regulation of *PIA1* in this resistance may proceed through an *avrRpm1/RPM1* pathway that is distinct from the *avrB/RPM1*-mediated defense.

### **3. Functional analysis of AtREM1.2 (At3g61260) for defense responses mediated by the *avrRpm1-RPM1* interaction**

Remorin was identified for the first time as a protein that is phosphorylated *in vitro* by galacturonide treatment of potato and tomato membranes (Reymond et al., 1996). It is present in many plant species, also in mosses and ferns, but not in algae, fungi, animals, archaeobacteria and eubacteria. There are 16 genes in *Arabidopsis* that encode remorins, which are divided into six different groups based on amino acid homologies (Raffaele et al., 2007). The characteristic feature of the remorin family is the conserved N-terminal proline-rich region and C-terminal coiled-coil domain, both of which imply protein-protein

interaction (Bariola et al., 2004; Raffaele et al., 2007; Reymond et al., 1996). Remorins associate with membranes even though they contain highly hydrophilic domains and lack any transmembrane domain or membrane anchor sequences (Bariola et al., 2004; Raffaele et al., 2007; Reymond et al., 1996). Many remorins harbor the C-terminal tetrapeptide motif CaaX (“a” = aliphatic amino acid, “X” = amino acid), a potential isoprenylation site for membrane association (Bariola et al., 2004), but not all remorins possess CaaX motifs, and they still associate strongly with membranes (Bariola et al., 2004). Remorin is highly expressed in meristems, leaf primordia, axillary buds and vascular tissues (Bariola et al., 2004).

AtREM1.2, which was found here to be differentially regulated during the RPM1-mediated defense response, belongs to the group 1b of the remorin family that contains a proline-rich region. Members of this group are the most ubiquitous remorins and most of them attach to membranes (Raffaele et al., 2007). Two members of this group have been found to be differentially regulated in defense responses. AtREM1.3, the closest homolog of AtREM1.2, was differentially phosphorylated on flg22-treated *Arabidopsis* cell cultures (Benschop et al., 2007), and Remorin 1 was up-regulated in tomato after infection with *Clavibacter michiganensis* subsp. *michiganensis* (Coaker et al., 2004). Despite many evidences of remorin accumulation upon abiotic and biotic stimuli, their function is still unclear since functional studies using over expressing and knockdown mutants did not give conclusive results (Bariola et al., 2004).

In this study, AtREM1.2 was consistently up-regulated very early in the artificial system (dexamethasone inducible system), as well as in the natural situation (bacterial infiltration). Interestingly, AtREM1.2 was found to be up-regulated after infiltration with *Pto* DC3000(*avrRpm1*), as well as with *Pto* DC3000(*avrB*). This is dissimilar to PIA1 up-regulation described above, and again emphasizes that there are separable and common pathway(s) between *avrRpm1* and *avrB* in the RPM1-mediated defense response.

AtREM1.2 was present in several isoforms that were differentially regulated during induction. Protein identification of AtREM1.2 using PMF MALDI-TOF/MS was problematic since each isoform was low in abundance. Even though AtREM1.2 could be identified with significant confidence, confirmation of protein identification was also pursued using immunological methods. Three protein spots identified as AtREM1.2 in Rubisco-depleted microsomal protein were detected on 2D Western blots by  $\alpha$ -Remorin, thus validating the protein identification. Furthermore,  $\alpha$ -Remorin was used to verify AtREM1.2 up-regulation observed on silver-stained 2D gels. This confirmation is important to exclude possible co-migration of other proteins in the same position of AtREM1.2, resulting in false quantification

of AtREM1.2. Comparison between  $\alpha$ -Remorin-detected 2D Western of “t=0 hpi” and “t=2 hpi” samples showed that isoform 2 was more intense in the “t=2 hpi” sample, which is in agreement with the result from silver-stained 2D gels.

The timing of AtREM1.2 up-regulation coincides with RIN4 phosphorylation, which is thought to be an *avrRpm1* target (Mackey et al., 2002). This up-regulation, like that of RIN4, was maintained until the occurrence of HR. By contrast, RIN4 phosphorylation did not require RPM1. Thus, even though there is similarity between RIN4 and AtREM1.2 regulation, it is unlikely that AtREM1.2 is another target of *avrRpm1* since AtREM1.2 up-regulation was only observed in the *RPM1* but not in the *rpm1-3* line. AtREM1.2 regulation is dependent on RPM1 and is most likely downstream of RIN4 phosphorylation (Fig 40).

### **3.1. AtREM1.2 regulation during the RPM1-mediated defense response might occur via phosphorylation and distribution to lipid rafts, but not by interaction with RIN4**

PTM analysis by ProMoST predicted at least dual phosphorylation events on AtREM1.2. Treatment with  $\lambda$ -phosphatase shifted isoforms 4/5 and 2 to a presumably more basic pI, but not isoform 1 and 3. Beside phosphorylation, AtREM1.2 might contain additional modification since there was a slight difference in migration on the second dimension of electrophoresis between isoform 2 and 3, as well as isoform 4 and 5. Further, *in silico* analysis using ELM (the Eukaryotic Linear Motif) (Puntervoll et al., 2003) predicted sites for interaction with cyclin to enhance phosphorylation, besides several phosphorylation motifs in the amino acid sequence.

Up-regulation of isoforms 2, 4 and 5 was actually an increase in AtREM1.2 phosphorylation, rather than an increase in protein abundance. This is also supported by RT-PCR analysis that showed a decrease in AtREM1.2 transcript levels during the RPM1-defense response, indicating that AtREM1.2 up-regulation was caused by post-transcriptional and/or post-translational regulation.

The concept of “lipid rafts” was initially introduced by Simons and Ikonen (1997) following the finding that certain lipids preferentially reside in the exoplasmic rather than in the cytoplasmic leaflets of plasma membranes (Simons and Ikonen, 1997; Simons and van Meer, 1988). Thus, various lipids are not uniformly distributed in the membrane, but spatially organized in small microdomains. These microdomains have unique lipid compositions that are highly rich in sphingolipids and cholesterol (Simons and Ikonen, 1997). The sphingolipids associate with one another through interactions between carbohydrate heads of glycosphingolipids and cholesterol fill the space between the interacting sphingolipids. This

assembly forms ordered microdomains that are supposed to float freely in the surrounding membrane which is more fluid (Simons and Ikonen, 1997). The existence of such microdomains in the membrane results in phase separation, which may promote recruitment of lipid raft-associated proteins, and excluding other proteins (Matko and Szollosi, 2002). This ability is presumably important in signal transduction processes by bringing together the signaling components in the rafts to promote interaction and segregating the negative regulator from the rafts (Matko and Szollosi, 2002). Some biological roles have been proposed for lipid raft, including signal transduction, regulation of exocytosis, endocytosis, and apoptosis, actin cytoskeleton organization as well as subversion of lipid raft function for pathogen entry (Bhat and Panstruga, 2005)

Association of proteins to lipid rafts can be achieved through transmembrane domains or lipid anchors. For example, the transmembrane domain of influenza virus neuraminidase (NA) is the determinant for apical membrane targeting of NA and interaction with lipid rafts plasma membrane (Kundu et al., 1996). GPI-anchored proteins and acylated tyrosine kinase of the Src family are associated with rafts *via* protein modification (Horejsi et al., 1999; Matko and Szollosi, 2002; Simons and Ikonen, 1997).

The most common procedure to isolate lipid rafts is enrichment of detergent-resistant fraction with non-ionic detergent at low temperature, which is based on the insolubility of sphingolipid-cholesterol in TritonX-100 at 4°C. Because of their high lipid content, these detergent-resistant fractions float to low density in gradient centrifugation, thus enabling purification of lipid rafts and any associated proteins (Brown and Rose, 1992). Using adapted protocols from Borner et al. (2005), detergent-resistant membrane (DRM) was isolated and AtREM1.2 was detected in this fraction. Since AtREM1.2 does not contain any transmembrane domain, its association to lipid rafts may be through protein lipidation. The final tetrapeptide at the carboxyl-terminus of AtREM1.2 sequence (CGCF) contains motifs similar to the carboxyl-terminal prenylation motif. Proteins containing a cysteine residue four amino acid from the carboxyl-terminus (CaaX motif) or two cysteine residues at or very near the carboxyl-terminus (XCXC, XXCC or CCXX motifs) can undergo prenylation (Casey, 1995; Crowell, 2000). Besides the isoprenylation motif, the final amino acid of AtREM1.2 is a phenylalanine residue, which can also contribute to the hydrophobicity of the potential isoprenyl moieties to promote association to lipid rafts. The isolation of lipid rafts using the mentioned procedure has several drawbacks. The lipid behaviour in the plasma membrane is temperature dependent, and the reduction of temperature during the extraction could potentially change lipid organization in the plasma membrane (Munro, 2003). Heerklotz

(2002) also demonstrated that Triton itself can induce domain formation in membranes, which will be resistant to Triton solubilization in the subsequent extraction (Heerklotz, 2002). Even though the procedure to isolate lipid rafts tends to overestimate its composition, the presence of remorins in lipid rafts has been reported by numerous studies (Lefebvre et al., 2007; Mongrand et al., 2004; Morel et al., 2006; Shahollari et al., 2004), supporting the finding of AtREM1.2 in lipid raft membranes.

The association of AtREM1.2 to lipid rafts seems to be partial since a fraction of AtREM1.2 can also be found in the detergent soluble fraction (DSM). Distribution of proteins to lipid rafts to regulate downstream signaling has been demonstrated. Translocation of raft-associated proteins to the microdomains can cause simultaneous distribution and activation of kinases localized in these micro domains, followed by phosphorylation of their substrate to trigger signaling cascade (Horejsi et al., 1999). Stimulation of Ramos B cells B cell receptor (BCR) results in rapid translocation of a subset of the BCR complex to lipid rafts, even though some percentage of the complex remains in the soluble fraction. Since the earliest BCR-mediated signaling event is the activation of Src family tyrosine kinases, which are also present in lipid rafts, it is possible that BCRs are recruited to lipid rafts to initiate downstream signaling. In agreement with this, stimulation of BCR also induced tyrosine phosphorylation of several substrates in lipid rafts. It is still unclear whether these phosphorylated proteins are moved to the lipid rafts, or whether they are lipid rafts residents that are phosphorylated by activated kinases (Petrie et al., 2000). It could be that during avrRpm1-RPM1 interaction, a fraction of AtREM1.2 is phosphorylated and distributed to lipid raft microdomains; alternatively there is a fraction of AtREM1.2 that is always localized to lipid rafts and this is phosphorylated after R gene activation. Since remorins are often found in lipid rafts, even in untreated samples, they may indeed be lipid-raft resident proteins.

In plant defense, the role of lipid rafts has been reported by two independent studies (Assaad et al., 2004; Bhat et al., 2005). The *PEN1* (*PENETRATION1*) locus of *Arabidopsis* was identified in a genetic screen for mutants with increased penetration by the non-adapted pathogen, *Blumeria graminis* f.sp *hordei*. Upon infection with adapted and non-adapted powdery mildew, PEN1 accumulated at papillae, and papillae formation was significantly delayed in *pen1-1* mutants. This suggests that PEN1 defines a cellular compartment upon fungal attack and is required for papillae formation (Assaad et al., 2004). MLO, a protein that is required for the entry of adapted powdery mildew species in leaf epidermal cells, also accumulated beneath fungal appressoria upon pathogen attack (Bhat et al., 2005). ROR2, which is required for full expression of *mlo* resistance, was co-localized at the same site (Bhat

et al., 2005). This accumulation of plasma membrane proteins at the infection site is not a general phenomena, since other plasma membrane proteins known to reside in the leaf epidermis did not show similar localization (Bhat et al., 2005). Furthermore, analysis with filipin staining at these sites indicates enrichment of sterols, which are the main components of lipid rafts membrane. This is evidence of pathogen-induced microdomain formation in the host plasma membrane, which recruits certain plasma membrane proteins, while excluding others. Since *Pto* DC3000(*avrRpm1*) infection does not involve pathogen penetration, AtREM1.2 seems to have different role(s) in this resistance.

Belkhadir et al. (2004) suggest that resistance proteins are activated following recruitment of signaling molecules into resistance protein complexes, where reversible interaction and modification of the signaling molecules takes place. Since AtREM1.2 and RIN4 are both localized to membranes and phosphorylated during RPM1-mediated resistance, they might interact to activate *R* gene-mediated responses. However, no interaction between RIN4 and AtREM1.2 could be detected by co-immunoprecipitation (co-IP) using  $\alpha$ -RIN4 and  $\alpha$ -Remorin. Nevertheless, the low abundance of AtREM1.2 and its resistance to detergent solubilization may be the cause of the failure in detecting RIN4 and AtREM1.2 interaction. AtREM1.2 is a potential lipid raft membrane protein that is insoluble even at high concentration of Triton X-100 (2%). It is possible that only a small fraction of AtREM1.2 was solubilized in the co-IP buffer that contains 0.1% Triton X-100 and NP-40, which could explain the difficulties to immunoprecipitate AtREM1.2 using  $\alpha$ -Remorin. An attempt to optimise the detergent concentration near the CMC (critical micelle concentration) did not result in enhanced solubilization of AtREM1.2 (data not shown). Higher concentration of detergent above the CMC was avoided since it will result in the formation of micelles that possibly trap many proteins even though they do not interact with one another, leading to false positive result.

### **3.2. AtREM1.2 may play a role in maintaining cell integrity**

Functional analysis of AtREM1.2 in RPM1-mediated resistance was initiated by searching for T-DNA knockout mutants. None of the two mutants obtained from the SALK database showed a T-DNA insert in *AtREM1.2* gene. Generation of over-expressing transgenic plant under control of the 35S promoter did not produce plants with enhanced *AtREM1.2* protein expression. Only two out of the 27 putative over-expressing lines were able to express some *AtREM1.2* protein. Since all the over-expressing lines were generated using tag-containing vectors, it is possible to differentiate between the endogenous and the

transgene-derived protein. CFP/YFP increase the molecular mass (MW) by roughly 27 kDa, while the Strep tag will add roughly 1 kDa to AtREM1.2 MW. Thus, all AtREM1.2 transgenes will produce proteins with higher MW compared to the endogenous proteins. All putative over-expressing lines with no transgene expression showed no expression of endogenous *AtREM1.2*, while the lines with transgene expression still retained the endogenous *AtREM1.2*. The reduction of endogenous and *AtREM1.2* transgene proteins suggests co-suppression.

The high incidence of co-suppression in the transgenic lines suggests that AtREM1.2 plays some important role in normal development. On the other hand, AtREM1.2 is not absolutely essential since the co-suppressed *AtREM1.2* plants did not show any morphological or developmental defects, at least in the T1 generation. AtREM1.2 over-expression might result in inappropriate timing, location or level of expression that leads to the disturbed regulation of a certain pathway important for the plant, thus needs to be inactivated (Elkind et al., 1990).

Agrobacterium-mediated transient expression using over-expressing constructs did not produce any sign of tissue collapse or necrosis. A faint AtREM1.2 band could be detected by  $\alpha$ -Remorin (not shown), suggesting that the binary construct is functional. In contrast, minor necrosis was observed when the *AtREM1.2* silencing construct was used in tobacco (Fig. 32). Whether this cross-species silencing is specific for remorin and, if so, what causes the necrosis phenotype upon *AtREM1.2* silencing is not clear. Bariola et al. (2004) demonstrated that remorin can form filamentous structures, and speculated that it may play roles in cell survival, perhaps in cell integrity related to development or damage. It may well be that silencing *AtREM1.2* will reduce cell integrity that renders the plant more susceptible to damage.

### **3.3. Silencing *AtREM1.2* increases resistance specifically to *Pto* DC3000 (*avrRpm1*)**

To bypass the co-silencing problem when attempting to overexpress AtREM1.2, transformation with an estradiol-inducible AtREM1.2 (*EsAtREM1.2/rpm1-3* and *EsAtREM1.2/RPM1*) was performed. For comparison, RNAi (*AtREM1.2R1/rpm1-3*, *AtREM1.2Ri/RPM1*) plants were also created. Comparison between *EsAtREM1.2/RPM1*, *AtREM1.2Ri/RPM1* and wild type plants (the *RPM1* line) after dexamethasone spraying (to induce *avrRpm1* expression) did not show any clear difference in HR phenotype. Ion leakage assays to quantify the change in HR formation did not show significant differences either. Thus, AtREM1.2 does not seem to regulate HR formation in RPM1-mediated resistance.

Although figure 35 depicts some effect on the growth of the virulent *Pto* DC3000, this is only in one of the transgenic lines and at only one of the two time points analysed. Hence, there is no reproducible difference in susceptibility against virulent *Pto* DC3000 after silencing *AtREM1.2* in the *rpm1-3* and *RPM1* plants or after estradiol-induced expression of *AtREM1.2*. The variation in bacterial growth between *AtREM1.2Ri/Rpm1* (Fig. 35B) and *EsAtREM1.2/Rpm1* (Fig. 35C) may be due to the ethanol solvent for the estradiol solution (to induce *AtREM1.2* expression one day prior to bacterial infiltration), which might affect either the plant or the bacteria or both. The growth of the avirulent strain *Pto* DC3000(*avrRpm1*) in two independent *AtREM1.2*-silenced lines was reduced about 10 fold less than the *RPM1* plants at two and four dpi (Fig 36B). The increased resistance after silencing *AtREM1.2* was not accompanied by the opposite phenotype after estradiol-induced expression of *AtREM1.2*. The *RPM1* and *EsAtREM1.2/RPM1* lines showed similar bacterial colonization (Fig. 36C).

Taken together, these data demonstrate that silencing *AtREM1.2* increases specific resistance against *Pto* DC3000(*avrRpm1*), but induced expression of *AtREM1.2* does not compromise resistance against the same strain of bacteria. The same observation was seen for *RIN4*, where *rin4* is partially compromised in *Pto* DC3000(*avrRpm1*) resistance, but over-expression of *RIN4* did not enhance the resistance to *Pto* DC3000(*avrRpm1*) (Mackey et al., 2002). This might be explained by saturating wild type levels of *RIN4* (and perhaps *AtREM1.2*) for the resistance. Therefore additional expression is not needed for enhanced resistance. In the case of *AtREM1.2*, another possibility may be the epitope tag added to *AtREM1.2*. The inducible transgenic plants were generated with a construct carrying a Strep tag at the C-terminus of *AtREM1.2*. Since this C-terminus contains a potential isoprenylation site for membrane anchoring, the introduction of the tag may disturb the proper distribution of *AtREM1.2* to the membrane and affect the protein function. Additional experiments will be required to see if the tagged protein is still membrane/lipid raft-associated.

### **3.4. *AtREM1.2* does not regulate *RIN4* phosphorylation and the expression of *RPM1* marker genes *MMP2*, *RIPK* and *TonB***

To investigate whether enhanced resistance in *AtREM1.2*-silenced plants was regulated *via* known *RPM1*-signaling components, *RIN4* and *RPM1*-specific marker genes were analysed. There was no change in *RIN4* phosphorylation and *RPM1*-marker gene expression between the RNAi and *RPM1* plants after dexamethasone induction. In summary, *AtREM1.2* is not required for regulation of *RIN4* phosphorylation and *avrRpm1*-induced expression of *MMP2*, *RIPK* and *TonB*.

Analysis of AtREM1.2 does not give a clear answer regarding its role in RPM1-mediated resistance. It is still an enigma as to why the AtREM1.2 protein was not expressed in *rpm1-3* background despite the presence of the mRNA (Fig. 39). Nevertheless, it seems to be a negative regulator of resistance against *Pto* DC3000(*avrRpm1*) (Fig. 36B). However, some caution is needed for this interpretation since it is possible that more than one member of the remorin family might have been silenced.

#### 4. Summary

In summary, the screening of putative signaling proteins in the *avrRpm1*-RPM1 interaction resulted in four candidates of which two, PIA1 (At2g20630) and AtREM1.2 (At3g61260), were analysed in more details. Based on the results from functional analysis using “gain-of-function” and “loss-of-function” approaches, a model for roles of PIA1 and AtREM1.2 in the RPM1-mediated defense response is proposed.

Under non-challenged conditions (see Fig. 40A), PIA1 negatively regulates the expression of *PR5*, *PDF1.2* and *ACS6*. Since the enhanced expression of *PR5* and *PDF1.2* is independent of SA and ET/JA levels, the regulation of PIA1 on the gene expression may be direct, for example by releasing repressor(s) or activating the promoters of these genes. Alternatively, PIA1 may act in the signaling pathways downstream of SA and ET/JA. Analysis using double mutants of *pial* and SA signaling such, as *npr1*, JA signaling, such as *jin1/coi1* and ET signaling, such as *ein2* (Glazebrook, 2005) will be useful to clarify this.

After *avrRpm1*, but not *avrB*, perception by RPM1 (Fig. 40B), PIA1 is activated and negatively regulates defense responses initiated by RPM1, and this is presumably downstream of RIN4 phosphorylation. PIA1 also negatively regulates the expression of *MMP2*, an *avrRpm1*-responsive gene, which may also contribute to the suppression of the defense response. The role of *MMP2* in *RPM1*-mediated resistance remains to be determined. The up-regulation of PIA1 as a potential negative regulator of the defense response is peculiar; the explanation for this may be that activation of defense responses needs to be fine-balanced to avoid excessive damage that can be detrimental to plant cells. Earlier studies also discovered early induction of negative regulators during the defense response. He et al. (2004) found rapid activation of *PP2Ac* in tomato after inoculation with *Pto* DC3000(*avrPto*) and showed that this *PP2Ac* is a potential negative regulator of defense (He et al., 2004). Similarly, the expression of WRKY11 and WRKY17, transcription factors that act as negative regulators of basal resistance, was activated upon challenge with *Pto* (Journot-Catalino et al., 2006).

During *RPM1*-mediated resistance, PIA1 positively regulates the expression of *PR* genes and this regulation may be downstream of SA accumulation. To find out whether *PR* gene expression in the *pia1* mutants is SA-dependent, analysis using mutants with defects in SA biosynthesis will be valuable. The candidates for this study are *sid2* and *eds5*, which are defect in SA biosynthesis, or *nahG* transgenic plants that do not accumulate SA (Glazebrook, 2005). Besides SA-regulated genes, PIA1 also affects the JA/ET-regulated gene, *PR3*. Since JA and ET levels were not affected similarly, the regulation might be directly on the gene or in the signaling pathway downstream of JA/ET.

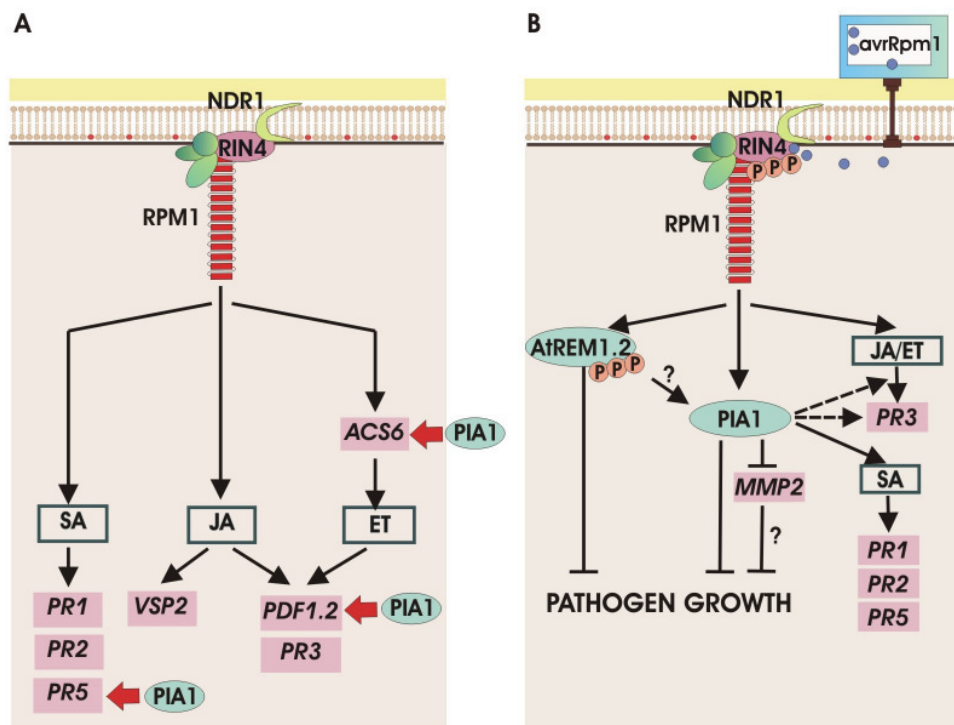


**Fig. 40** Model for the roles of PIA1 and AtREM1.2 in RPM1-mediated resistance. Under non-challenged condition PIA1 negatively regulates the expression of *PR5*, *PDF1.2* and *ACS6* (A). After the introduction of *avrRpm1* into plant cells, both PIA1 and AtREM1.2 act as negative regulators of the defense response in terms of growth of *Pto* DC3000(*avrRpm1*) (B). PIA also positively regulates *PR* gene expression possibly *via* SA-dependent pathway. PIA1 is specifically regulated by *avrRpm1* (but not *avrB*).

The second candidate, AtREM1.2, seems to also act as a negative regulator for RPM1-mediated resistance since silenced plants showed enhanced resistance to avirulent bacteria (Fig 36B). Particularly interesting for AtREM1.2 is the differential phosphorylation. This phosphorylation is likely downstream of RIN4 phosphorylation and might be upstream, or independent, of PIA1 up-regulation. The mechanism of AtREM1.2 regulation is still not clear, and requires further investigation. Since AtREM1.2 may be regulated through phosphorylation, analysis of phosphorylation site(s) and generation of mutants with altered phosphorylation states may provide better understanding of the mechanism.

## V. References

- Aarts, N., Metz, M., Holub, E., Staskawicz, B.J., Daniels, M.J. and Parker, J.E. (1998) Different requirements for EDS1 and NDR1 by disease resistance genes define at least two R gene-mediated signaling pathways in Arabidopsis. *Proc Natl Acad Sci U S A*, **95**, 10306-10311.
- Abramovitch, R.B., Kim, Y.J., Chen, S., Dickman, M.B. and Martin, G.B. (2003) Pseudomonas type III effector AvrPtoB induces plant disease susceptibility by inhibition of host programmed cell death. *Embo J*, **22**, 60-69.
- Abramovitch, R.B. and Martin, G.B. (2004) Strategies used by bacterial pathogens to suppress plant defenses. *Curr Opin Plant Biol*, **7**, 356-364.
- Alfano, J.R. and Collmer, A. (2004) Type III secretion system effector proteins: double agents in bacterial disease and plant defense. *Annu Rev Phytopathol*, **42**, 385-414.
- Anderson, N.L. and Anderson, N.G. (1998) Proteome and proteomics: new technologies, new concepts, and new words. *Electrophoresis*, **19**, 1853-1861.
- Andersson, M.X., Kourtschenko, O., Dangl, J.L., Mackey, D. and Ellerstrom, M. (2006) Phospholipase-dependent signalling during the AvrRpm1- and AvrRpt2-induced disease resistance responses in Arabidopsis thaliana. *Plant J*, **47**, 947-959.
- Asai, T., Tena, G., Plotnikova, J., Willmann, M.R., Chiu, W.L., Gomez-Gomez, L., Boller, T., Ausubel, F.M. and Sheen, J. (2002) MAP kinase signalling cascade in Arabidopsis innate immunity. *Nature*, **415**, 977-983.
- Assaad, F.F., Qiu, J.L., Youngs, H., Ehrhardt, D., Zimmerli, L., Kalde, M., Wanner, G., Peck, S.C., Edwards, H., Ramonell, K., Somerville, C.R. and Thordal-Christensen, H. (2004) The PEN1 syntaxin defines a novel cellular compartment upon fungal attack and is required for the timely assembly of papillae. *Mol Biol Cell*, **15**, 5118-5129.
- Ausubel, F.M. (2005) Are innate immune signaling pathways in plants and animals conserved? *Nat Immunol*, **6**, 973-979.
- Axtell, M.J., Chisholm, S.T., Dahlbeck, D. and Staskawicz, B.J. (2003) Genetic and molecular evidence that the Pseudomonas syringae type III effector protein AvrRpt2 is a cysteine protease. *Mol Microbiol*, **49**, 1537-1546.
- Axtell, M.J. and Staskawicz, B.J. (2003) Initiation of RPS2-specified disease resistance in Arabidopsis is coupled to the AvrRpt2-directed elimination of RIN4. *Cell*, **112**, 369-377.
- Baker, C.J., O'Neill, N.R., Dale Keppeler, L. and Orlandi, E.W. (1991) Early responses during plant-bacteria interactions in tobacco cell suspensions. *Phytopathol*, **81**, 1504-1507.
- Bariola, P.A., Retelska, D., Stasiak, A., Kammerer, R.A., Fleming, A., Hijri, M., Frank, S. and Farmer, E.E. (2004) Remorins form a novel family of coiled coil-forming oligomeric and filamentous proteins associated with apical, vascular and embryonic tissues in plants. *Plant Mol Biol*, **55**, 579-594.
- Belkadir, Y., Nimchuk, Z., Hubert, D.A., Mackey, D. and Dangl, J.L. (2004) Arabidopsis RIN4 negatively regulates disease resistance mediated by RPS2 and RPM1 downstream or independent of the NDR1 signal modulator and is not required for the virulence functions of bacterial type III effectors AvrRpt2 or AvrRpm1. *Plant Cell*, **16**, 2822-2835.
- Belkadir, Y., Subramaniam, R. and Dangl, J.L. (2004) Plant disease resistance protein signaling: NBS-LRR proteins and their partners. *Curr Opin Plant Biol*, **7**, 391-399.
- Benschop, J.J., Mohammed, S., O'Flaherty, M., Heck, A.J., Slijper, M. and Menke, F.L. (2007) Quantitative phosphoproteomics of early elicitor signaling in Arabidopsis. *Mol Cell Proteomics*, **6**, 1198-1214.

- Bhat, R.A., Miklis, M., Schmelzer, E., Schulze-Lefert, P. and Panstruga, R. (2005) Recruitment and interaction dynamics of plant penetration resistance components in a plasma membrane microdomain. *Proc Natl Acad Sci U S A*, **102**, 3135-3140.
- Bhat, R.A. and Panstruga, R. (2005) Lipid rafts in plants. *Planta*, **223**, 5-19.
- Bijlmakers, M.J. and Marsh, M. (2003) The on-off story of protein palmitoylation. *Trends Cell Biol*, **13**, 32-42.
- Blum, H., Beier, H. and Gross, H.J. (1987) Improved silver staining of plant proteins, RNA, and DNA in polyacrylamide gels. *Electrophoresis*, **8**, 93-99.
- Boyes, D.C., Nam, J. and Dangl, J.L. (1998) The Arabidopsis thaliana RPM1 disease resistance gene product is a peripheral plasma membrane protein that is degraded coincident with the hypersensitive response. *Proc Natl Acad Sci U S A*, **95**, 15849-15854.
- Brown, D.A. and Rose, J.K. (1992) Sorting of GPI-anchored proteins to glycolipid-enriched membrane subdomains during transport to the apical cell surface. *Cell*, **68**, 533-544.
- Bruce, A., Johnson, A.R., Lewis, J., Raff, M., Roberts, K. and Walters, P. (2002) Molecular Biology of the Cell. **Fourth Edition**.
- Büttner, D. and Bonas, U. (2003) Common infection strategies of plant and animal pathogenic bacteria. *Curr Opin Plant Biol*, **6**, 312-319.
- Casey, P.J. (1995) Protein lipidation in cell signaling. *Science*, **268**, 221-225.
- Chang, J.H., Urbach, J.M., Law, T.F., Arnold, L.W., Hu, A., Gombar, S., Grant, S.R., Ausubel, F.M. and Dangl, J.L. (2005) A high-throughput, near-saturating screen for type III effector genes from *Pseudomonas syringae*. *Proc Natl Acad Sci U S A*, **102**, 2549-2554.
- Charles, J., Travers, P., Walport, M. and Shlomchik, M. (2001) *Immunobiology*, **Fifth Edition**.
- Chisholm, S.T., Coaker, G., Day, B. and Staskawicz, B.J. (2006) Host-microbe interactions: shaping the evolution of the plant immune response. *Cell*, **124**, 803-814.
- Clarke, J.D., Volko, S.M., Ledford, H., Ausubel, F.M. and Dong, X. (2000) Roles of salicylic acid, jasmonic acid, and ethylene in cpr-induced resistance in Arabidopsis. *Plant Cell*, **12**, 2175-2190.
- Clough, S.J., Fengler, K.A., Yu, I.C., Lippok, B., Smith, R.K., Jr. and Bent, A.F. (2000) The Arabidopsis dnd1 "defense, no death" gene encodes a mutated cyclic nucleotide-gated ion channel. *Proc Natl Acad Sci U S A*, **97**, 9323-9328.
- Coaker, G.L., Willard, B., Kinter, M., Stockinger, E.J. and Francis, D.M. (2004) Proteomic analysis of resistance mediated by Rcm 2.0 and Rcm 5.1, two loci controlling resistance to bacterial canker of tomato. *Mol Plant Microbe Interact*, **17**, 1019-1028.
- Conrath, U., Silva, H. and Klessig, D.F. (1997) Protein dephosphorylation mediates salicylic acid-induced expression of PR-1 genes in tobacco. *Plant J*, **11**, 747-757.
- Coppinger, P., Repetti, P.P., Day, B., Dahlbeck, D., Mehlert, A. and Staskawicz, B.J. (2004) Overexpression of the plasma membrane-localized NDR1 protein results in enhanced bacterial disease resistance in Arabidopsis thaliana. *Plant J*, **40**, 225-237.
- Crowell, D.N. (2000) Functional implications of protein isoprenylation in plants. *Prog Lipid Res*, **39**, 393-408.
- Dangl, J.L., Dietrich, R.A. and Richberg, M.H. (1996) Death Don't Have No Mercy: Cell Death Programs in Plant-Microbe Interactions. *Plant Cell*, **8**, 1793-1807.
- Day, B., Dahlbeck, D. and Staskawicz, B.J. (2006) NDR1 interaction with RIN4 mediates the differential activation of multiple disease resistance pathways in Arabidopsis. *Plant Cell*, **18**, 2782-2791.
- de Torres, M., Sanchez, P., Fernandez-Delmond, I. and Grant, M. (2003) Expression profiling of the host response to bacterial infection: the transition from basal to induced defence responses in RPM1-mediated resistance. *Plant J*, **33**, 665-676.

- DeRoy, S., Thilmony, R., Kwack, Y.B., Nomura, K. and He, S.Y. (2004) A family of conserved bacterial effectors inhibits salicylic acid-mediated basal immunity and promotes disease necrosis in plants. *Proc Natl Acad Sci U S A*, **101**, 9927-9932.
- Dekker, L.V. and Parker, P.J. (1997) Regulated binding of the protein kinase C substrate GAP-43 to the V0/C2 region of protein kinase C-delta. *J Biol Chem*, **272**, 12747-12753.
- Delorme, V.G., McCabe, P.F., Kim, D.J. and Leaver, C.J. (2000) A matrix metalloproteinase gene is expressed at the boundary of senescence and programmed cell death in cucumber. *Plant Physiol*, **123**, 917-927.
- Deslandes, L., Olivier, J., Peeters, N., Feng, D.X., Khounlotham, M., Boucher, C., Somssich, I., Genin, S. and Marco, Y. (2003) Physical interaction between RRS1-R, a protein conferring resistance to bacterial wilt, and PopP2, a type III effector targeted to the plant nucleus. *Proc Natl Acad Sci U S A*, **100**, 8024-8029.
- Despres, C., Subramaniam, R., Matton, D.P. and Brisson, N. (1995) The Activation of the Potato PR-10a Gene Requires the Phosphorylation of the Nuclear Factor PBF-1. *Plant Cell*, **7**, 589-598.
- Devadas, S.K., Enyedi, A. and Raina, R. (2002) The Arabidopsis hrl1 mutation reveals novel overlapping roles for salicylic acid, jasmonic acid and ethylene signalling in cell death and defence against pathogens. *Plant J*, **30**, 467-480.
- Dinesh-Kumar, S.P., Tham, W.H. and Baker, B.J. (2000) Structure-function analysis of the tobacco mosaic virus resistance gene N. *Proc Natl Acad Sci U S A*, **97**, 14789-14794.
- Dodds, P.N., Lawrence, G.J., Catanzariti, A.M., Teh, T., Wang, C.I., Ayliffe, M.A., Kobe, B. and Ellis, J.G. (2006) Direct protein interaction underlies gene-for-gene specificity and coevolution of the flax resistance genes and flax rust avirulence genes. *Proc Natl Acad Sci U S A*, **103**, 8888-8893.
- Dodds, P.N., Lawrence, G.J. and Ellis, J.G. (2001) Six amino acid changes confined to the leucine-rich repeat beta-strand/beta-turn motif determine the difference between the P and P2 rust resistance specificities in flax. *Plant Cell*, **13**, 163-178.
- Dong, X. (1998) SA, JA, ethylene, and disease resistance in plants. *Curr Opin Plant Biol*, **1**, 316-323.
- Dunigan, D.D. and Madlener, J.C. (1995) Serine/threonine protein phosphatase is required for tobacco mosaic virus-mediated programmed cell death. *Virology*, **207**, 460-466.
- Eitas, T.K., Nimchuk, Z.L. and Dangl, J.L. (2008) Arabidopsis TAO1 is a TIR-NB-LRR protein that contributes to disease resistance induced by the *Pseudomonas syringae* effector AvrB. *Proc Natl Acad Sci U S A*, **105**, 6475-6480.
- Elkind, Y., Edwards, R., Mavandad, M., Hedrick, S.A., Ribak, O., Dixon, R.A. and Lamb, C.J. (1990) Abnormal plant development and down-regulation of phenylpropanoid biosynthesis in transgenic tobacco containing a heterologous phenylalanine ammonia-lyase gene. *Proc Natl Acad Sci U S A*, **87**, 9057-9061.
- Ellis, J.G., Lawrence, G.J., Luck, J.E. and Dodds, P.N. (1999) Identification of regions in alleles of the flax rust resistance gene L that determine differences in gene-for-gene specificity. *Plant Cell*, **11**, 495-506.
- Falk, A., Feys, B.J., Frost, L.N., Jones, J.D., Daniels, M.J. and Parker, J.E. (1999) EDS1, an essential component of R gene-mediated disease resistance in Arabidopsis has homology to eukaryotic lipases. *Proc Natl Acad Sci U S A*, **96**, 3292-3297.
- Felix, G., Duran, J.D., Volko, S. and Boller, T. (1999) Plants have a sensitive perception system for the most conserved domain of bacterial flagellin. *Plant J*, **18**, 265-276.
- Flor, H.H. (1971) Current status of the Gene-for-Gene Concept. *Annu Rev Phytopathol*, **9**, 275-296.

- Fritz-Laylin, L.K., Krishnamurthy, N., Tor, M., Sjolander, K.V. and Jones, J.D. (2005) Phylogenomic analysis of the receptor-like proteins of rice and Arabidopsis. *Plant Physiol*, **138**, 611-623.
- Fu, Z.Q., Guo, M., Jeong, B.R., Tian, F., Elthon, T.E., Cerny, R.L., Staiger, D. and Alfano, J.R. (2007) A type III effector ADP-ribosylates RNA-binding proteins and quells plant immunity. *Nature*, **447**, 284-288.
- Glazebrook, J. (2001) Genes controlling expression of defense responses in Arabidopsis--2001 status. *Curr Opin Plant Biol*, **4**, 301-308.
- Glazebrook, J. (2005) Contrasting mechanisms of defense against biotrophic and necrotrophic pathogens. *Annu Rev Phytopathol*, **43**, 205-227.
- Glazebrook, J., Zook, M., Mert, F., Kagan, I., Rogers, E.E., Crute, I.R., Holub, E.B., Hammerschmidt, R. and Ausubel, F.M. (1997) Phytoalexin-deficient mutants of Arabidopsis reveal that PAD4 encodes a regulatory factor and that four PAD genes contribute to downy mildew resistance. *Genetics*, **146**, 381-392.
- Golldack, D., Popova, O.V. and Dietz, K.J. (2002) Mutation of the matrix metalloproteinase At2-MMP inhibits growth and causes late flowering and early senescence in Arabidopsis. *J Biol Chem*, **277**, 5541-5547.
- Gomez-Gomez, L. and Boller, T. (2000) FLS2: an LRR receptor-like kinase involved in the perception of the bacterial elicitor flagellin in Arabidopsis. *Mol Cell*, **5**, 1003-1011.
- Görg, A., Weiss, W. and Dunn, M.J. (2004) Current two-dimensional electrophoresis technology for proteomics. *Proteomics*, **4**, 3665-3685.
- Grant, M.R., Godiard, L., Straube, E., Ashfield, T., Lewald, J., Sattler, A., Innes, R.W. and Dangl, J.L. (1995) Structure of the Arabidopsis RPM1 gene enabling dual specificity disease resistance. *Science*, **269**, 843-846.
- Grant, S.R., Fisher, E.J., Chang, J.H., Mole, B.M. and Dangl, J.L. (2006) Subterfuge and manipulation: type III effector proteins of phytopathogenic bacteria. *Annu Rev Microbiol*, **60**, 425-449.
- Gray, M.O., Karliner, J.S. and Mochly-Rosen, D. (1997) A selective epsilon-protein kinase C antagonist inhibits protection of cardiac myocytes from hypoxia-induced cell death. *J Biol Chem*, **272**, 30945-30951.
- Gygi, S.P., Rist, B., Gerber, S.A., Turecek, F., Gelb, M.H. and Aebersold, R. (1999) Quantitative analysis of complex protein mixtures using isotope-coded affinity tags. *Nat Biotechnol*, **17**, 994-999.
- Hahlbrock, K. and Scheel, D. (1989) Physiology and molecular biology of phenylpropanoid metabolism. *Annu Rev Plant Physiol Plant Mol Biol*, **40**, 347-369.
- Halim, V.A., Hunger, A., Macioszek, V., Landgraf, P., Nurnberger, T., Scheel, D. and Rosahl, S. (2004) The oligopeptide elicitor Pep-13 induces salicylic acid-dependent and -independent defense reactions in potato. *Physiol Mol Plant Pathol*, **64**, 311-318.
- Halligan, B.D., Ruotti, V., Jin, W., Laffoon, S., Twigger, S.N. and Dratz, E.A. (2004) ProMoST (Protein Modification Screening Tool): a web-based tool for mapping protein modifications on two-dimensional gels. *Nucleic Acids Res*, **32**, W638-644.
- Hammond-Kosack, K.E. and Jones, J.D. (1996) Resistance gene-dependent plant defense responses. *Plant Cell*, **8**, 1773-1791.
- Hauck, P., Thilmony, R. and He, S.Y. (2003) A *Pseudomonas syringae* type III effector suppresses cell wall-based extracellular defense in susceptible Arabidopsis plants. *Proc Natl Acad Sci U S A*, **100**, 8577-8582.
- He, P., Chintamanani, S., Chen, Z., Zhu, L., Kunkel, B.N., Alfano, J.R., Tang, X. and Zhou, J.M. (2004) Activation of a COI1-dependent pathway in Arabidopsis by *Pseudomonas syringae* type III effectors and coronatine. *Plant J*, **37**, 589-602.

- He, X., Anderson, J.C., del Pozo, O., Gu, Y.Q., Tang, X. and Martin, G.B. (2004) Silencing of subfamily I of protein phosphatase 2A catalytic subunits results in activation of plant defense responses and localized cell death. *Plant J*, **38**, 563-577.
- Heerklotz, H. (2002) Triton promotes domain formation in lipid raft mixtures. *Biophys J*, **83**, 2693-2701.
- Horejsi, V., Drbal, K., Cebecauer, M., Cerny, J., Brdicka, T., Angelisova, P. and Stockinger, H. (1999) GPI-microdomains: a role in signalling via immunoreceptors. *Immunol Today*, **20**, 356-361.
- Hubert, D.A., Tornero, P., Belkhadir, Y., Krishna, P., Takahashi, A., Shirasu, K. and Dangl, J.L. (2003) Cytosolic HSP90 associates with and modulates the Arabidopsis RPM1 disease resistance protein. *Embo J*, **22**, 5679-5689.
- Hunt, D.F., Yates, J.R., 3rd, Shabanowitz, J., Winston, S. and Hauer, C.R. (1986) Protein sequencing by tandem mass spectrometry. *Proc Natl Acad Sci U S A*, **83**, 6233-6237.
- Ideker, T., Galitski, T. and Hood, L. (2001) A new approach to decoding life: systems biology. *Annu Rev Genomics Hum Genet*, **2**, 343-372.
- Janjusevic, R., Abramovitch, R.B., Martin, G.B. and Stebbins, C.E. (2006) A bacterial inhibitor of host programmed cell death defenses is an E3 ubiquitin ligase. *Science*, **311**, 222-226.
- Jia, Y., McAdams, S.A., Bryan, G.T., Hershey, H.P. and Valent, B. (2000) Direct interaction of resistance gene and avirulence gene products confers rice blast resistance. *Embo J*, **19**, 4004-4014.
- Jirage, D., Tootle, T.L., Reuber, T.L., Frost, L.N., Feys, B.J., Parker, J.E., Ausubel, F.M. and Glazebrook, J. (1999) Arabidopsis thaliana PAD4 encodes a lipase-like gene that is important for salicylic acid signaling. *Proc Natl Acad Sci U S A*, **96**, 13583-13588.
- Jones, A.M., Thomas, V., Bennett, M.H., Mansfield, J. and Grant, M. (2006) Modifications to the Arabidopsis defense proteome occur prior to significant transcriptional change in response to inoculation with *Pseudomonas syringae*. *Plant Physiol*, **142**, 1603-1620.
- Jones, A.M., Thomas, V., Truman, B., Lilley, K., Mansfield, J. and Grant, M. (2004) Specific changes in the Arabidopsis proteome in response to bacterial challenge: differentiating basal and R-gene mediated resistance. *Phytochemistry*, **65**, 1805-1816.
- Jones, D.A. and Jones, J.D.G. (1997) The role of leucine-rich repeat proteins in plant defense. *Adv Bot Res Adv Plant Pathol*, **24**, 89-167.
- Jones, J.D. and Dangl, J.L. (2006) The plant immune system. *Nature*, **444**, 323-329.
- Journot-Catalino, N., Somssich, I.E., Roby, D. and Kroj, T. (2006) The transcription factors WRKY11 and WRKY17 act as negative regulators of basal resistance in Arabidopsis thaliana. *Plant Cell*, **18**, 3289-3302.
- Kay, S., Hahn, S., Marois, E., Hause, G. and Bonas, U. (2007) A bacterial effector acts as a plant transcription factor and induces a cell size regulator. *Science*, **318**, 648-651.
- Kim, H.S., Desveaux, D., Singer, A.U., Patel, P., Sondek, J. and Dangl, J.L. (2005) The *Pseudomonas syringae* effector AvrRpt2 cleaves its C-terminally acylated target, RIN4, from Arabidopsis membranes to block RPM1 activation. *Proc Natl Acad Sci U S A*, **102**, 6496-6501.
- Kim, M.G., da Cunha, L., McFall, A.J., Belkhadir, Y., DebRoy, S., Dangl, J.L. and Mackey, D. (2005) Two *Pseudomonas syringae* type III effectors inhibit RIN4-regulated basal defense in Arabidopsis. *Cell*, **121**, 749-759.
- Kim, S.T., Cho, K.S., Jang, Y.S. and Kang, K.Y. (2001) Two-dimensional electrophoretic analysis of rice proteins by polyethylene glycol fractionation for protein arrays. *Electrophoresis*, **22**, 2103-2109.
- Kumar, A., Dhawan, S., Mukhopadhyay, A. and Aggarwal, B.B. (1999) Human immunodeficiency virus-1-tat induces matrix metalloproteinase-9 in monocytes

- through protein tyrosine phosphatase-mediated activation of nuclear transcription factor NF-kappaB. *FEBS Lett*, **462**, 140-144.
- Kundu, A., Avalos, R.T., Sanderson, C.M. and Nayak, D.P. (1996) Transmembrane domain of influenza virus neuraminidase, a type II protein, possesses an apical sorting signal in polarized MDCK cells. *J Virol*, **70**, 6508-6515.
- Kunkel, B.N. and Brooks, D.M. (2002) Cross talk between signaling pathways in pathogen defense. *Curr Opin Plant Biol*, **5**, 325-331.
- Lacomme, C. and Santa Cruz, S. (1999) Bax-induced cell death in tobacco is similar to the hypersensitive response. *Proc Natl Acad Sci U S A*, **96**, 7956-7961.
- Lee, J., Rudd, J.J., Macioszek, V.K. and Scheel, D. (2004) Dynamic changes in the localization of MAPK cascade components controlling pathogenesis-related (PR) gene expression during innate immunity in parsley. *J Biol Chem*, **279**, 22440-22448.
- Lee, M.W., Jelenska, J. and Greenberg, J.T. (2008) Arabidopsis proteins important for modulating defense responses to *Pseudomonas syringae* that secrete HopW1-1. *Plant J*, **54**, 452-465.
- Lee, Y.H., Kolade, O.O., Nomura, K., Arvidson, D.N. and He, S.Y. (2005) Use of dominant-negative HrpA mutants to dissect Hrp pilus assembly and type III secretion in *Pseudomonas syringae* pv. tomato. *J Biol Chem*, **280**, 21409-21417.
- Lefebvre, B., Furt, F., Hartmann, M.A., Michaelson, L.V., Carde, J.P., Sargueil-Boiron, F., Rossignol, M., Napier, J.A., Cullimore, J., Bessoule, J.J. and Mongrand, S. (2007) Characterization of lipid rafts from *Medicago truncatula* root plasma membranes: a proteomic study reveals the presence of a raft-associated redox system. *Plant Physiol*, **144**, 402-418.
- Liang, X., Abel, S., Keller, J.A., Shen, N.F. and Theologis, A. (1992) The 1-aminocyclopropane-1-carboxylate synthase gene family of *Arabidopsis thaliana*. *Proc Natl Acad Sci U S A*, **89**, 11046-11050.
- Liu, Y., Dammann, C. and Bhattacharyya, M.K. (2001) The matrix metalloproteinase gene GmMMP2 is activated in response to pathogenic infections in soybean. *Plant Physiol*, **127**, 1788-1797.
- Liu, Y. and Zhang, S. (2004) Phosphorylation of 1-aminocyclopropane-1-carboxylic acid synthase by MPK6, a stress-responsive mitogen-activated protein kinase, induces ethylene biosynthesis in *Arabidopsis*. *Plant Cell*, **16**, 3386-3399.
- Loh, Y.T., Zhou, J. and Martin, G.B. (1998) The myristylation motif of Pto is not required for disease resistance. *Mol Plant Microbe Interact*, **11**, 572-576.
- Mackey, D., Belkhadir, Y., Alonso, J.M., Ecker, J.R. and Dangl, J.L. (2003) Arabidopsis RIN4 is a target of the type III virulence effector AvrRpt2 and modulates RPS2-mediated resistance. *Cell*, **112**, 379-389.
- Mackey, D., Holt, B.F., 3rd, Wiig, A. and Dangl, J.L. (2002) RIN4 interacts with *Pseudomonas syringae* type III effector molecules and is required for RPM1-mediated resistance in *Arabidopsis*. *Cell*, **108**, 743-754.
- Martin, G.B., Bogdanove, A.J. and Sessa, G. (2003) Understanding the functions of plant disease resistance proteins. *Annu Rev Plant Biol*, **54**, 23-61.
- Martin, G.B., Brommonschenkel, S.H., Chunwongse, J., Frary, A., Ganai, M.W., Spivey, R., Wu, T., Earle, E.D. and Tanksley, S.D. (1993) Map-based cloning of a protein kinase gene conferring disease resistance in tomato. *Science*, **262**, 1432-1436.
- Matko, J. and Szollosi, J. (2002) Landing of immune receptors and signal proteins on lipid rafts: a safe way to be spatio-temporally coordinated? *Immunol Lett*, **82**, 3-15.
- Mellor, H. and Parker, P.J. (1998) The extended protein kinase C superfamily. *Biochem J*, **332** (Pt 2), 281-292.
- Melotto, M., Underwood, W., Koczan, J., Nomura, K. and He, S.Y. (2006) Plant stomata function in innate immunity against bacterial invasion. *Cell*, **126**, 969-980.

- Mongrand, S., Morel, J., Laroche, J., Claverol, S., Carde, J.P., Hartmann, M.A., Bonneau, M., Simon-Plas, F., Lessire, R. and Bessoule, J.J. (2004) Lipid rafts in higher plant cells: purification and characterization of Triton X-100-insoluble microdomains from tobacco plasma membrane. *J Biol Chem*, **279**, 36277-36286.
- Morel, J., Claverol, S., Mongrand, S., Furt, F., Fromentin, J., Bessoule, J.J., Blein, J.P. and Simon-Plas, F. (2006) Proteomics of plant detergent-resistant membranes. *Mol Cell Proteomics*, **5**, 1396-1411.
- Mudgett, M.B. (2005) New insights to the function of phytopathogenic bacterial type III effectors in plants. *Annu Rev Plant Biol*, **56**, 509-531.
- Munro, S. (2003) Lipid rafts: elusive or illusive? *Cell*, **115**, 377-388.
- Naqvi, S.M., Park, K.S., Yi, S.Y., Lee, H.W., Bok, S.H. and Choi, D. (1998) A glycine-rich RNA-binding protein gene is differentially expressed during acute hypersensitive response following Tobacco Mosaic Virus infection in tobacco. *Plant Mol Biol*, **37**, 571-576.
- Newton, A.C. and Johnson, J.E. (1998) Protein kinase C: a paradigm for regulation of protein function by two membrane-targeting modules. *Biochim Biophys Acta*, **1376**, 155-172.
- Nimchuk, Z., Marois, E., Kjemtrup, S., Leister, R.T., Katagiri, F. and Dangl, J.L. (2000) Eukaryotic fatty acylation drives plasma membrane targeting and enhances function of several type III effector proteins from *Pseudomonas syringae*. *Cell*, **101**, 353-363.
- Nomura, K., Melotto, M. and He, S.Y. (2005) Suppression of host defense in compatible plant-*Pseudomonas syringae* interactions. *Curr Opin Plant Biol*, **8**, 361-368.
- Nürnberg, T., Brunner, F., Kemmerling, B. and Piater, L. (2004) Innate immunity in plants and animals: striking similarities and obvious differences. *Immunol Rev*, **198**, 249-266.
- Palmgren, M.G. and Christensen, G. (1994) Functional comparisons between plant plasma membrane H(+)-ATPase isoforms expressed in yeast. *J Biol Chem*, **269**, 3027-3033.
- Patterson, S.D. and Aebersold, R.H. (2003) Proteomics: the first decade and beyond. *Nat Genet*, **33 Suppl**, 311-323.
- Penninckx, I.A., Eggermont, K., Terras, F.R., Thomma, B.P., De Samblanx, G.W., Buchala, A., Metraux, J.P., Manners, J.M. and Broekaert, W.F. (1996) Pathogen-induced systemic activation of a plant defensin gene in *Arabidopsis* follows a salicylic acid-independent pathway. *Plant Cell*, **8**, 2309-2323.
- Penninckx, I.A., Thomma, B.P., Buchala, A., Metraux, J.P. and Broekaert, W.F. (1998) Concomitant activation of jasmonate and ethylene response pathways is required for induction of a plant defensin gene in *Arabidopsis*. *Plant Cell*, **10**, 2103-2113.
- Peterhansel, C., Freialdenhoven, A., Kurth, J., Kolsch, R. and Schulze-Lefert, P. (1997) Interaction Analyses of Genes Required for Resistance Responses to Powdery Mildew in Barley Reveal Distinct Pathways Leading to Leaf Cell Death. *Plant Cell*, **9**, 1397-1409.
- Petrie, R.J., Schnetkamp, P.P., Patel, K.D., Awasthi-Kalia, M. and Deans, J.P. (2000) Transient translocation of the B cell receptor and Src homology 2 domain-containing inositol phosphatase to lipid rafts: evidence toward a role in calcium regulation. *J Immunol*, **165**, 1220-1227.
- Pieterse, C.M., van Wees, S.C., Hoffland, E., van Pelt, J.A. and van Loon, L.C. (1996) Systemic resistance in *Arabidopsis* induced by biocontrol bacteria is independent of salicylic acid accumulation and pathogenesis-related gene expression. *Plant Cell*, **8**, 1225-1237.
- Pugin, A., Frachisse, J.M., Tavernier, E., Bigny, R., Gout, E., Douce, R. and Guern, J. (1997) Early Events Induced by the Elicitor Cryptogein in Tobacco Cells: Involvement of a Plasma Membrane NADPH Oxidase and Activation of Glycolysis and the Pentose Phosphate Pathway. *Plant Cell*, **9**, 2077-2091.

- Puntervoll, P., Linding, R., Gemund, C., Chabanis-Davidson, S., Mattingsdal, M., Cameron, S., Martin, D.M., Ausiello, G., Brannetti, B., Costantini, A., Ferre, F., Maselli, V., Via, A., Cesareni, G., Diella, F., Superti-Furga, G., Wyrwicz, L., Ramu, C., McGuigan, C., Gudavalli, R., Letunic, I., Bork, P., Rychlewski, L., Kuster, B., Helmer-Citterich, M., Hunter, W.N., Aasland, R. and Gibson, T.J. (2003) ELM server: A new resource for investigating short functional sites in modular eukaryotic proteins. *Nucleic Acids Res*, **31**, 3625-3630.
- Raffaele, S., Mongrand, S., Gamas, P., Niebel, A. and Ott, T. (2007) Genome-wide annotation of remorins, a plant-specific protein family: evolutionary and functional perspectives. *Plant Physiol*, **145**, 593-600.
- Rehmany, A.P., Gordon, A., Rose, L.E., Allen, R.L., Armstrong, M.R., Whisson, S.C., Kamoun, S., Tyler, B.M., Birch, P.R. and Beynon, J.L. (2005) Differential recognition of highly divergent downy mildew avirulence gene alleles by RPP1 resistance genes from two Arabidopsis lines. *Plant Cell*, **17**, 1839-1850.
- Reymond, P., Kunz, B., Paul-Pletzer, K., Grimm, R., Eckerskorn, C. and Farmer, E.E. (1996) Cloning of a cDNA encoding a plasma membrane-associated, uronide binding phosphoprotein with physical properties similar to viral movement proteins. *Plant Cell*, **8**, 2265-2276.
- Ritter, C. and Dangl, J.L. (1995) The avrRpm1 gene of *Pseudomonas syringae* pv. *maculicola* is required for virulence on Arabidopsis. *Mol Plant Microbe Interact*, **8**, 444-453.
- Ritter, C. and Dangl, J.L. (1996) Interference between Two Specific Pathogen Recognition Events Mediated by Distinct Plant Disease Resistance Genes. *Plant Cell*, **8**, 251-257.
- Rojo, E., Titarenko, E., Leon, J., Berger, S., Vancanneyt, G. and Sanchez-Serrano, J.J. (1998) Reversible protein phosphorylation regulates jasmonic acid-dependent and -independent wound signal transduction pathways in Arabidopsis thaliana. *Plant J*, **13**, 153-165.
- Römer, P., Hahn, S., Jordan, T., Strauss, T., Bonas, U. and Lahaye, T. (2007) Plant pathogen recognition mediated by promoter activation of the pepper Bs3 resistance gene. *Science*, **318**, 645-648.
- Ron, D., Luo, J. and Mochly-Rosen, D. (1995) C2 region-derived peptides inhibit translocation and function of beta protein kinase C in vivo. *J Biol Chem*, **270**, 24180-24187.
- Rooney, H.C., Van't Klooster, J.W., van der Hoorn, R.A., Joosten, M.H., Jones, J.D. and de Wit, P.J. (2005) Cladosporium Avr2 inhibits tomato Rcr3 protease required for Cf-2-dependent disease resistance. *Science*, **308**, 1783-1786.
- Rose, J.K., Bashir, S., Giovannoni, J.J., Jahn, M.M. and Saravanan, R.S. (2004) Tackling the plant proteome: practical approaches, hurdles and experimental tools. *Plant J*, **39**, 715-733.
- Ruhul Amin, A.R., Oo, M.L., Senga, T., Suzuki, N., Feng, G.S. and Hamaguchi, M. (2003) SH2 domain containing protein tyrosine phosphatase 2 regulates concanavalin A-dependent secretion and activation of matrix metalloproteinase 2 via the extracellular signal-regulated kinase and p38 pathways. *Cancer Res*, **63**, 6334-6339.
- Sambrook, J., Fritsch, E.F. and Maniatis, T. (1989) Molecular Cloning: A Laboratory Manual. **Second edition**.
- Sanabria, N., Goring, D., Nurnberger, T. and Dubery, I. (2008) Self/nonsel perception and recognition mechanisms in plants: a comparison of self-incompatibility and innate immunity. *New Phytol*, **178**, 503-514.
- Schmidt, F., Dahlmann, B., Janek, K., Kloss, A., Wacker, M., Ackermann, R., Thiede, B. and Jungblut, P.R. (2006) Comprehensive quantitative proteome analysis of 20S proteasome subtypes from rat liver by isotope coded affinity tag and 2-D gel-based approaches. *Proteomics*, **6**, 4622-4632.

- Schmidt, F., Donahoe, S., Hagens, K., Mattow, J., Schaible, U.E., Kaufmann, S.H., Aebbersold, R. and Jungblut, P.R. (2004) Complementary analysis of the Mycobacterium tuberculosis proteome by two-dimensional electrophoresis and isotope-coded affinity tag technology. *Mol Cell Proteomics*, **3**, 24-42.
- Schrattenholz, A. (2004) Proteomics: how to control highly dynamic patterns of millions of molecules and interpret changes correctly? *Drug Discovery Today: Technologies*, **1**, 1-8.
- Schulze-Lefert, P. and Panstruga, R. (2003) Establishment of biotrophy by parasitic fungi and reprogramming of host cells for disease resistance. *Annu Rev Phytopathol*, **41**, 641-667.
- Schweighofer, A., Hirt, H. and Meskiene, I. (2004) Plant PP2C phosphatases: emerging functions in stress signaling. *Trends Plant Sci*, **9**, 236-243.
- Schweighofer, A., Kazanaviciute, V., Scheikl, E., Teige, M., Doczi, R., Hirt, H., Schwanninger, M., Kant, M., Schuurink, R., Mauch, F., Buchala, A., Cardinale, F. and Meskiene, I. (2007) The PP2C-type phosphatase AP2C1, which negatively regulates MPK4 and MPK6, modulates innate immunity, jasmonic acid, and ethylene levels in Arabidopsis. *Plant Cell*, **19**, 2213-2224.
- Shah, J., Kachroo, P. and Klessig, D.F. (1999) The Arabidopsis *ssi1* mutation restores pathogenesis-related gene expression in *npr1* plants and renders defensin gene expression salicylic acid dependent. *Plant Cell*, **11**, 191-206.
- Shahollari, B., Peskan-Berghoefler, T. and Oelmueller, R. (2004) Receptor kinases with leucine-rich repeats are enriched in Triton X-100 insoluble plasma membrane microdomains from plants. *Physiol Plant*, **122**, 397-403.
- Shao, F., Golstein, C., Ade, J., Stoutemyer, M., Dixon, J.E. and Innes, R.W. (2003) Cleavage of Arabidopsis PBS1 by a bacterial type III effector. *Science*, **301**, 1230-1233.
- Shen, Y. and Ronald, P. (2002) Molecular determinants of disease and resistance in interactions of *Xanthomonas oryzae* pv. *oryzae* and rice. *Microbes Infect*, **4**, 1361-1367.
- Simons, K. and Ikonen, E. (1997) Functional rafts in cell membranes. *Nature*, **387**, 569-572.
- Simons, K. and van Meer, G. (1988) Lipid sorting in epithelial cells. *Biochemistry*, **27**, 6197-6202.
- Sutherland, M.W. (1991) The generation of oxygen radicals during host plant responses to infection. *Physiol Mol Plant Pathol*, **39**, 79-93.
- Tao, Y., Xie, Z., Chen, W., Glazebrook, J., Chang, H.S., Han, B., Zhu, T., Zou, G. and Katagiri, F. (2003) Quantitative nature of Arabidopsis responses during compatible and incompatible interactions with the bacterial pathogen *Pseudomonas syringae*. *Plant Cell*, **15**, 317-330.
- Thordal-Christensen, H. (2003) Fresh insights into processes of nonhost resistance. *Curr Opin Plant Biol*, **6**, 351-357.
- Thordal-Christensen, H., Zhang, Z.G., Wei, Y.D. and Collinge, D.B. (1997) Subcellular localization of H<sub>2</sub>O<sub>2</sub> in plants. H<sub>2</sub>O<sub>2</sub> accumulation in papillae and hypersensitive response during the barley-powdery mildew interaction. *Plant J*, **11**, 1187-1194.
- Tornero, P., Chao, R.A., Luthin, W.N., Goff, S.A. and Dangl, J.L. (2002) Large-scale structure-function analysis of the Arabidopsis RPM1 disease resistance protein. *Plant Cell*, **14**, 435-450.
- Tornero, P., Merritt, P., Sadanandom, A., Shirasu, K., Innes, R.W. and Dangl, J.L. (2002) RAR1 and NDR1 contribute quantitatively to disease resistance in Arabidopsis, and their relative contributions are dependent on the R gene assayed. *Plant Cell*, **14**, 1005-1015.

- Truman, W., de Zabala, M.T. and Grant, M. (2006) Type III effectors orchestrate a complex interplay between transcriptional networks to modify basal defence responses during pathogenesis and resistance. *Plant J*, **46**, 14-33.
- Uknes, S., Mauch-Mani, B., Moyer, M., Potter, S., Williams, S., Dincher, S., Chandler, D., Slusarenko, A., Ward, E. and Ryals, J. (1992) Acquired resistance in Arabidopsis. *Plant Cell*, **4**, 645-656.
- van den Burg, H.A., Westerink, N., Francoijs, K.J., Roth, R., Woestenenk, E., Boeren, S., de Wit, P.J., Joosten, M.H. and Vervoort, J. (2003) Natural disulfide bond-disrupted mutants of AVR4 of the tomato pathogen *Cladosporium fulvum* are sensitive to proteolysis, circumvent Cf-4-mediated resistance, but retain their chitin binding ability. *J Biol Chem*, **278**, 27340-27346.
- Van der Biezen, E.A. and Jones, J.D. (1998) Plant disease-resistance proteins and the gene-for-gene concept. *Trends Biochem Sci*, **23**, 454-456.
- van Loon, L.C., Bakker, P.A. and Pieterse, C.M. (1998) Systemic resistance induced by rhizosphere bacteria. *Annu Rev Phytopathol*, **36**, 453-483.
- Van Loon, L.C. and Van Strien, E.A. (1999) The families of pathogenesis-related proteins, their activities, and comparative analysis of PR-1 type proteins. *Physiol Mol Plant Pathol*, **55**, 85-97.
- Wang, K.L., Li, H. and Ecker, J.R. (2002) Ethylene biosynthesis and signaling networks. *Plant Cell*, **14 Suppl**, S131-151.
- Warren, R.F., Merritt, P.M., Holub, E. and Innes, R.W. (1999) Identification of three putative signal transduction genes involved in R gene-specified disease resistance in Arabidopsis. *Genetics*, **152**, 401-412.
- Washburn, M.P., Wolters, D. and Yates, J.R., 3rd. (2001) Large-scale analysis of the yeast proteome by multidimensional protein identification technology. *Nat Biotechnol*, **19**, 242-247.
- Whisson, S.C., Boevink, P.C., Moleleki, L., Avrova, A.O., Morales, J.G., Gilroy, E.M., Armstrong, M.R., Grouffaud, S., van West, P., Chapman, S., Hein, I., Toth, I.K., Pritchard, L. and Birch, P.R. (2007) A translocation signal for delivery of oomycete effector proteins into host plant cells. *Nature*, **450**, 115-118.
- Yu, I.C., Parker, J. and Bent, A.F. (1998) Gene-for-gene disease resistance without the hypersensitive response in Arabidopsis *dnd1* mutant. *Proc Natl Acad Sci U S A*, **95**, 7819-7824.
- Zhao, Y., Thilmony, R., Bender, C.L., Schaller, A., He, S.Y. and Howe, G.A. (2003) Virulence systems of *Pseudomonas syringae* pv. tomato promote bacterial speck disease in tomato by targeting the jasmonate signaling pathway. *Plant J*, **36**, 485-499.
- Zhu, W., Yang, B., Chittoor, J.M., Johnson, L.B. and White, F.F. (1998) AvrXa10 contains an acidic transcriptional activation domain in the functionally conserved C terminus. *Mol Plant Microbe Interact*, **11**, 824-832.
- Zipfel, C., Robatzek, S., Navarro, L., Oakeley, E.J., Jones, J.D., Felix, G. and Boller, T. (2004) Bacterial disease resistance in Arabidopsis through flagellin perception. *Nature*, **428**, 764-767.

List of abbreviations for effector proteins

Avr2	Avirulence protein 2 from <i>Cladosporium fulvum</i> (also Avr4/9)
Avr3a	Avirulence protein 3a from <i>Phytophthora infestans</i>
AvrB	Avirulence protein B from <i>Psg</i>
Avrb6	Avirulence protein b6 from <i>Xanthomonas campestris</i> pv. <i>malvacearum</i>
AvrBs3	Avirulence protein Bs3 from <i>Xcv</i> (also AvrBsT)
AvrE	Avirulence protein E from <i>Pto</i> DC3000
AvrL	Avirulence protein L from flax rust fungus ( <i>Melampsora lini</i> )
Avr-PITA	Avirulence protein from <i>Magnaporthe grisea</i>
AvrPphB	Avirulence protein B from <i>Pph</i> (also AvrPphC, AvrPphE, AvrPphF)
AvrPpiB1 <sub>Pto</sub>	Avirulence protein from <i>Pseudomonas syringae</i> pv. <i>pisi</i> race 3A strain 870A
AvrPto	Avirulence protein from <i>Pto</i>
AvrPtoB	Avirulence protein from <i>Pto</i> with functional similarity to AvrPto
AvrRpm1	Avirulence protein 1 from <i>Pma</i>
AvrRps4	Avirulence protein from <i>Pseudomonas syringae</i> pv. <i>pisi</i> strain 151
AvrRpt2	Avirulence protein 2 from <i>Pto</i>
AvrXa7	Avirulence protein from <i>Xanthomonas oryzae</i> pv. <i>oryzae</i>
AvrXa10	Avirulence protein from <i>Xanthomonas oryzae</i> pv. <i>oryzae</i>
AvrXv4	Avirulence protein from <i>Xcv</i>
Hop	Hrp outer protein in <i>Pseudomonas</i>
HopPtoD2	Effector protein from <i>Pto</i> DC3000 (initially designated as AvrPphD2 <sub>Pto</sub> )
HopPtoE	Effector protein from <i>Pto</i> DC3000
HopPtoF	Effector protein from <i>Pto</i> DC3000 (AvrPphF homolog)
HopPtoK	Effector protein from <i>Pto</i> DC3000 (AvrRps4 homolog)
HopPtoM	Effector protein from <i>Pto</i> DC3000
HopPsyA	Effector protein from <i>Pseudomonas syringae</i> pv. <i>syringae</i> 61
HopU1	Effector protein from <i>Pto</i> DC3000 (initially designated as hopPtoS2)
HopW1	Effector protein from <i>Pma</i> strain ES4326
<i>PthA</i>	<i>Pathogenicity gene</i> from <i>Xanthomonas citri</i>
Pop	<i>Pseudomonas</i> outer protein in <i>Ralstonia</i>
Pop2	Avirulence protein from <i>Ralstonia solanacearum</i>
<i>VirPphA</i>	Virulence gene A from <i>Pph</i>
Xop	<i>Xanthomonas</i> outer protein in <i>Xanthomonas</i>
XopD	Effector protein from <i>Xcv</i>

List of abbreviations for resistance proteins

Bs3	Resistance to <i>Xcv</i> expressing AvrBs3
Cf-2	Resistance to <i>Cladosporium fulvum</i> 2
Cf-9	Resistance to <i>Cladosporium fulvum</i> 9
Pi-ta	Resistance to <i>Magnaporthe grisea</i>
Pto	Resistance to <i>Pseudomonas syringae</i> expressing AvrPto
R3a	Resistance to <i>Phytophthora infestans</i> expressing <i>avr3a</i>
RPM1	Resistance to <i>Pma</i> 1

---

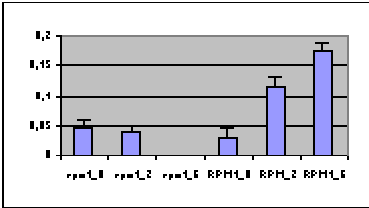
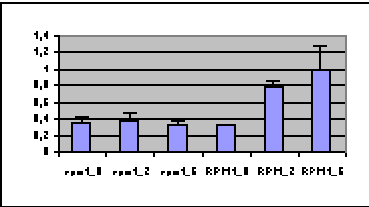
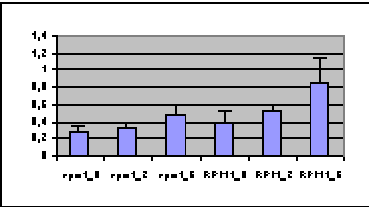
RPP2	Resistance to <i>Hyaloperonospora parasitica</i> 2 (also RPP4/5/7/8/10/13714)
RPS2	Resistance to <i>Pseudomonas syringae</i> expressing <i>avrRpt2</i>
RPS4	Resistance to <i>Pseudomonas syringae</i> expressing <i>avrRps4</i>
RPS5	Resistance to <i>Pseudomonas syringae</i> expressing <i>avrPphB</i>
RPW8	Resistance to powdery mildew 8
RRS1-R	Resistance to <i>Ralstonia solanacearum</i>
Xa21	Resistance to <i>Xanthomonas oryzae</i> pv. <i>oryzae</i>

List of abbreviations for pathogens

<i>Pma</i>	<i>Pseudomonas syringae</i> pv. <i>maculicola</i> (previously known as <i>Psm</i> )
<i>Psg</i>	<i>Pseudomonas syringae</i> pv. <i>glycinea</i>
<i>Pph</i>	<i>Pseudomonas syringae</i> pv. <i>phaseolicola</i> (previously known as <i>Psh</i> )
<i>Pto</i>	<i>Pseudomonas syringae</i> pv. <i>tomato</i> (previously known as <i>Pst</i> )
<i>Xcv</i>	<i>Xanthomonas campestris</i> pv. <i>vesicatoria</i>

	Name	Oligonucleotide sequence	T <sub>m</sub> (°C)	Cycle
RPM1-marker genes	RIPK fwd	5'-AAA GTT TCA TGG AGA TCA CTA ATC G-3'	58.1	28
	RIPK rev	5'-AAA GCT GTA TAC GTC ACT TCT TGC T-3'	59.7	
	TonB fwd	5'-AAT CAT AAT CTG TTC GAA GAT GAG C-3'	58.1	28
	TonB rev	5'-GAA GTT CCA AAT GTC ATA CAA ATC C-3'	58.1	
	MMP2 fwd	5'-GTT GAT GGT CTC TAC CGT ATC AAA A-3'	59.7	28
	MMP2 rev	5'-TCC TCA ACT GAA GAA TGT CCT AAA C-3'	59.7	
ET biosynthesis genes	ACS6 fwd	5'-CCC TTA TTA TCC AGG GTT TGA T-3'	56.5	28
	ACS6 rev	5'-TCG GAT TGA CCA AAA GTA GTA GC-3'	58.9	
	EFE fwd	5'-GCG AAG TTC AAC CTC TTA ACG-3'	57.9	28
	EFE rev	5'-CGC GCA CTT CTG TTT CTC TT-3'	57.3	
PR genes	PR1 fwd	5'-AAT TTT ACT GGC TAT TCT CG-3'	51.1	28
	PR1 rev	5'-GTG AAC GAG AAG CCA TAC-3'	53.7	
	PR2 fwd	5'-CTT CTC AGC CTT GTA ATA GCT TCC-3'	61.0	28
	PR2 rev	5'-GCC CAC AAA GTC TCT AAG GAT TAG T-3'	61.3	
	PR3 fwd	5'-GCC CAT CCA CCT GTA GTT TC-3'	59.4	28
	PR3 rev	5'-AGC AAT GTG GTC GCC AAG-3'	56.0	
	PR5 fwd	5'-CTC CAG TAT TCA CAT TCT CTT CCT CG-3'	63.2	28
	PR5 rev	5'-ACC CGA CTG TAT CTA ACT CGA AGC-3'	62.7	
JA/ET-regulated genes	PDF1.2 fwd	5'-AGA AGT TGT GCG AGA AGC CAA G-3'	60.0	28
	PDF1.2 rev	5'-TTG TAA CAA CAA CGG GAA AAT AAA C-3'	58.0	
	VSP2 fwd	5'-CTC TTG GTC TTG GGC GCT AC-3'	60.3	28
	VSP2 rev	5'-GTT CGA ACC ATT AGG CTT CAA TAT G-3'	59.7	
Constitutive controls	EF1 $\alpha$ fwd	5'-TCA CAT CAA CAT TGT GGT CAT TGG C-3'	61.3	22
	EF1 $\alpha$ rev	5'-TTG ATC TGG TCA AGA GCC TCA AG-3'	60.6	
	Actin8 fwd	5'-GCT GGA TTC GCT GGA GAT GA-3'	59.3	22
	Actin8 rev	5'-AGG TCT CCA TCT CTT GCT CG-3'	59.3	
	PIA fwd	5'-CAC CAT GGC AGG CAG AGA GAT TCT CC-3'	68.0	35
	PIA rev	5'-CTG GAA CCT TAC AAC TAT ACA AGA AAT G-3'	60.7	

**Table A1** Primers combination, melting temperatures and number of cycles for gene expression analysis using RT-PCR

Accession Number	Protein Name	Theoretical pI/MW	Experimental pI/MW	PMF Score	%Sequence Coverage	Matched peptide	Pairwise t-Test			Expression Profile
							T <sub>2/0</sub> <sup>a)</sup>	T <sub>6/0</sub> <sup>b)</sup>	T <sub>6/2</sub> <sup>c)</sup>	
<b>TOTAL PROTEIN</b>										
<b>DEFENSE</b>										
At3g53260	Phenylalanine ammonia-lyase 2	6.41 / 77	6.41 / 72	98	14,2	8	**d)	**	**	
At3g52960	Peroxiredoxin type 2, putative/Prx IIE	9.57 / 24	4.85 / 16	65	15,8	5	**	**	ns <sup>f)</sup>	
At1g02930	Glutathione transferase/GSTF6 <sup>1)</sup>	6.17 / 23	6.26 / 24	159	38,0	9	ns	*e)	*	

At1g02930 Glutathione transferase/GSTF6<sup>2)</sup>

6.17 / 23

6.44 / 24

191

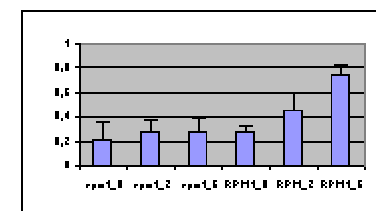
43,8

12

\*

\*\*

\*



At1g02920 Glutathione transferase /GSTF7

6.61 / 23

6.70 / 24

148

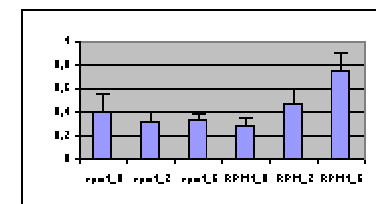
30,1

8

\*

\*\*

\*

**RNA PROCESSING**

At2g37220 29 kDa, ribonucleoprotein, chloroplast putative/RNA-binding protein

4.78 / 30

4.46 / 26

81

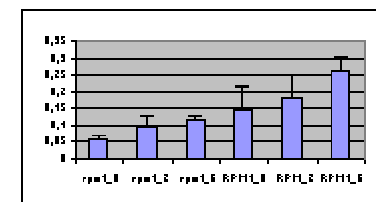
20,1

5

ns

\*

\*

**METABOLISM AND PHOTOSYNTHESIS**

At3g01500 Carbonic anhydrase 1, chloroplast precursor

5.45 / 29

5.41 / 62

66

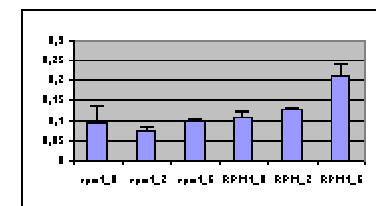
14,4

4

\*

\*\*

\*\*



Atcg00490 RBCL<sup>1)</sup>

6.24 / 53

5.97 / 62

145

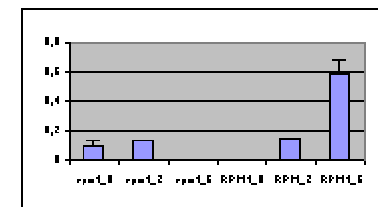
25,9

12

ns

\*\*

\*\*



Atcg00490 RBCL<sup>3)</sup>

6.24 / 53

06.05.1963

150

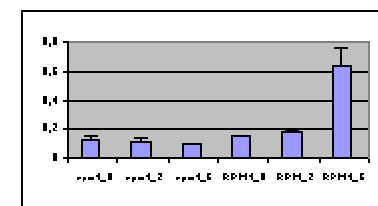
25,1

12

ns

\*\*

\*\*



At5g66570 Oxygen evolving complex subunit 33 kDa  
OEC33

5.28 / 35

4.64 / 32

109

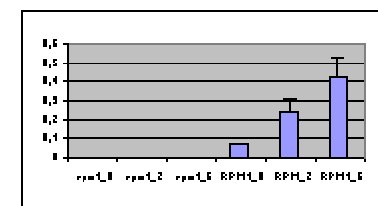
15,4

8

\*\*

\*\*

\*



At5g09660 Similar to malate dehydrogenase

8.11 / 37

5.99 / 36

68

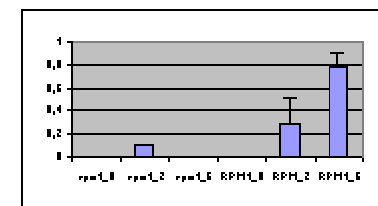
17,4

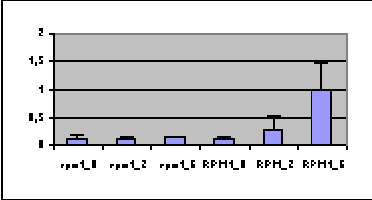
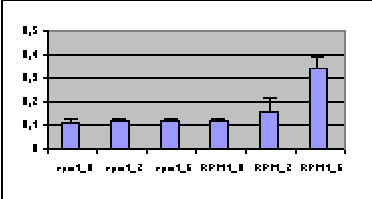
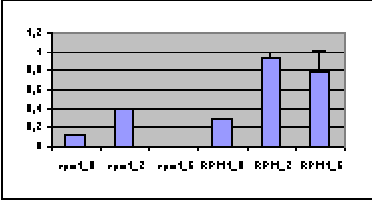
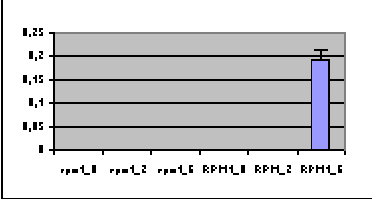
4

\*

\*\*

\*\*



At1g06680	Oxygen evolving complex subunit 23 kDa PSII-P	7.49 / 28	4.69 / 26	100	30,0	5	*	**	*	
At5g11670	The malic enzyme, encoded by AtNADP_ME2	6.36 / 64	6.24 / 63	122	16,3	9	*	**	**	
At5g35630	Chloroplastic glutamine synthase	6.86 / 47	4.97 / 45	124	19,8	9	**	**	ns	
At4g37930	Serine hydroxymethyltransferase 1	8.36 / 57	6.63 / 55	168	19,9	13	na	**	**	

## UNKNOWN

At1g12870 S locus F-box-related

8.83 / 48

4.90 / 32

60

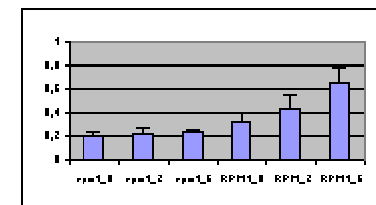
10,8

5

\*

\*\*

\*



## MICROSOMAL PROTEIN

## DEFENSE

At3g53260 Phenylalanine ammonia-lyase 2

6.42 / 78

6.44 / 81

182

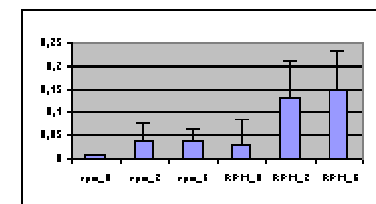
24,4

14

\*

\*

ns

At3g14210 Myrosinase-associated protein like<sup>1)</sup>

7.28 / 44

5.82 / 44

149

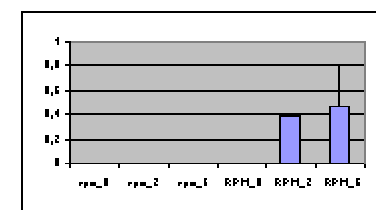
24,5

7,28

ns

\*

ns

At3g14210 Myrosinase-associated protein like<sup>2)</sup>

7.28 / 44

5.79 / 44

101

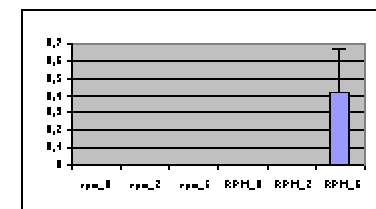
20,7

9

na

\*

\*



At1g02920 Glutathione transferase/GSTF7

6.61 / 24

6.76 / 19

135

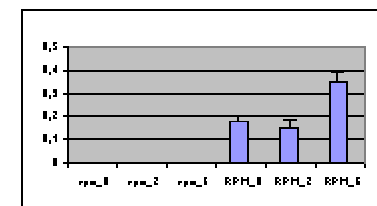
33,5

8

ns

\*

\*\*

**SIGNALING**At3g61260 AtREM1.2<sup>1)</sup>

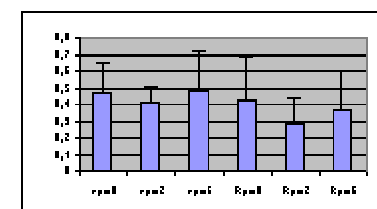
5.32 / 23

5.37 / 35

ns

ns

ns

At3g61260 AtREM1.2<sup>2)</sup>

5.32 / 23

05.12.1935

126

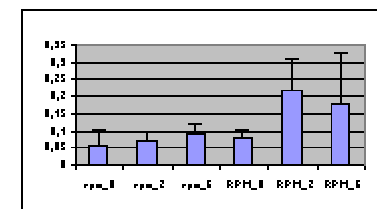
40,6

8

\*

ns

ns

**METABOLISM AND PHOTOSYNTHESIS**Atcg00490 RBCL<sup>1)</sup>

6.24 / 53

5.92 / 65

66

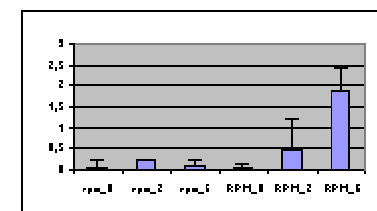
12,5

6

ns

\*\*

\*



Appendix

Atcg00490 RBCL<sup>2)</sup>

6.24 / 53

6.00 / 64

135

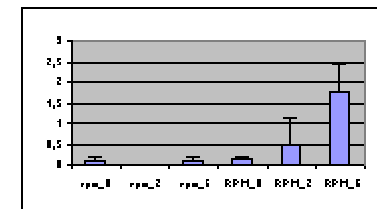
26,9

13

ns

\*\*

\*



Atcg00490 RBCL<sup>4)</sup>

6.24 / 53

06.09.1968

170

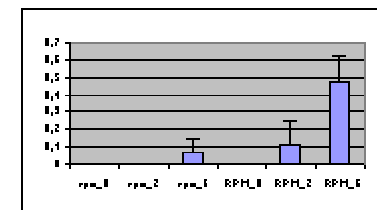
29,6

14

ns

\*\*

\*\*



Atcg00490 RBCL<sup>5)</sup>

6.24 / 53

6.17 / 68

102

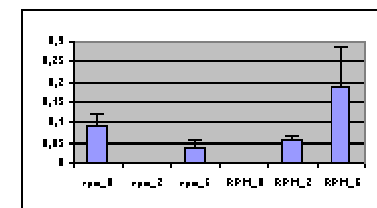
19,4

9

ns

\*\*

\*



RUBISCO-DEPLETED TOTAL PROTEIN

RNA PROCESSING

At1g11650 Similar to RNA-binding protein 45

5.95 / 33

5.45 / 54

150

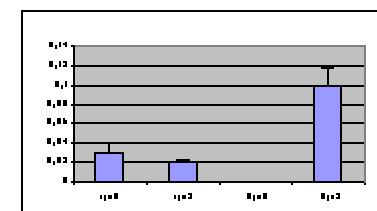
27,9

12

\*\*

na<sup>g)</sup>

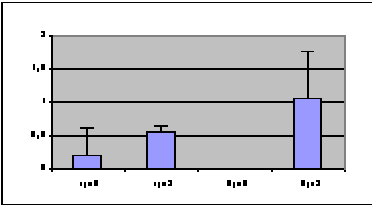
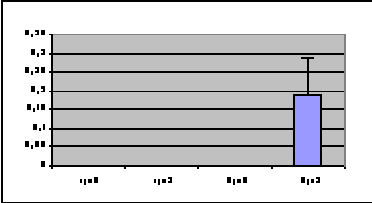
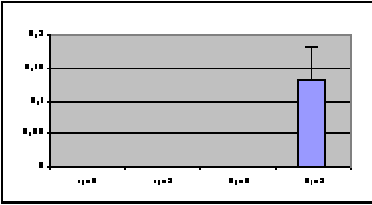
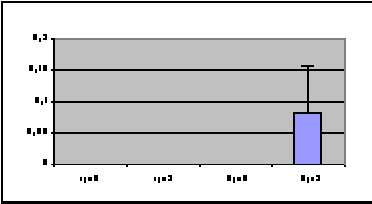
na



## SIGNALING

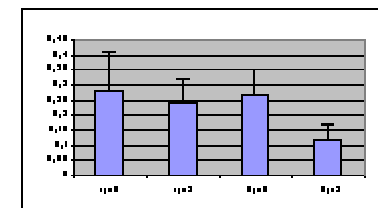
At2g20630 Protein Phosphatase 2C, putative	6.05 / 30	5.82 / 32	272	61,6	21	**	na	na	<table border="1"> <thead> <tr> <th>Genotype</th> <th>Value</th> </tr> </thead> <tbody> <tr> <td>rpp1</td> <td>~0,05</td> </tr> <tr> <td>rpp2</td> <td>~0,01</td> </tr> <tr> <td>Rpp1</td> <td>~0,08</td> </tr> <tr> <td>Rpp2</td> <td>~0,18</td> </tr> </tbody> </table>	Genotype	Value	rpp1	~0,05	rpp2	~0,01	Rpp1	~0,08	Rpp2	~0,18
Genotype	Value																		
rpp1	~0,05																		
rpp2	~0,01																		
Rpp1	~0,08																		
Rpp2	~0,18																		
At3g61260 AtREM1.2 <sup>1)</sup>	5.32 / 23	5.39 / 35	87,9	35,8	7	ns	na	na	<table border="1"> <thead> <tr> <th>Genotype</th> <th>Value</th> </tr> </thead> <tbody> <tr> <td>rpp1</td> <td>~0,75</td> </tr> <tr> <td>rpp2</td> <td>~0,70</td> </tr> <tr> <td>Rpp1</td> <td>~0,65</td> </tr> <tr> <td>Rpp2</td> <td>~0,60</td> </tr> </tbody> </table>	Genotype	Value	rpp1	~0,75	rpp2	~0,70	Rpp1	~0,65	Rpp2	~0,60
Genotype	Value																		
rpp1	~0,75																		
rpp2	~0,70																		
Rpp1	~0,65																		
Rpp2	~0,60																		
At3g61260 AtREM1.2 <sup>2)</sup>	5.32 / 23	5.18 / 35	87,9	35,8	7	ns <sup>h)</sup>	na	na	<table border="1"> <thead> <tr> <th>Genotype</th> <th>Value</th> </tr> </thead> <tbody> <tr> <td>rpp1</td> <td>~0,25</td> </tr> <tr> <td>rpp2</td> <td>~0,18</td> </tr> <tr> <td>Rpp1</td> <td>~0,20</td> </tr> <tr> <td>Rpp2</td> <td>~0,38</td> </tr> </tbody> </table>	Genotype	Value	rpp1	~0,25	rpp2	~0,18	Rpp1	~0,20	Rpp2	~0,38
Genotype	Value																		
rpp1	~0,25																		
rpp2	~0,18																		
Rpp1	~0,20																		
Rpp2	~0,38																		
At3g61260 AtREM1.2 <sup>3)</sup>	5.32 / 23	5.22 / 35	91,5	36,8	7	ns	na	na	<table border="1"> <thead> <tr> <th>Genotype</th> <th>Value</th> </tr> </thead> <tbody> <tr> <td>rpp1</td> <td>~0,28</td> </tr> <tr> <td>rpp2</td> <td>~0,28</td> </tr> <tr> <td>Rpp1</td> <td>~0,22</td> </tr> <tr> <td>Rpp2</td> <td>~0,12</td> </tr> </tbody> </table>	Genotype	Value	rpp1	~0,28	rpp2	~0,28	Rpp1	~0,22	Rpp2	~0,12
Genotype	Value																		
rpp1	~0,28																		
rpp2	~0,28																		
Rpp1	~0,22																		
Rpp2	~0,12																		

## METABOLISM AND PHOTOSYNTHESIS

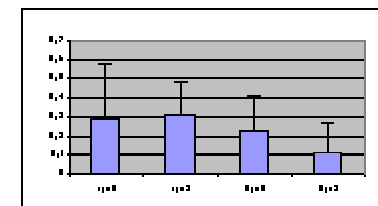
At2g39730 Rubisco activase	5.93 / 52	4.84 / 51	157	22,6	11	**	na	na	
At1g06680 Oxygen evolving complex subunit 23 kDa PSII-P	7.49 / 28	4.73 / 27	122	39,9	9	**	na	na	
At4g05180 Oxygen evolving complex subunit 16 kDa PSII-Q	10.28 / 25	5.67 / 12	100	33,9	6	**	na	na	
At5g05600 Oxidoreductase	6.24 / 42	7.75 / 48	87,8	18,3	7	**	na	na	

## UNKNOWN

At5g48930 Hydroxycinnamoyl-Coenzyme A shikimate/  
 quinate hydroxycinnamoyl transferase 6.65 / 48 6.88 / 54 129 25,6 14 \*\* na na



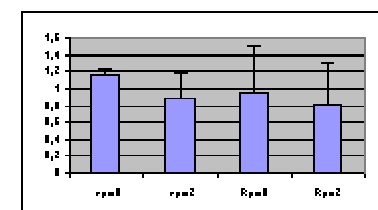
At4g39260 Encodes a glycine-rich protein 5.30 / 16 5.35 / 10 181 72,8 11 \* na na



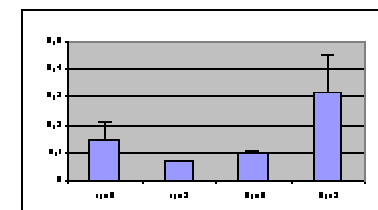
## RUBISCO-DEPLETED MICROSOMAL PROTEIN

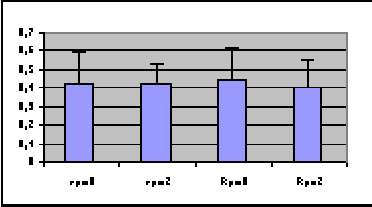
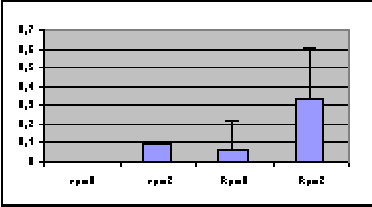
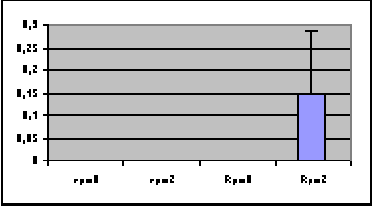
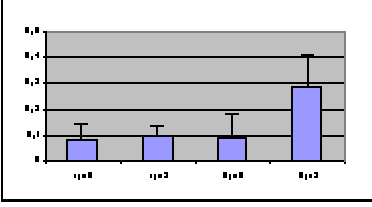
## SIGNALING

At3g61260 AtREM1.2<sup>1)</sup> 5.32 / 23 5.44 / 37 180 62,7 14 ns na na

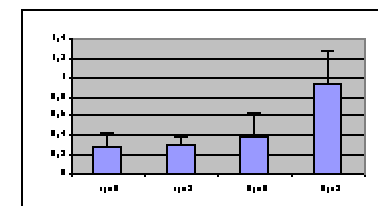


At3g61260 AtREM1.2<sup>2)</sup> 5.32 / 23 5.21 / 37 96,5 39,2 7 \*\* na na



At3g61260 AtREM1.2 <sup>3)</sup>	5.32 / 23	5.25 / 37	109	42,5	11	ns	na	na	
At3g61260 AtREM1.2 <sup>4)</sup>	5.32 / 23	05.08.1937	80,6	40,6	8	*	na	na	
At3g61260 AtREM1.2 <sup>5)</sup>	5.32 / 23	05.07.1937	74,4	37,7	11	**	na	na	
At2g20630 Protein Phosphatase 2C, putative	6.05 / 30	5.72 / 38	170	50,2	18	*	na	na	

At4g34150 C2-domain containing protein	7.47 / 27	6.58 / 39	113	40,5	11	*	na	na
----------------------------------------	-----------	-----------	-----	------	----	---	----	----



- a) The p values of t-test between samples at 2 and 0 hours after dexamethasone induction
- b) The p values of t-test between samples at 6 and 0 hours after dexamethasone induction
- c) The p values of t-test between samples at 6 and 2 hours after dexamethasone induction
- d) The p value less than 0.01 (\*\*)
- e) The p value less than 0.05 (\*)
- f) not significant (ns)
- g) not applicable (na)
- h)  $p = 0.053$ , It failed the t-test marginally but p-values are  $< 0.05$  for the same spot in the microsomal protein samples (with/without fractionation)

**Table A2** The identified up-regulated and down-regulated proteins after dexamethasone induction in different fraction according to their biological functions

## **Acknowledgements**

My sincere thanks to you...

Prof. Dr. Dierk Scheel for the opportunity to do my PhD in his lab, for the supervision during my PhD and for the supports during my stay in Germany.

Dr. Justin Lee for the supervision during my PhD, for helping me to organize the experiments and critically evaluate the results and for sharing his knowledge and experiences.

I also like to thank Dr. Lee and Prof. Scheel for editing this manuscript.

I am grateful for the continuous supports and encouragements from my husband, Vincent, during this PhD. Thank you for the patience for my long work at weekends though that is the only time for us to meet.

The analysis of SA was done with the assistance from Franziska Handmann. Simone Altmann and Birgit Ortel helped me to perform JA and OPDA analysis. I thank Dr. Kai Naumann for protein identification by LC-MS/MS and Gerit Bethke for FRET analysis and Botrytis assay. Many thanks to Dr. Steffen Neuman and Dr. Jens Boch for the fruitful discussion.

I would like to thank every one in the group of cellular signaling and department of stress and developmental biology for the help during my PhD and for the friendly environment during my stay.

This thesis would not be possible without people who may not even know their contribution:

Prof. Dr. Gunawan Indrayanto, the first person who introduces me to research and encourages me to pursue higher education.

I am very lucky to have a father who always supports me and a mother who devotes a constant prayer for me. Thank you for always being there for me.

## **Curriculum Vitae**

### Personal details

Name: Ivy Widjaja  
Address: Kencanasari Timur IV / F-27, Surabaya 60225, Indonesia  
Date and place of birth: 2<sup>nd</sup> November 1974 in Surabaya, Indonesia

### Education and work experience

1981 – 1987 Primary School, SDK “St. Xaverius” in Surabaya  
1987 – 1990 Junior High School, SMPK “Angelus Custos” in Surabaya  
1990 – 1993 Senior High School, SMAK “Frateran” in Surabaya  
1993 – 1998 Bachelor of Science in Pharmacy, University of Airlangga, Surabaya  
1998 – 1999 Apothecary degree, University of Airlangga, Surabaya  
1999 – 2000 Technical assistant, Laboratory of Pharmaceutical Biotechnology, University of Airlangga, Surabaya  
2000 – 2002 Master of Science in Natural Products, University of Leiden, The Netherlands  
2002 – 2004 Research assistant, Genome Institute of Singapore, Singapore  
2004 – 2008 PhD work, Leibniz Institute of Plant Biochemistry, Halle/Saale, Germany